

# Funkcionalno istraživanje fosforilacije proteina CENP-E kinazama Aurora A i B

---

Kubat, Mirela

Master's thesis / Diplomski rad

2020

*Degree Grantor / Ustanova koja je dodijelila akademski / stručni stupanj:* **University of Zagreb, Faculty of Science / Sveučilište u Zagrebu, Prirodoslovno-matematički fakultet**

*Permanent link / Trajna poveznica:* <https://urn.nsk.hr/urn:nbn:hr:217:125685>

*Rights / Prava:* [In copyright](#) / [Zaštićeno autorskim pravom.](#)

*Download date / Datum preuzimanja:* **2024-04-25**



*Repository / Repozitorij:*

[Repository of the Faculty of Science - University of Zagreb](#)



University of Zagreb

Faculty of Science

Division of Biology

Mirela Kubat

**Functional study of CENP-E phosphorylation  
by Aurora kinases A and B**

Graduate Thesis

Zagreb, 2020.



This thesis was performed in Cell Division and Cytoskeleton Lab, Danish Cancer Society Research Center, Copenhagen, Denmark under supervision of Associate Professor Marin Barišić and Postdoctoral Researcher Susana Eibes-Gonzalez, co-supervised by Associate Professor Inga Marijanović. Thesis is submitted on evaluation to Department of Biology, Faculty of Science, University of Zagreb, Zagreb, Croatia in order to acquire academic title of Master of Molecular Biology.



## Acknowledgements

Firstly, I would like to thank assoc. prof. Marin Barišić, for having me as a part of his group and allowing me to conduct my master's thesis project under his supervision. Thank you for all the support, knowledge, and invested time. Not only were you the best boss I ever had, but also one of the best teachers. I have never met somebody so committed and in love with what they do, and passionate to pass the knowledge they have. I am certain your group will continue to grow and be very successful, and I wish you all the best.

Biggest thanks to Susana Eibes-Gonzalez, my direct mentor and supervisor in Marin's group. Not only were you an amazing teacher and mentor, you were one of the few friends I had while in Denmark, and your support and kindness were sometimes the only thing that made me push through. I am extremely grateful for your patience, the knowledge you passed onto me, invested time, guidance, but most importantly your friendship. I couldn't have wished for a better mentor and thank you for always being there for me.

Thanks to Claudia Guasch-Boldu, Girish Rajendraprasad and Yulia Steblyanko. You immediately made me feel like an equal member of your group, and together with Marin and Susana, as a part of a family when I was far away from mine. Thank you for all your help and advice and making my days at work not feel like work at all.

Thanks to Inga Marijanović, my mentor at University of Zagreb. For your advice and invested time, and for being one of the most approachable and kindest professors I had.

I want to thank my closest friends – Andrea, Flavija, Hana, Karlo, Lucija, Patricia, Vanja and Zorana (please notice the alphabetical order). For all the laughs, support, kindness, patience, understanding, nights out, fun and love. I feel so fortunate to have you in my life, and I never thought I would have so many amazing people that understand me and support me. You are my family and I love you very much.

Thank you to my brother Ilija, for your love and support, and for always looking up to me. I know how much you are proud of me, and you don't even know how many times you were my motivation to keep staying true to my path. I am extremely proud of you, the man you are becoming and the person you are. You are my rock. I love you.

Thank you to my sister Irena, for everything you have done for me. I can not even put into words what an amazing sister and person you are. I couldn't be prouder of you, the person you are, how you treat other people, how you are always there for the people you love, and how amazing

you are as a mother. Laura is very blessed to have you as a mother, as are Ilija and me to have you as a sister. I am looking forward to a packed dinner table when our big families will come together. I love you.

I na kraju, hvala mojim roditeljima, Vesni i Vladi. Bez vas ne bih bila to što jesam. Isprike na svakom putu kada je bilo teško sa mnom. Hvala vam na sigurnosti, što uvijek znam da se mogu pouzdati u vas i da uz vas imam dom. Hvala vam što ste uvijek vjerovali u mene, posebno kada ja nisam. Hvala vam što ste uvijek bili ponosni na mene, jer mi je to bila najveća motivacija. I hvala vam na neizmjernoj ljubavi, koju ću vam vraćati cijelog života.





## **BASIC DOCUMENTATION CARD**

---

University of Zagreb

Faculty of Science

Division of Biology

Graduate Thesis

### **Functional study of CENP-E phosphorylation by Aurora kinases A and B**

Mirela Kubat

Rooseveltovej trg 6, 10000 Zagreb, Hrvatska

Spatial layout of chromosomes enables equal allocation of genetic material during cell division. Congression of chromosomes that are positioned on the poles of the mitotic spindle is mediated by kinesin-7/CENP-E, a microtubule plus-end directed motor protein. Currently, there are two models that explain how CENP-E directs chromosomes exclusively towards cell equator. In the first model, CENP-E drives chromosome movements from high Aurora A kinase concentration on the poles, towards the cell equator, then binds protein phosphatase 1 which dephosphorylates it and enables stable binding of kinetochores to microtubules. The second model is based on different preferences of two motor proteins with opposite directionalities, namely CENP-E and dynein, for detyrosinated and tyrosinated microtubules, respectively, which control the directionality of chromosome movements during cell division. However, the relationship of individual contributions of activity regulation of CENP-E by phosphorylation and microtubule detyrosination remains to be elucidated. This set of experiments focused on clarifying the role of CENP-E phosphorylation by Aurora A and B and its impact on CENP-E-dynein activity switch and potential interaction. The hypothesis is that T422 phosphorylation of CENP-E prevents its premature stripping by Dynein from bioriented chromosomes' kinetochores, thus facilitating the accurate cell division. The methods used were molecular cloning, lentiviral infection, immunofluorescence following protein inhibition and siRNA knock down, confocal microscopy, Western blot and immunoprecipitation.

(88 pages, 44 figures, 9 tables, 210 references, original in: English)

Thesis deposited in the Central biological library.

Key words: CENP-E, Aurora A, Aurora B, kinase, dynein-mediated stripping, mitosis, chromosome congression.

Supervisor: Dr. Marin Barišić, Assist. Prof.

Assistant supervisor: Dr. Inga Marijanović, Assist. Prof.

Reviewers: Dr. Inga Marijanović, Assist. Prof.

Dr. Sven Jelaska, Prof.

Dr. Goran Kovačević, Prof.

Replacement reviewer: Dr. Sc. Nenad Malenica, Assist. Prof.

Thesis accepted: February 20<sup>th</sup>, 2020

# TEMELJNA DOKUMENTACIJSKA TABLICA

---

Sveučilište u Zagrebu

Prirodoslovno-matematički fakultet

Biološki odsjek

Diplomski rad

## **Funkcionalno istraživanje fosforilacije proteina CENP-E Aurora kinazama A i B**

Mirela Kubat

Rooseveltov trg 6, 10000 Zagreb, Hrvatska

Ispravan prostorni raspored kromosoma omogućava ravnopravnu raspodjelu genetičkog materijala prilikom stanične diobe. Kongresija kromosoma koji se nalaze na polovima mitotskog vretena je posredovana proteinom kinezinom-7/CENP-E. Trenutno postoje dva modela koji objašnjavaju kako CENP-E usmjerava kromosome isključivo prema staničnom ekvatoru. U prvom modelu, CENP-E pogoni kretanje kromosoma od visoke koncentracije kinaze Aurora A na polovima prema staničnom ekvatoru, zatim veže protein fosfatazu 1, koja ga defosforilira i omogućuje stabilno vezanje kinetohora na mikrotubule. Drugi model se bazira na različitim preferencijama dvaju motornih protein suprotnih usmjerenja, proteina CENP-E i dineina za detirozinirane i tirozinirane mikrotubule, koji kontroliraju smjer putovanja kromosoma tijekom stanične diobe. Odnos pojedinačnih doprinosa regulacije aktivnosti proteina CENP-E direktnom fosforilacijom i detirozinacijom mikrotubula ostaje za razjasniti. Ovaj set eksperimenata je fokusiran na raščišćavanje funkcije fosforilacije proteina CENP-E kinazama Aurora A i B, kao i na utjecaj fosforilacije na prekidač aktivnosti između proteina CENP-E i dineina. Metode koje su korištene su molekularno kloniranje, lentivirusna infekcija, imunofluorescencija nakon tretmana inhibitorima proteina i siRNA knock down, konfokalna mikroskopija, Western blot te imunoprecipitacija.

(88 stranica, 44 slike, 9 tablica, 210 literaturnih navoda, jezik izvornika: engleski)

Rad pohranjen u Središnjoj biološkoj knjižnici.

Ključne riječi: CENP-E, Aurora A, Aurora B, dinein, uklanjanje posredovano dineinom, mitozu, kongresija kromosoma.

Voditelj: izv. prof. dr. sc. Marin Barišić

Suvoditelj: izv. prof. dr. sc. Inga Marijanović

Ocijenitelji: izv. prof. dr. sc. Inga Marijanović

prof. dr. sc. Sven Jelaska

prof. dr. sc. Goran Kovačević

Zamjena: izv. prof. dr. sc. Nenad Malenica

Rad prihvaćen: 20.02.2020.

# Table of contents

1. Introduction .....	1
1.1. The Cell Cycle.....	1
1.2. Mitosis.....	5
1.2.1. Prophase .....	5
1.2.2. Prometaphase and metaphase .....	5
1.2.3. Anaphase and telophase .....	7
1.3. Aurora kinases.....	7
1.3.1. Roles in mitosis .....	8
1.4. Kinetochore-microtubule interface.....	10
1.5. Spindle assembly checkpoint (SAC) .....	11
1.5.1. SAC silencing.....	13
1.6. CENP-E.....	15
1.6.1. Congression of pole proximal chromosomes .....	17
1.6.2. Regulation .....	17
1.7. Aims of the thesis .....	20
2. Materials and methods.....	21
2.1. Cell culture and transfections .....	21
2.2. Generation of new cell line.....	21
2.2.1. Verification of plasmids .....	21
2.2.2. Restriction-ligation cloning .....	22
2.2.3. Gateway cloning.....	23
2.2.4. Lentiviral infection .....	23
2.3. Drug treatments .....	24
2.4. Western blot .....	24
2.5. Immunofluorescence .....	24
2.6. Live-cell imaging .....	25
2.7. Immunoprecipitation .....	26
2.8. Statistical analysis .....	26
3. Results .....	30
3.1. Establishing a stable cell line with CC1-box and T422A mutations .....	30
3.2. GFP-CENP-E expression is highest after 16 hours of adding doxycycline .....	38
3.3. Phosphorylation by Aurora A prevents stripping of CENP-E towards the spindle poles .....	39
3.4. Microtubules have a role in CENP-E stripping.....	41
3.5. Accumulation of CENP-E at the poles is not due to uncongressed chromosomes.....	43

3.6. CENP-E stripping is dependent upon Spindly .....	44
3.7. Characterization of CENP-E CC1-box mutant.....	49
3.8. Quantification of CENP-E amount at the poles after siRNA treatments.....	52
3.9. Immunoprecipitation .....	56
3.10. T422A mutant establishes bipolar spindles under treatment with STLC .....	58
3.10. Establishment of bipolarity is due to CENP-E's phosphorylation state, not activity .....	62
4. Discussion .....	66
5. Conclusions .....	69
6. References .....	70
7. Curriculum vitae.....	88

# 1. Introduction

## 1.1. The Cell Cycle

The cell cycle is a core process in every cell which main goal is the production of two daughter cells. In prokaryotes and yeasts, each cell division results in a complete new organism. In eukaryotes, its roles go beyond growth and proliferation of cells, while it is crucial in organismal development, regulation of DNA damage repair, response to injury, cancer etc.

The cell cycle is divided into interphase (subdivided into G1, S and G2) and M phase. Interphase itself is a period of DNA synthesis and preparation for cell division. At the beginning, in G1 phase, the cell is preparing for DNA synthesis, with abundant protein and mRNA synthesis, as well as growth of the cell. The longest phase in the process is the S phase, taking as much as 12 hours of the 24-hour cycle in a mammalian cell. The DNA is being replicated, and the cells finish the phase with a  $4n$  DNA content. Subsequently, in the G2 phase, the cell is preparing for cell division, growing and making certain the DNA has been correctly replicated. If there are no mistakes or damage, the cell progresses to the M phase. The M phase lasts less than an hour and comprises nuclear division (mitosis), during which the chromosomes are being distributed, and cytoplasmic division (cytokinesis), which is defined as physical separation in two cells.

The cell cycle process is extensively regulated, with numerous regulatory proteins which secure that the cell first replicates its genome in two complete copies, and that the copied chromosomes are accurately segregated to the two daughter cells. Most important regulatory proteins in this process are cyclin-dependent kinases (Cdks) and cyclin proteins. Cyclins regulate the cell cycle progression through activation of Cdks, with which they form complexes. The levels of Cdk/cyclin complexes oscillate throughout the cycle, thus controlling the progression between cell cycle phases (Alberts, 2014).

To further ensure the proper progression throughout the cell cycle phases, these proteins are under control of internal checkpoints. If the system detects problems at either one of the checkpoints, it leads to cell cycle arrest (Hartwell *et al.*, 1989). In order to enter the cell cycle, adult cells must activate the expression of cell cycle genes, since most of them are in a quiescent state and therefore do not express many of these proteins. (Malumbres and Barbacid, 2001).

In G1, if the environment is favorable, mitogenic signals transcriptionally induce cyclins (D1, D2 and D3), leading to the activation of Cdk4 and Cdk6, which then phosphorylate pRb. This

modification by Cdk4/6-cyclin D complexes disrupts the pRb repression program and leads to high expression levels of genes required for following cell cycle phases (Malumbres and Barbacid, 2001; Malumbres *et al.*, 2009).

Among those proteins are cyclin A, E and Cdk2, which have a role in promoting G1/S checkpoint progression. The G1/S checkpoint, also denoted the DNA damage checkpoint, pauses the cell cycle if DNA damage occurred during G1 phase. The damage repair is mostly comprised of a p53-dependent mechanism feeding into the pRb pathway (Sherr and McCormick, 2002). Damage- activated protein kinases phosphorylate p53, which leads to release from its suppressor MDM2. p53 then transcriptionally activates a Cdk inhibitor p21. p21 consequentially binds and inhibits Cdk2-cyclin A/E, leading to diminished phosphorylation of pRb and consequent arrest of the cell cycle in G1 phase (Henley and Dick, 2012; Nelson *et al.*, 1997).

If there is no damage present, the levels of cyclin E are high, favoring formation of the complexes with Cdk2, thus enabling DNA synthesis. An internal S phase replication checkpoint is responsible for delaying S phase progression and preventing mitosis in case of stalled replication forks. Centrosome duplication also occurs and is partially coupled with the mechanism that controls DNA replication by the activity of Cdk2-cyclin A/E. After completion of the replication process, the cell enters the G2 phase, where it prepares for mitosis (Masai *et al.*, 2010; Hinchcliffe and Sluder, 2001; Dynlacht *et al.*, 1997).

Mitotic entry is under control of the G2/M checkpoint, which delays the onset of mitosis if there is unreplicated or damaged DNA present (Nurse, 1990) by negatively regulating the activity of Cdk1-cyclin B complex. A phosphorylation/dephosphorylation activating loop ensures high Cdk1-cyclin B levels required for the mitotic entry (Fung and Poon, 2005; Ma and Poon, 2011; Lindqvist *et al.*, 2009). During mitosis, several important events occur, such as chromosome condensation, nuclear envelope breakdown, formation of mitotic spindles, attachment of chromosomes to the mitotic spindle, congression of the chromosomes to the metaphase plate and separation of sister chromatids, happening during 5 subphases (prophase, prometaphase, metaphase, anaphase and telophase). An in-phase checkpoint, called spindle assembly checkpoint (SAC) is activated by the presence of unattached kinetochores or the absence of tension between paired kinetochores. It is crucial for metaphase to anaphase transition, e.g. proper chromosome segregation (Musacchio and Salmon, 2007).

If all kinetochores are properly attached, the SAC is silenced, and mitotic exit is driven by APC/C-dependent ubiquitination. Degradation of securin and cyclin B promotes sister chromatid



separation, spindle disassembly, chromosome decondensation, cytokinesis and reformation of the nuclear envelope (Mapelli *et al.*, 2007; Lesage *et al.*, 2011).

The last step of transition from M to G1 phase that yields two daughter cells, is called cytokinesis and is completed by abscission. Cytokinesis is coordinated with chromosome segregation (Maiato *et al.*, 2015) and the presence of chromatin in the cleavage plane can cause cytokinetic failure and tetraploidy, chromosome breaks and formation of micronuclei (Carlton *et al.*, 2012; Ganem *et al.*, 2012) which can lead to cancer development (Bakhoun and Compton, 2012; Holland and Cleveland, 2012). Recently, a machinery that delays completion of the final steps of abscission in the presence of trapped chromatin in the cleavage plane was described and is under control of the chromosomal passenger complex, comprised of INCENP, Survivin, Borealin and Aurora B (Steigemann, 2009).

Abscission timing is tightly controlled by Aurora B activity as part of the abscission checkpoint. Decline in Aurora B activity is necessary for abscission, and its inactivation accelerates abscission by leading to furrow regression in cells with chromatin bridges, whereas persistent Aurora B activity delays abscission. Targeting of Aurora B depends on its partners in the CPC- INCENP, Survivin, and Borealin (Cuylen, 2013).

Also, high membrane tension (Caballe, 2015; Lafaurie-Janvire, 2013), defective nuclear pore complex (NPC) integrity (Mackay, 2010), and DNA replication stress (Mackay and Ullman, 2015) have been shown to cause cytokinetic delay through the same pathway.

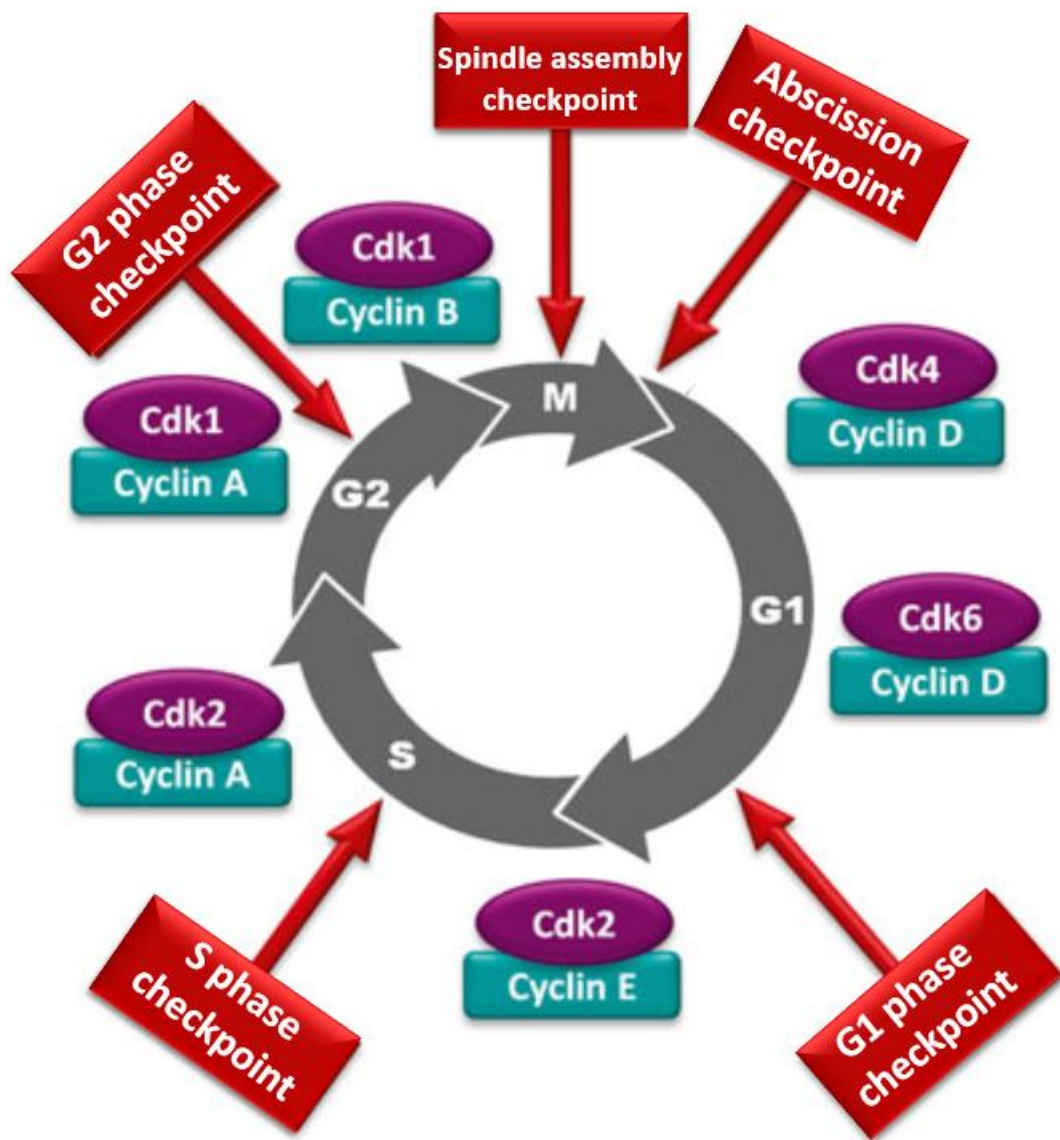


**Figure 1.** The cell cycle and its checkpoints. Cyclins are synthesised and degraded in a specific phase of the cell cycle and bind and activate specific Cdks which controls progression of the cell cycle phases. Four main checkpoints, respond to different types of errors and promote cell cycle arrest and repair (modified from Spoerri, 2015).

## 1.2. Mitosis

In mitosis, the duplicated DNA has to be accurately segregated into daughter cells. In the first stage of mitosis, prophase, chromosomes are being condensed. The mitotic spindle forms during prometaphase, attaches to the chromosomes and organizes them in the center of the cell in metaphase. Chromosomes start to segregate in anaphase, and when they are separated enough, two distinct nuclei can form in distant parts of the cell during telophase. Cytokinesis is the finishing step, where a contractile ring forms and separates two daughter cells (Glotzer, 2016)

### 1.2.1. Prophase

Onset of prophase is defined by visible chromosome condensation. DNA compaction in prophase acts on chromatin, the DNA fibers wrapped around histone octamers. Chromatin gets supercoiled in chromosomes, and each chromosome gets shorter and thicker and can be distinguished from other chromosomes (Martinez-Balbas *et al.*, 1995). In accordance, the nucleolus disperses by releasing many nucleoproteins into the nucleoplasm. The lamin network that lines the inner surface of the nuclear envelope weakens, and the nuclear envelope starts to break down (NEBD). Interphase microtubules disappear, and centrosomes initiate new microtubules that will form the spindle. Dispersal of the nuclear envelope marks the end of prophase, but the spindle formation begins even before the end of NEBD. At the time of NEBD, centrosomes can either be close to each other when the microtubule growth begins and then they can separate as the spindle forms, or in another setup, they can already lie on the opposite side of the nucleus and microtubules form as distinct asters (the “prophase” and “prometaphase” pathways of spindle assembly) (Chou *et al.*, 1990; Steinhardt and Alderton, 1988; O’Toole *et al.*, 2003).

### 1.2.2. Prometaphase and metaphase

To properly attach to microtubules, each chromosome needs a protein structure, called the kinetochore, to be formed on each chromatid. Kinetochores are complex structures, made from as much as 100 proteins in humans (Cheeseman *et al.*, 2014). These proteins form several layers of kinetochore structure with the most outer layer (the so-called “fibrous corona”) consisting of fibrous proteins that bind microtubule walls, but also of motor proteins that bind microtubules and generate forces to position chromosomes and have a role in microtubule dynamics. Among these motor proteins, CENP-E and dynein play a crucial role.

How microtubules bind chromosomes is still a matter of extensive research. The “search and capture” model is a proposed solution, and it resides on the dynamic nature of microtubules.

Spindle microtubules display dynamic instability, frequently growing and shortening. Together with diffusive rotations, microtubules are probing the region where chromosomes are, amplifying their chance to encounter a kinetochore. Kinetochore binding stabilizes them, and they are removed from the dynamic pool (Belmont *et al.*, 1990; Kalinina *et al.*, 2013; Kirschner and Mitchinson, 1986; Magidson *et al.*, 2015).

After NEBD, microtubules instantly grow into the nuclear space. If centrosomes are already separated, they approach chromosomes from opposite sides. Microtubules outnumber kinetochores, increasing their chance of binding. Microtubule-kinetochore binding is firstly not stable and needs a specific level of tension between sister chromatids to stabilize. When sister kinetochores are attached to opposite poles, they are being pulled in opposite directions. The pulling puts the centromere under tension, which promotes stable attachment. Microtubule attachment to kinetochores is under control of the Spindle Assembly Checkpoint (SAC) (Nicklas, 1997; Petry *et al.*, 2013; Bakhoum *et al.*, 2014).

To minimize the chance of improper chromosome segregation, chromosomes are being put in the equatorial plane of the spindle, obtaining the same distance from both spindle poles. Chromosomes can congress either directly, due to microtubule polymerization and depolymerization at kinetochores, with help of chromokinesins and polar ejection force, or indirectly, being transported by motor proteins, dynein and CENP-E. In the first case, the chromosome arms are being pushed toward the spindle equator and then outward from the spindle axis, which contributes to the motion of prometaphase chromosomes to the spindle equator. More on the motor proteins-mediated chromosome congression later (Rieder and Salmon, 1994; Brouhard and Hunt, 2005; Kapoor *et al.*, 2006)

Although prometaphase should end upon the last chromosome being aligned at the metaphase plate, because chromosomes oscillate along the spindle axis at the metaphase plate, the line between prometaphase and metaphase is not quite clear. The amplitude of oscillation varies between chromosomes and cells. On the other hand, the metaphase-anaphase transition is well defined – it is the moment sister chromatids start to separate. It is also one of the most important moments in mitosis, because of its irreversibility. The transition can not happen without SAC silencing, which happens when proper attachment of all chromosomes is achieved. SAC silencing then activates polyubiquitination of numerous proteins – most important being securin and cyclin B, causing inactivation of CDK1. Phosphatases undo the phosphorylation which was crucial in mitotic entry (McIntosh, 1991; Hardwick and Murray, 1995; Rieder *et al.*, 1995; Kapoor *et al.*, 2006; Cheeseman *et al.*, 2014).

### 1.2.3. Anaphase and telophase

Anaphase can be divided in two parts: anaphase A during which chromosomes are being pulled away from each other and their distance from the poles decreases, and anaphase B, during which the distance between the poles increases. When, due to the securin degradation, separase cleaves cohesins that held sister chromatids, each chromatid becomes an anaphase chromosome. The movement is an interplay between microtubule dynamics (changes in microtubule length and microtubule motions relative to one another) and motor proteins' activity (Uhlmann, 2001).

Shortening of kinetochore microtubules by loss of tubulin subunits at kinetochores marks the onset of anaphase A. It is presumed that either dynein or kinesin-14 could have a role in pulling the chromosomes poleward as kinetochore microtubules depolymerize. Relative sliding of the overlapping non-kinetochore microtubules is characteristic of anaphase B. It has also been shown that microtubules themselves elongate, polymerizing at their plus ends where they overlap near the spindle midplane. Elongation and sliding of microtubules assure that chromosomes are sufficiently apart for proper cytokinesis (Kirschner and Mitchinson, 1986; LaFountain *et al.*, 2004, Brust-Mascher and Scholey, 2011).

In telophase, the cells aim to restore an interphase nucleus. Cdk1 activity drops and alters activity in other mitotic kinases. Chromatin masses concentrate next to the spindle poles. Inner nuclear envelope proteins associate with the chromosomes and nuclear membrane surrounds them. When membranes come in contact, they fuse, and reform the nuclear envelope. Chromatin decondensation can commence, and afterwards transcription. By reorganizing actin, a cleavage furrow forms between the two new nuclei, and during cytokinesis two new daughter cells separate (Renshaw *et al.*, 2010; Gupta *et al.*, 2013).

## 1. 3. Aurora kinases

The majority of cell cycle regulators belong to the mitotic kinome, consisting of kinase families and their counteracting phosphatases or kinase inhibitors (Manning, 2002). To this day, there have been more than 1000 phosphoproteins identified, whose phosphorylation and dephosphorylation are cell-cycle regulated. One-third of mitotic proteins have at least 10 phosphorylation sites. (Dephoure *et al.*, 2008). Phosphorylation either activates mitotic proteins or leaves them in an inactive state. Phosphoproteins are then usually degraded through E3 ubiquitin ligase APC/C (anaphase promoting complex/cyclosome) when mitosis is finished (Barr *et al.*, 2007; Ma *et al.*, 2011).

Aurora kinase family members have roles in mitotic entry, spindle assembly and cytokinesis, and it has been noticed that mutations in the AURKA gene can cause monopolar spindles (Glover, 1995). While Aurora A (AurA) controls centrosome maturation and bipolar spindle assembly, Aurora B and C (AurB and AurC) have roles in condensation, attachment to kinetochores and alignment of chromosomes during prometaphase, metaphase and cytokinesis. (Wang *et al.*, 2014; Carmena *et al.*, 2009; Damodaran *et al.*, 2017).

Aurora A and B are constitutively expressed in mitotically active cells, while AurC is present only in germ cell during meiosis. During G2 phase, AurA expression levels increase, and it accumulates within cell nuclei (Zheng *et al.*, 2016). After NEBD, AurA mainly concentrates by centrosomes. The targeting to the centrosomes is enabled by the N-terminal domain in a microtubule-dependent manner. Depletion of this domain impairs proper spindle formation, chromosome alignment and mitotic onset (Li *et al.*, 2015; Liu *et al.*, 20016). The C-terminal domain of AurA impacts mitotic progression by altering AurA conformation and kinase activity (Giet *et al.*, 2005).

In contrast, AurB localization is regulated by its C-terminal domain. Survivin targets AurB to the centrosomes during prophase, to mediate the function of the chromosomal passenger complex (CPC) in proper kinetochore attachment. CPC is composed of the enzymatic component Aurora B and the three regulatory and targeting components: INCENP (inner centromere protein), Survivin and Borealin (Kelly *et al.*, 2009; van der Waal *et al.*, 2012). CPC has an important regulatory role, and its localization throughout mitosis ensures proper temporo-spatial phosphorylation of substrates involved in chromosome condensation, correction of erroneous kinetochore–microtubule attachments, activation of the spindle assembly checkpoint (SAC) and cytokinesis. When localization or function of the regulatory CPC components is perturbed, the other subunits of the CPC do not localize properly, Aurora B activity is diminished which leads to improper cell division (Vader *et al.*, 2006; Gassmann *et al.*, 2004; Carvalho *et al.*, 2003; Honda *et al.*, 2003; Adams *et al.*, 2001).

### **1.3.1. Roles in mitosis**

AurA promotes centrosome maturation which involves microtubule nucleation and recruitment of pericentriolar material to the microtubule organizing center (MTOC) (Petretti *et al.*, 2006). AurA roles prevail in centrosome growing, rather than duplication (Meraldi *et al.*, 2002) - it recruits the gamma-TuRC (γ-tubulin ring complex) and Centrosomin, which are required for elongation and nucleation of microtubules. (Hsu *et al.*, 1998; Hanna *et al.*, 2001; Glet *et al.*, 2002;

Ouchi *et al.*, 2004; Kapltein *et al.*, 2005; Barros *et al.*, 2005; Wang *et al.*, 2014). Moreover, AurA activates and targets the Cdk-cyclin B complex at centrosomes, having an important part in the transition from G2 to the M phase in cell cycle.

After maturation, centrosomes have to be separated to form opposite cell poles in order to establish the bipolar spindle (Hannak Ouchi *et al.*, 2001; Hirota Ouchi *et al.*, 2003; Cowley *et al.*, 2009). Amongst other proteins, AurA phosphorylates Eg5, a kinesin responsible for anti-parallel sliding of spindle microtubules, and consequently responsible for forming the bipolar spindle. Also, AurA activity balances the cycles of microtubule assembly and disassembly and controls the mitotic spindle dynamics. It does so through inhibition of Kif2a (a microtubule depolymerase), recruitment of TACC3 (transforming complex acidic coiled-coil-containing protein 3, induces microtubule growth), and antagonizing Kif2C (destabilizes microtubules around the centrosomes). (Barros *et al.*, 2005; Cowley *et al.*, 2009; Walczak *et al.*, 2008; De luca *et al.*, 2008; Jang *et al.*, 2009; Kinoshita *et al.*, 2005; Zhang *et al.*, 2008).

In the late prophase, AurA contributes to the second wave of Cdk-cyclin B phosphorylation. The activity of the complex then induces the release of spindle assembly factors and activates pathways responsible for NEBD. (Barr *et al.*, 2007; Carmena *et al.*, 2009).

As for Aurora B, during prophase it localizes at the kinetochores and mediates attachment between chromosomes and microtubules. AurB allows chromosome bi-orientation through the regulation of SAC. AurB also recruits and phosphorylates Kif2C to depolymerize the incorrectly attached kinetochores. It phosphorylates the Centromere Protein A, which is needed for recruitment of additional kinetochore proteins prior chromosome segregation. After SAC has been passed, APC/C are being activated, and mitosis can come to its end. (Lan *et al.*, 2004; Ma *et al.*, 2011; Shimada *et al.*, 2016).

AurB also has a role in chromosome separation, after being recruited to centromeres and the midzone together with other CPC components (being essential part of the abscission checkpoint (also termed the NoCut checkpoint). During cytokinesis, AurB has a role in actin polymerization and myosin activation, both required for the formation of the contractile ring. It also phosphorylates additional substrates to organize the cleavage furrow (Carmena *et al.*, 2009; Gachet *et al.*, 2016; Gruneberg *et al.*, 2004; Surnara *et al.*, 2007; Dal *et al.*, 2006). AurB functions as part of a sensor that responds to unsegregated chromatin in the cleavage plane, thus controlling abscission timing. The presence of chromosome bridges prevents Aurora B inactivation and leads to its localization to a narrow ring at the intercellular canal upon midbody disassembly which stabilizes the

intercellular canal for delayed abscission. Premature inactivation of Aurora B in cells with chromosome bridges leads to furrow regression, due to premature destabilization of the intercellular canal at a stage that is not ready for abscission (Steigemann *et al.*, 2009). In this context, the most important Aurora B phosphorylation target is mitotic kinesin-like protein 1 (Mklp1), which has a role in stabilization of the midbody and anchoring the ingressed furrow during telophase.

## **1. 4. Kinetochore-microtubule interface**

At the basis of kinetochore, a centromeric protein CENP-A binds centromeric DNA, and recruits a complex of kinetochore proteins termed the Constitutive Centromere- Associated Network (CCAN) (McKinley *et al.*, 2016). During mitosis, the CCAN targets other kinetochore proteins facilitating the assembly of the outer kinetochore, with the core outer kinetochore proteins comprising the KMN network (KNL1/Mis12/Ndc80 network). Three different subcomplexes make the KMN network; KNL1 (Kn11-Zwint1), Mis12 (Mis12, Dsn1/Mis13, Nsl1/Mis14 and Nnfl1) and Ndc80C (Hec1/Ndc80, Nuf2, Spc24 and Spc25) (De Wulf *et al.*, 2003; Cheeseman *et al.*, 2004). Phosphorylation of a CCAN member CENP-T promotes direct binding of Mis12C during mitosis (Gascoigne *et al.*, 2013; Nishino *et al.*, 2013; Rago *et al.*, 2015; Sadasivam *et al.*, 2016). The KMN network has a well-established role as an interface between microtubules and kinetochores (Cheeseman *et al.*, 2006; De Wulf *et al.*, 2003; Cheeseman *et al.*, 2004; Alushin *et al.*, 2008).

A prerequisite of accurate chromosome segregation is the generation of end-on kinetochore–microtubule attachments, where the plus-end of microtubule is embedded within the kinetochore. Some kinetochores will initially form lateral associations with microtubules (Barisic, 2014; Kapoor, 2006; Magidson, 2011; Tanaka, 2005) and then expanding their reach by forming a structure called the fibrous corona (Jokelainen, 1967; Magidson *et al.*, 2015; McEwen *et al.*, 1993; Rieder, 1982) consisting of CENP-E (Cooke *et al.*, 1997), CENP-F (Rattner, 1993; Zhu *et al.*, 1995), dynein (Wordeman, 1991), and the Rod–ZW10–Zwilch (RZZ) complex (Basto *et al.*, 2004; Starr *et al.*, 1998). In the absence of microtubules, this crescent-shaped structure surrounds the kinetochore creating a large platform to capture microtubules (Dong *et al.*, 2007; Echeverri, 1996; Hoffman *et al.*, 2001; Thrower, 1996).

In most organisms, each kinetochore binds a bundle of microtubules (McEwen *et al.*, 2001; Wendell *et al.*, 1993), termed the kinetochore fiber (k-fiber). In comparison to other populations of



mitotic microtubules, k-fibers are more stable, and this stability is partially a result of their plus-ends being embedded within kinetochores, cross-linking and bundling of adjacent microtubules. The complex of TACC3, colonic and hepatic tumor overexpressed gene protein (ch-TOG) and clathrin (Gulluni *et al.*, 2017), crosslinks microtubules and has a role in organization of the mitotic spindle. Together, the stabilization and organization of k-fibers contributes to the generation of sufficient force to drive accurate chromosome segregation (Booth *et al.*, 2011; Nixon *et al.*, 2017).

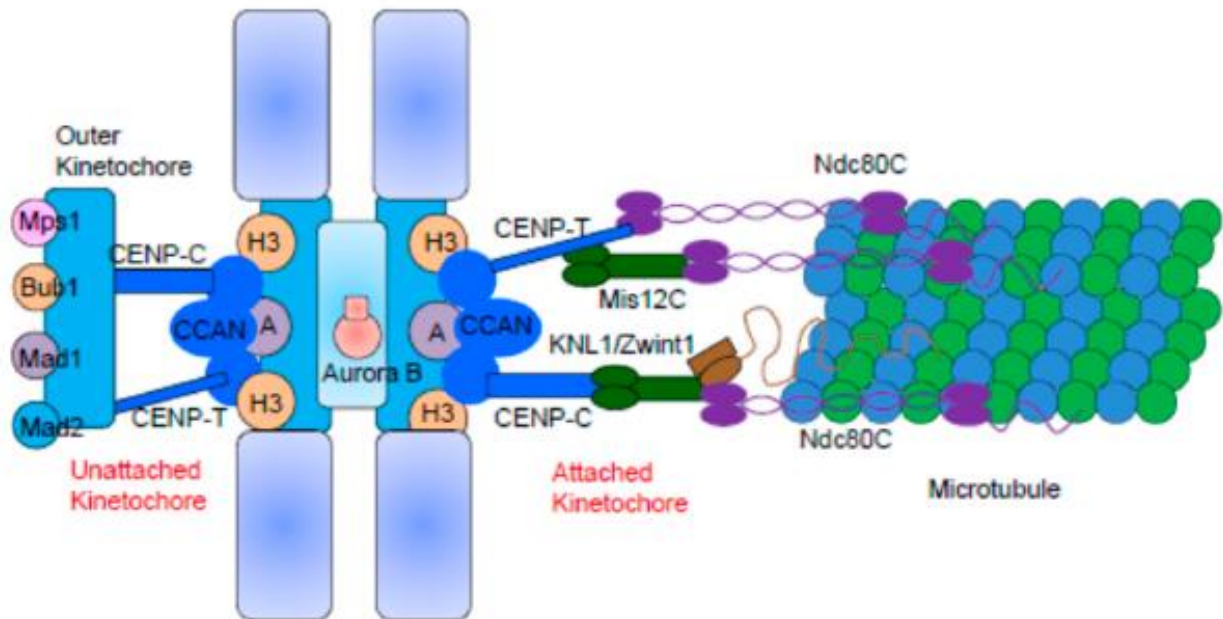


**Figure 2.** Kinetochore-microtubule interface. Cenp-A (A) mediates the recruitment of the constitutive centromere-associated network (CCAN) subcomplexes that form the inner kinetochore layer (dark blue). Members of the CCAN, CENP-C and CENP-T are involved in the recruitment of members of the KMN complex (Knl1-Mis12-Ndc80), a part of the outer kinetochore layer and mediate the interaction between the kinetochore and microtubules (modified from Dou *et al.*, 2019).

## 1.5. Spindle assembly checkpoint (SAC)

As already mentioned, the metaphase to anaphase transition is one of the defining moments of mitosis. When kinetochores achieve end-on attachments and bi-orient, they can successfully be pulled towards opposing poles. Improper attachments are corrected by an error-correction machinery, regulated by Aurora B kinase. AurB localizes at the centromeric DNA and phosphorylates its substrates from the outer kinetochore, resulting in a reduced affinity for microtubules and destabilization of KT-MT attachments (Cheeseman *et al.*, 2006; Deluca *et al.*, 2006; Chan *et al.*, 2012). Moreover, AurB also phosphorylates MCAK, promoting its recruitment to the centromere where it helps correcting improper attachments through its microtubule

depolymerase activity (Andrews *et al.*, 2004; Lan *et al.*, 2004; Kline-Smith *et al.*, 2004). When proper attachments are achieved and chromosomes are bi-oriented, the distance between two sister kinetochores increases, resulting in displacement and physical separation of AurB from its substrates (Liu *et al.*, 2009; Welburn *et al.*, 2010). Kinetochore-microtubule interactions are therefore created and destroyed until all kinetochores are properly attached. This lack of proper attachments is a sign to pause chromosome segregation (onset of anaphase) and links activation of SAC signaling to the repair machinery.

The SAC pauses anaphase by assembling a direct inhibitor (called the mitotic checkpoint complex (MCC)) of APC/C at kinetochores that are not properly attached. APC/C is a ubiquitin ligase which tags inhibitors of mitotic exit for proteasome degradation. The kinetochore interface for contacting microtubules and the main target of the error correction pathway is the KMN. MCC assembly is under control of kinase Mps1, which associates with the NDC80 subcomplex of the KMN (Carmenta *et al.*, 2012).

AurB activity promotes efficient Mps1 recruitment to unattached kinetochores, allowing rapid Mps1 activation at the onset of mitosis (Saurin *et al.*, 2013; Vigneron *et al.*, 2004; Santaguida *et al.*, 2010; Dou *et al.*, 2011). During prophase, Mps1 acts as the initiator of SAC signaling, while AurB prevents its substrates from attaching to microtubules. At the KMN, it orchestrates the recruitment of a network of SAC proteins: Bub1, Bub3, Mad1, Mad2 and Mad3/BubR1. Mad2, Bub3 and BubR1 constitute the MCC, and its assembly depends on Bub1 and Mad1.

Mad2 is a core component of MCC and it forms a constitutive heterotetramer with Mad1, and the complex then recruits more Mad2 to the kinetochore (Lou *et al.*, 2018; Jin *et al.*, 1998; Chen *et al.*, 1999; Sironi *et al.*, 2002; Sironi *et al.*, 2001). Once at the kinetochores, Mad2 is converted from an open (O-Mad2) to a closed (C-Mad2) conformation, which is critical for its checkpoint activity (Luo *et al.*, 2008; Mapelli *et al.*, 2007). In humans and other higher eukaryotes, there is a separate pathway of recruiting Mad2, through the RZZ (Rod-Zwilch-ZW10) complex (Wang *et al.*, 2004; Barisic and Geley *et al.*, 2011; Zhang *et al.*, 2015; Caldas *et al.*, 2015; Silió *et al.*, 2015).

The assembled MCC can prevent Cdc20 from activating APC/C (Uzunova *et al.*, 2012), by displacing Cdc20 away from APC/C, and preventing the formation of a recognition site for ubiquitination (Chao *et al.*, 2012; Herzog *et al.*, 2009). Upon microtubule attachment, the MCC is disassembled, and the free Cdc20 binds to the APC/C complex and activates it, resulting in the

ubiquitination and subsequent proteasome-dependent degradation of its substrates cyclin B and securin (Sudakin *et al.*, 1995; Cohen-Fix *et al.*, 1996).

### 1.5.1. SAC silencing

Removal of Mad1, Mad2, Bub1, BubR1 and outer kinetochore components, such as the RZZ complex from kinetochores is a crucial step in silencing the SAC signal (Jelluma, 2010; Maldonado *et al.*, 2011). This removal is performed by a microtubule motor complex dynein, which strips SAC proteins poleward. Dynein is recruited to kinetochores prior to their microtubule attachments, and the recruitment occurs through the RZZ complex and Spindly, a dynein/dynactin adaptor (Starr, 1998). Dynein's processivity depends on interaction with the dynactin complex, its general adaptor, and different cargo-specific effectors – BICD2 (McKenney *et al.*, 2014; Splinter *et al.*, 2012), Hook1/3 (McKenney *et al.*, 2014; Olenick *et al.*, 2016; Schroeder *et al.*, 2016), FIP3 (McKenney *et al.*, 2014), Spindly (McKenney *et al.*, 2014) and NIN/NINL (Redwine *et al.*, 2017). Lee *et al.* (2018) have shown that a conserved amphipathic helix within the unstructured C-terminal region of dynein Light Intermediate Chain 1 (LIC1) interacts with a series of dynein-dynactin effectors.

Dynein LICs (LIC1 and LIC2), have two domains – an N-terminal GTP-ase like domain that interacts with dynein heavy chain (DHC), and an effector-binding C-terminal domain (Schroeder *et al.*, 2014). It has already been shown that the LIC-effector binding domain interacts with above mentioned effectors. Also, Gama *et al.* have in 2017 identified a coiled-coil segment – termed the CC1-box, that is conserved among BICD2, Spindly, HAP1 and TRAK, and has been implicated in binding LIC1.

With mutating the conserved alanines in the CC1 box to valine (figure 6, alanines marked with asterisks), Gama and colleagues showed that disruption of this motif abrogates binding of both Spindly and BICD2 to LIC1 and that Spindly and BICD2 compete for LIC1 binding. Spindly and BICD2 engage with the C-terminal region of LIC1 through a similar mechanism that involves a conserved region in their N-terminal coiled-coil segment. They also showed that point mutations in the Spindly motif, which is located more C-terminally to the CC1 box in Spindly's coiled-coil region, abrogate Dynein and Dynactin recruitment to kinetochores. Given the similarities between Spindly and BICD2, they presumed that other adaptors also use their CC1 box to interact with the LIC domain. A multiple alignment (figure 6) of different proteins shows that they share a conserved region. Interestingly, this region can also be found in CENP-E and potentially be linked to LIC1 binding.

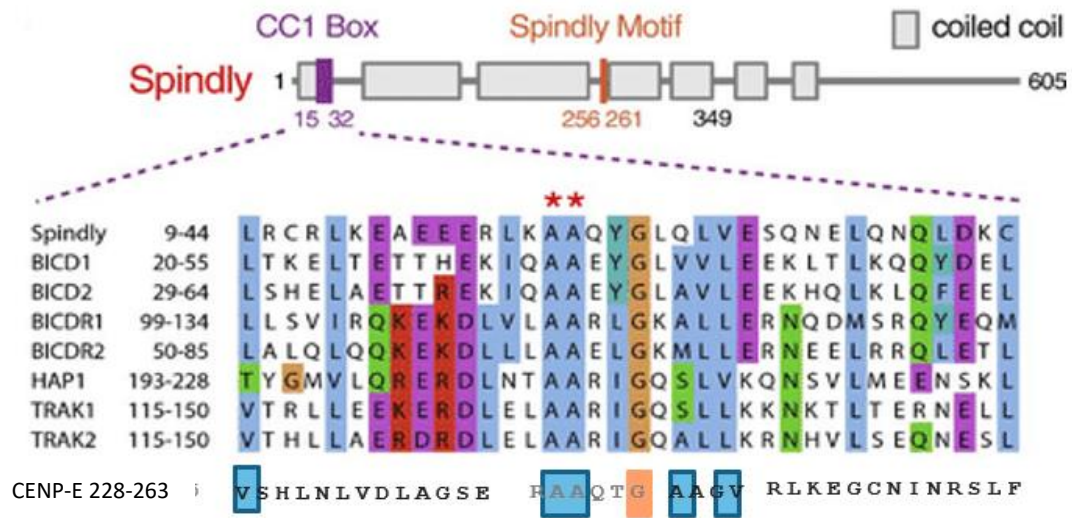


**Figure 3.** Sequence alignment showing a conserved region in the first coiled-coil segment of Spindly and other dynein adaptors (CC1 box) including CENP-E region (modified from Gama *et al.*, 2017).

Kinetochores localization of dynein is also regulated by phosphorylation of its intermediate chain, promoting its binding to ZW10. Moreover, dynein dephosphorylation promotes its interaction with dynactin and acts as a switch to start the stripping of SAC proteins from the kinetochore (Whyte *et al.*, 2008). There have been studies showing the role of CENP-F and NudE/Nde1/Lis1 in dynein recruitment to kinetochores, as depletion of these proteins disrupted dynein's localization (Stehman *et al.*, 2007; Vergnolle and Taylor, 2007). Dynactin has a proposed role in establishing proper microtubule-kinetochore attachments by promoting recruitment of polo-like kinase-1 (Plk1) to kinetochores, which recruits Mad1 for checkpoint signaling (Yeh *et al.*, 2013).

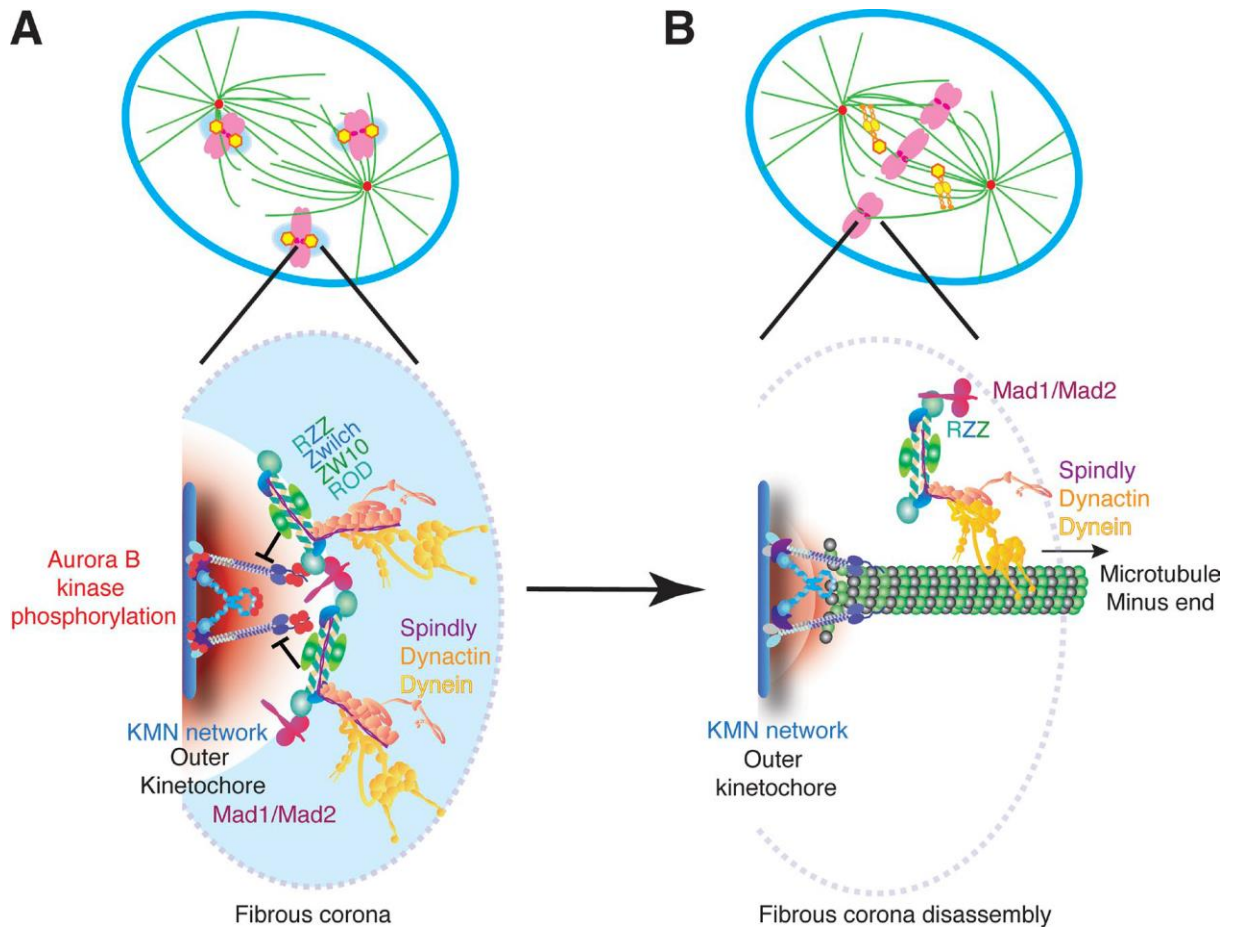


**Figure 4.** SAC silencing by Dynein-mediated stripping. The Spindly–dynein–dynactin complex binds to the RZZ complex and initiates the disassembly of the fibrous corona and removal of checkpoint proteins when correct kinetochore–microtubule attachment is achieved (A) At unattached kinetochores, binding of the KMN network to microtubules is inhibited by the presence of the RZZ complex and by Aurora B kinase phosphorylation. The RZZ complex assembles into the fibrous corona and recruits Mad1/Mad2 and Spindly, which recruit dynein. (B) After stabilization of kinetochore–microtubule attachment, Spindly–dynein–dynactin complex walks to the minus end of microtubules with its spindle checkpoint cargo. Dynein silences the spindle checkpoint by stripping the checkpoint proteins away from the outer kinetochore (modified from McHugh and Welburn, 2017).

## 1.6. CENP-E

CENP-E is a kinesin which accumulates at G2 phase of the cell cycle and is rapidly degraded at the completion of mitosis (Brown, 1994). Kinesin motors are microtubule associated motor proteins, with a role in vesicle and cargo transport, chromosome alignment and microtubule dynamics. CENP-E belongs to a kinesin-7 subfamily and is also known as KIF10 (kinesin family member 10). Its molecular weight is 316 kDa and it is made of 2701 amino acids (Yen, 1991; Wood *et al.*, 1997; Lawrence *et al.*, 2004).

It is comprised of three functional domains; an N-terminal motor domain (amino acids 6-329), a central coiled-coil domain (amino acids 336-2510) and a C-terminal tail domain (2511-2701) (Garcia-Saez *et al.*, 2004). An ATP-dependent microtubule binding domain is located in the motor domain and is essential for CENP-E localization at mitotic spindles. CENP-E generates mechanical forces along microtubules by hydrolysis of ATP in the motor domain, and this motor activity is needed for establishment and maintenance of stable connections between chromosomes and spindle microtubules (Mao *et al.*, 2005; Kumar and Purohit, 2012).

An 11 amino acid neck linker region connects the motor and coiled-coil domains. The coiled-coil domain of CENP-E is essential in homodimerization, which is needed for its activity. It forms a long fibrous extension emanating from the kinetochores, with a role in microtubule searching. In the C-terminal domain, there is another microtubule binding site, which is ATP-independent. Between amino acids 2126 and 2476, there is a kinetochore-binding site, needed for CENP-E localization at the outer layer of kinetochores (Chan *et al.*, 1998; Garcia-Saez *et al.*, 2004; Kim *et al.*, 2008; Gudimchuck *et al.*, 2018).

CENP-E is one of the essential kinetochore components, and its loss leads to high rates of chromosome missegregation (Weaver *et al.*, 2003). CENP-E is directly responsible for stable capture of spindle microtubules by kinetochores (Schaar, 1997), so its loss not only leads to chromosome misalignment, leaving chromosomes unattached and closer to a spindle pole, but also results in reduced number of microtubules bound on bi-oriented chromosomes (McEwen *et al.*, 2001).

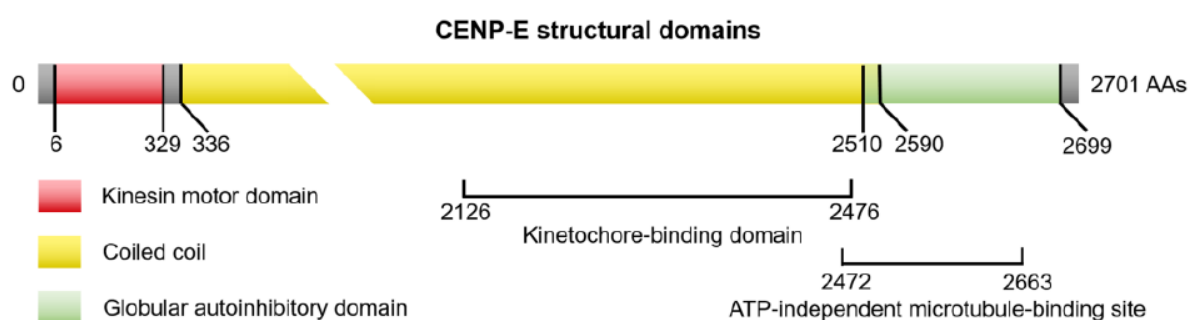


**Figure 5.** Domain structures of human CENP-E protein. The full length of is 2701 amino acids, and consists of a long coiled-coil domain, a motor domain located in the N-terminus and the tail domain located in the C-terminus (modified from Yu *et al.*, 2019).

### 1.6.1. Congression of pole proximal chromosomes

As already mentioned, the way chromosomes bi-orient depends on their position relative to the spindle pole at the moment of nuclear envelope breakdown. Chromosomes that are equidistant from the poles, directly bi-orient and their end-on kinetochore microtubule attachment stabilizes via the KMN (Cheeseman and Desai, 2008). Chromosomes that are located relatively closer to one pole than the other, are less likely to be reached by microtubules emanating from both spindle poles. Kinetochores of these chromosomes first become laterally attached by astral microtubules and are then being transported towards the pole by Dynein. Dynein is a minus-end directed motor protein, exerting the dominant force required for poleward movement of peripheral chromosomes. Initially, this force overcomes the activity of CENP-E and chromokinesins, thus preventing the formation of premature end-on kinetochore microtubule attachments and the ejection of chromosomes towards the cell cortex (Barisic *et al.*, 2014; Rieder and Alexander, 1990; Li *et al.*, 2007; Vorozhko *et al.*, 2008; Yang *et al.*, 2007).

When chromosomes reach the pole, CENP-E is a key player in promoting congression towards the cell equator. It attaches kinetochores, and transports chromosomes towards the plus ends of microtubules. It does so by powering movements of a monooriented chromosome by attachment to and translocation along the kinetochore fiber of another already bi-oriented chromosome (Kapoor *et al.*, 2006). CENP-E dimers can processively walk along microtubules for more than 250 steps in hand-over hand manner without dissociating (Rosenfeld *et al.*, 2009). After chromosomes are congressed and bi-oriented, CENP-E enhances their binding to plus ends of microtubules. Once at microtubule ends, it switches its role from a lateral transporter to a microtubule tip tracker and has a role in the formation of stable microtubule end-on attachments (Gudimchuck *et al.*, 2013).

### 1.6.2. Regulation

Human CENP-E has multiple consensus sites (T422, S454, S611, S1211, T1267, S2601, S2613 and S2616) which can be phosphorylated during cell division. The T422 site has been identified as the crucial phosphorylation site for kinetochore-microtubule attachment (Kim *et al.*, 2010; Nousiainen *et al.*, 2006). In 2010., Kim et al. showed that this particular site is being phosphorylated by Aurora kinases A and B. The group has also shown that PP1 interacts with the same site and dephosphorylates the T422 residue. Phosphorylation of CENP-E by Aurora kinases inhibits the PP1-CENP-E interactions and reduces the affinity of CENP-E to bind microtubules.

PP1 is also needed for stable microtubule capture of chromosomes through dephosphorylation of other kinetochore proteins (such as Ndc80 and KNL1).

Kim *et al.* have proposed a model, in which this Aurora kinase/PP1 phosphorylation switch regulates polar chromosome congression through T422 phosphorylation, and also regulates chromosome bi-orientation through CENP-E recruitment of PP1 to the outer kinetochore. When at the poles, phosphorylation by Aurora A is required for CENP-E function and was proposed to reduce its affinity for individual microtubules, consequently favoring its interaction with bundled kinetochore fibers (Kim *et al.*, 2010). However, it has been shown that CENP-E can mediate chromosome congression even in the absence of k-fibers (Cai *et al.*, 2009; Iemura and Tanaka, 2015) which raised a question whether this phosphorylation is the only factor regulating the switch between Dynein and CENP-E once chromosomes reach the spindle pole.

Further clarification on the mechanism of polar chromosome congression came in 2015, when Barisic *et al.* proposed tubulin code as the navigation system for CENP-E and Dynein. It was beforehand shown that some tubulin post-translational modifications influence motor activities of some kinesins and dynein (Hammond *et al.*, 2010; Kaul *et al.*, 2014; Sirajuddin *et al.*, 2014). In the model, the antipodal preferences of CENP-E and Dynein for detyrosinated and tyrosinated microtubules, respectively, control the directionality of the chromosome movements during cell division.

Dynein's preference for tyrosinated microtubules (astral microtubules, emanating from the spindle pole towards the cell cortex) is the reason for its dominance over CENP-E during initial poleward movement of peripheral chromosomes. When at the poles, CENP-E becomes the dominant force, transporting the chromosomes along detyrosinated pre-stabilized spindle microtubules. Nevertheless, phosphorylation of CENP-E by Aurora A could have a role in CENP-E activation and prevention of premature end-on kinetochore-microtubule attachments (Barisic *et al.*, 2015).



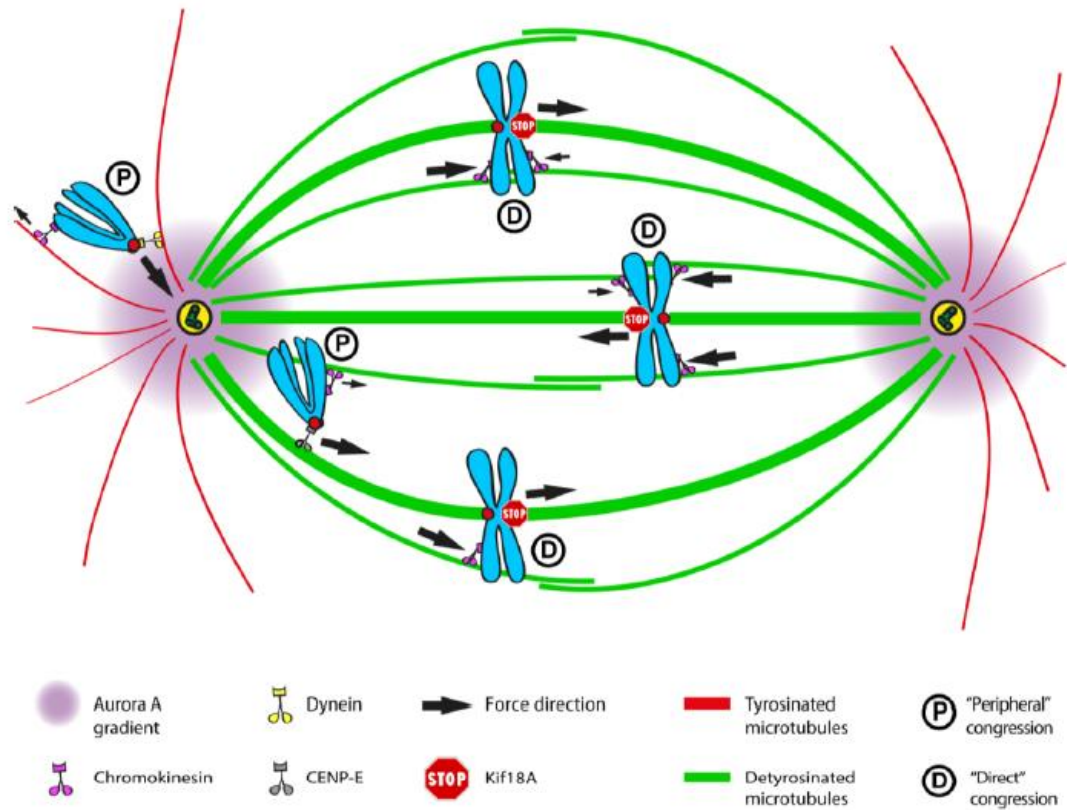


**Figure 6.** Integrated model of chromosome congression in human cells. Dynein/Dynactin have a preference for tyrosinated astral microtubules. By bringing chromosomes to the vicinity of the spindle pole-localized Aurora A kinase, Dynein/Dynactin prevents premature stabilization of erroneous end-on attachments and contributes to the local activation of CENP-E. At the pole, CENP-E interacts with detyrosinated microtubules, becoming dominant over Dynein to move chromosomes towards the equator. The levels of microtubule (de)tyrosination provide the directional bias for CENP-E-mediated chromosome transport and regulate the Dynein/CENP-E activity switch that facilitates chromosome congression. Kif18A is shown to restrict k-fiber length, contributing to a directional switch and regulating chromosome oscillations after bi-orientation (modified from Maiato *et al.*, 2017).

## **1.7. Aims of the thesis**

This set of experiments will work on clarifying the role of CENP-E phosphorylation by Aurora kinases A and B and its impact on chromosome movements and potential CENP-E-Dynein interaction. The hypothesis is, that the phosphorylation of T422 by Aurora kinases has a role in preventing premature dynein-dependent stripping of CENP-E from kinetochores, therefore facilitating accurate cell division. In order to do so, specific aims have to be met:

- 1) To investigate whether CENP-E T422 phosphorylation by Aurora kinases affects chromosome congression and segregation by regulating dynein-mediated stripping of CENP-E from kinetochores.
- 2) To test if CENP-E directly interacts with dynein.
- 3) To identify the potential sites on CENP-E that are required for interaction with dynein.
- 4) To test whether CENP-E T422 phosphorylation by Aurora kinases facilitates bipolar mitotic spindle formation.

## **2. Materials and methods**

### **2.1. Cell culture and transfections**

Human bone osteosarcoma epithelial cells (U2OS) and human embryonic kidney cells (HEK 293T) were cultured in Dulbecco's Modified Eagle Medium (DMEM, Thermo Fisher Scientific, USA) supplemented with 10% fetal bovine serum (FBS, Thermo Fisher Scientific, USA) and 5% Penicillin-Streptomycin (10,000 U/mL, Thermo Fisher Scientific, USA) at 37 °C with 5% of CO<sub>2</sub> in Hera cell 150 (Thermo Fisher Scientific, USA) incubator.

For knockdown experiments, U2OS cells were transfected for 48 h with the indicated siRNAs (Sigma-Aldrich, USA; see table 1 for the sequences and concentrations used) using Lipofectamine RNAi MAX Reagent (Thermo Fisher Scientific, USA). Right volumes of siRNAs and 5 µl of lipofectamine were mixed with 150 µl of Opti-MEM® I Reduced Serum Medium (Thermo Fisher Scientific, USA), respectively. After 5 minutes of incubation at room temperature, the diluted siRNA and diluted Lipofectamine RNAiMAX Reagent were mixed (1:1 ratio). After 20 minutes of incubation at room temperature, the siRNA-lipid complex was added to cells growing in 6-well plates (50% confluent).

### **2.2. Generation of new cell line**

#### **2.2.1. Verification of plasmids**

Plasmids used for cloning were digested with FastDigest EcoRI (Thermo Fisher Scientific, USA). The digestion mix consisted of 1 µL enzyme (1U), 1 µL 10 x FastDigest Green buffer (Thermo Fisher Scientific, USA), 100 ng of plasmid solution and autoclaved water till 10 µL total volume. The digestion reaction was performed for 30 minutes at 37°C in AccuBlock Digital dry Bath (Labnet Inc., USA). Patterns of digestion were analyzed after horizontal gel electrophoresis (1% UltraPure™ Agarose (Thermo Fisher Scientific, USA), 50 ml 1x TAE buffer (TAE buffer 50X UltraPure Grade (VWR) diluted with distilled water), 1:10000x SyBr Safe DNA Gel Stain (Thermo Fisher Scientific, USA). Molecular marker used was GeneRuler 1 kb DNA Ladder (Thermo Fisher Scientific, USA). Electrophoresis was conducted in Power Pac 200 system (Bio-Rad, USA), for 10 minutes at 90V then 20 minutes at 100V in TAE 1x buffer. Digestion patterns were visualized in ChemiDoc XRS+ (Bio-Rad, USA) transilluminator, with exposition time according to DNA amount.

### 2.2.2. Restriction-ligation cloning

5 µg of plasmids pBluescript-CENP-E 422A/CC1 (contains CENP-E cDNA with three mutated residues – T422A, A242V and A243V) and pENTR4-GFP (an entry plasmid for Gateway cloning, with a GFP tag) was digested with mix of 1.5U Fast Digest KpnI (Thermo Fisher Scientific, USA) and 1.5U FastDigest BamHI (Thermo Fisher Scientific, USA), 1 µL 10 x FastDigest Green buffer (Thermo Fisher Scientific, USA) and autoclaved water till 10 µL total volume for 2 hours at 37°C. To purify the digested fragments horizontal electrophoresis was performed (0.8% UltraPure™ Agarose (Thermo Fisher Scientific, USA), in 50 ml 1x TAE buffer (TAE buffer 50X UltraPure Grade (VWR) diluted with distilled water), 1:10000x SyBr Safe DNA Gel Stain (Thermo Fisher Scientific, USA). Molecular marker used was GeneRuler 1 kb DNA Ladder (Thermo Fisher Scientific, USA). Electrophoresis was conducted in Power Pac 200 system (Bio-Rad, USA), for 10 minutes at 90V then 20 minutes at 100V in TAE 1x buffer. Digestion patterns were visualized in ChemiDoc XRS+ (Bio-Rad, USA) transilluminator, with exposition time according to DNA amount. The right band was cut out of gel and purified from gel with QIAquick Gel Extraction Kit (Qiagen, Germany) according to manufacturer's instructions.

For ligation, 40 ng of vector (pENTR4-GFP cut) and 108 ng of insert (CENP-E insert from pBluescript-CENP-E 422A/CC1) were used (1:1 ratio). The ligation reaction was performed at room temperature for 2h, with 1 µl T4 DNA Ligase, LC (1 U/µL, Thermo Fisher Scientific, USA), 1 µl T4 DNA Ligase Buffer 10X (Thermo Fisher Scientific, USA), proper volumes of vector and insert solutions and autoclaved water till 10 µl volume. The ligation mix was used to transform 50 µl *E.coli* One Shot® TOP10 (Thermo Fisher Scientific, USA) . The bacteria were left 20 minutes on ice, heat-shocked for 30 seconds on 42°C and then left for 2 minutes on ice. 300 µl of Super Optimal Broth with Catabolite Repression (SOC) liquid medium was used for the recovery of competent *E. coli*, left shaking for 2h at 37°C. Bacteria was then plated on Luria-Bertani (LB) media supplemented with 1:1000 Kanamycin (Kan) (Thermo Fisher Scientific, USA) and left growing at 37°C overnight. 5 colonies were selected and grown overnight on 37°C, shaking in Falcon tubes with 2ml LB media and 1:1000 Kan. To purify plasmids, miniprep of each colony was done, with NucleoSpin Plasmid (Macherey-Nagel, Germany) according to the manufacturer's instructions. To verify the plasmid, an EcoRI digestion and 1% agarose gel electrophoresis were performed, same protocol as for plasmids mentioned earlier.

### 2.2.3. Gateway cloning

150 ng of plasmid obtained in the step before, pENTRY-GFP-CENP-E 422A/LIC (a plasmid containing CENP-E cDNA with target mutations, an N-terminal tag and attL1 and attL2 sites for Gateway cloning), was put in a LR reaction with 150ng of pLenti CMV/TO (containing a CMV promoter and tet-operator, for inducible expression after the addition of doxycycline), 1  $\mu$ L LR clonase (Invitrogen, Thermo Fisher Scientific, USA), 2  $\mu$ L of TE buffer (Macherey-Nagel, Germany), and left for 1h on room temperature. 1  $\mu$ L of Proteinase K was added to the mix and incubated for 10 minutes at 37°C. 50  $\mu$ L of One Shot™ Stbl3™ Chemically Competent *E. coli* was transformed with the mix and recovered by the same protocol as in the step earlier. Bacteria was then plated on Luria-Bertani (LB) media supplemented with 1:1000 Ampicilin (Amp) and left growing at 37°C overnight. 5 colonies were selected and grown overnight on 37°C, shaking in Falcon tubes with 2ml LB media and 1:1000 Amp. To purify plasmids, miniprep of each colony was done, with NucleoSpin Plasmid (Macherey-Nagel, Germany) according to the manufacturer's instructions. To verify the plasmid, an EcoRI digestion and 1% agarose gel electrophoresis were performed, same as for plasmids mentioned earlier.

### 2.2.4. Lentiviral infection

Lentiviruses were produced in a 6-well plate by co-transfecting HEK 293T cells with 4  $\mu$ g of the pLenti-GFP-CENP-E 422A/LIC plasmid containing CENP-E cDNA, 1  $\mu$ g of the lentiviral packaging plasmid (psPAX2) and 1  $\mu$ g of the lentiviral envelope plasmid (pVSV-G), using Metafectene (Biontex Laboratories GmbH, Germany) according to manufacturer's instructions. Two days after transfection, the supernatant from HEK293T cells containing the viruses was collected, filtered and added to U2OS cells. A second round of infection was performed the day after, using the supernatant from HEK293T cells three days after transfection with lentiviral plasmids. Two days after the second infection, U2OS cells were selected with 5  $\mu$ g/ml puromycin (InvivoGen, USA). The cells were trypsinized (1ml of Trypsin-EDTA (0.5%), no phenol red, Thermo Fisher Scientific, USA), counted in a Burker-Turk chamber, diluted and seeded in a 96-well plate. 100  $\mu$ L of DMEM was added to each well, and the cells were left growing.

### 2.3. Drug treatments

To induce the expression of CENP-E under CMV-TO promoter, 1 µg/ml doxycycline (doxycycline hyclate, Sigma-Aldrich, USA) was added 16 hours before filming, fixing or harvesting cells. To inhibit CENP-E, 20 nM GSK-923295 (MedChemexpress, USA) was added to the media and cells were fixed after 3 h. For Aurora A kinase inhibition 250 nM MLN-8054 (Selleck Chemicals, USA) and for Aurora B kinase inhibition 4 µM ZM447439 (AstraZeneca, UK) were added respectively to the cells 2 h before fixation. To deplete microtubules 3.3 µM nocodazole (Sigma-Aldrich, USA) was used 3 h before fixation. A 0.5 µM or 5 µM *S*-trityl-L-cysteine (STLC; Sigma-Aldrich, USA) concentration was used in the cell culture media 3 h before fixation to induce monopolar spindles by inhibiting Eg5.

### 2.4. Western blot

Cells were collected after the treatments and lysed in 150 mM NaCl, 50 mM Tris-HCl pH 8, 5 mM EDTA pH 8, 0.5% NP-40, 1x EDTA-free protease inhibitors (Sigma-Aldrich, USA), 1x phosphatase inhibitor cocktail (Sigma-Aldrich, USA), 1 mM PMSF (Santa Cruz Biotechnology, USA). Cells were then subjected to two cycles of liquid-nitrogen freezing and thawing and centrifuged at 14000 rpm for 15 minutes at 4°C. Subsequently, the supernatants were collected, the amount of protein was quantified and the appropriate amount of Laemmli buffer was added (Bio-Rad, USA, final concentration 0,25x) before boiling the samples for 5 minutes at 95°C. The protein lysates were then applied to SDS-PAGE at constant voltage (100 V/gel) for approximately one and a half hours, and transferred to nitrocellulose membranes (iBlot system – 20V 1 minute, 23V 4 minutes, 25V 4 minutes, Invitrogen, USA) followed by analysis with the indicated antibodies (see table 2). Incubation with primary antibodies was done in 5 % non-fat milk (Powdered Milk, Roth, USA) overnight at 4°C, whereas secondary antibodies were incubated in 0.25 % non-fat milk ((Powdered Milk, Roth, USA)) for 1 h at room temperature, shaking. Detection was performed by chemiluminescence, using Clarity Western ECL substrate (Bio-Rad, USA) in a ChemiDoc MP imaging system (Bio-Rad, USA).

### 2.5. Immunofluorescence

U2OS cells were grown on 12 mm diameter round glass coverslips (VWR) and fixed using ice-cold methanol for 4 minutes at -20°C. Cells were then washed with 1x phosphate-buffered saline (PBS) before the immunostaining with antibodies (see table 2). Primary and secondary antibodies were diluted in IF stain (1x PBS, 5% FBS, 0.5% Triton (Sigma-Aldrich, USA)), and the

incubations were performed at room temperature in a humidified chamber for one hour and 30 minutes, respectively. DNA was counterstained with DAPI (Sigma-Aldrich, USA, final concentration 0.1 µg/ml). Coverslips were mounted on glass slides using Fluoromount-G mounting media (Southern Biotech, USA). Images were acquired in a Zeiss AxioObserver Z1 wide-field microscope (63x Plan-Apochromatic oil differential interference contrast objective lens, 1.4 NA) equipped with a CoolSNAP HQ2 CCD camera using the Metamorph software or Plan-Apochromat 63x/1.4NA with differential interference contrast oil objective mounted on an inverted Zeiss Axio Observer Z1 microscope (Marianas Imaging Workstation from Intelligent Imaging and Innovations Inc. (3i), Denver, CO, USA), equipped with a CSU-X1 spinning-disk confocal head (Yokogawa Corporation of America) and three laser lines (488 nm, 561 nm and 640 nm) and an iXon Ultra 888 EM-CCD camera (Andor Technology, UK). Maximum projections of the representative images were processed using Image J. For the quantification of fluorescence intensities at centrosomes: ImageJ: M -> measure intensity area, min&max gray value (intensity, integrated density, mean grey value). Fluorescence intensities of the protein of interest were normalized against median signal at centrosomes of the control and were plotted using GraphPad Prism 8.1.1.

## **2.6. Live-cell imaging**

U2OS CENP-E inducible cells were cultured in 35 mm glass-bottomed dishes (14 mm, No. 1.5, MatTek Corporation, USA) with DMEM media supplemented with 10% FBS and 5% pen-strep. 16 h after seeding, cells were infected with Ad-H2B-RFP. After 6h, the cells were washed with DMEM 6x. New 2ml DMEM was added, induced with 1 µg/ml doxycycline ((doxycycline hyclate, Sigma-Aldrich, USA), verapamil (Spirochrome, USA, final concentration 50 nM) and siRTubulin dye (Spirochrome, USA, final concentration of 100 nM) 16 h before imaging. Time-lapse imaging was performed in a heated chamber (37°C, 5% CO<sub>2</sub>) using a Plan-Apochromat 63x/1.4NA with differential interference contrast oil objective mounted on an inverted Zeiss Axio Observer Z1 microscope (Marianas Imaging Workstation from Intelligent Imaging and Innovations Inc. (3i), Denver, CO, USA), equipped with a CSU-X1 spinning-disk confocal head (Yokogawa Corporation of America) and three laser lines (488 nm, 561 nm and 640 nm). Images were detected using an iXon Ultra 888 EM-CCD camera (Andor Technology, UK). Fifteen 1 µm-separated z-planes covering the entire volume of the cell were collected every 3 minutes. The maximum projections of each movie were exported and analyzed in ImageJ.

## 2.7. Immunoprecipitation

U2OS (expressing CENP-E) cells were lysed in a buffer containing 20 mM Hepes, 10mM K, 1 mM MgCl<sub>2</sub>, Cl, 1mM EDTA, 1mM EGTA, 1x EDTA-free protease inhibitors (Sigma-Aldrich, USA), 1x phosphatase inhibitor cocktail (Sigma-Aldrich, USA) and 1 mM PMSF (Santa Cruz Biotechnology, USA). Protein lysates were then subjected to two liquid nitrogen freezing-thawing cycles and centrifuged at 14000 rpm for 15 minutes at 4°C. Supernatants were collected and the protein concentration was measured. Dynabeads protein G (Thermo Fisher Scientific, USA) were coupled to the antibody by incubation for 1 h at room temperature, shaking with 1 or 1.5 µg of Anti -GFP Goat IgG (Rockland, USA) or Donkey Anti-Goat IgG H&L (Abcam, USA). 1 mg or more of protein was incubated with the antibody-coupled beads for 2 h at 4°C, washed with wash buffer: 50mM tris HCL, 150mM NaCl, 2mM EDTA, 0.2 mM EGTA, 1mM DTT (Sigma-Aldrich, USA), and eluted from the beads by resuspension with 1x Laemmli buffer (Bio-Rad, USA) followed by 5 minutes boiling at 95°C. The eluted proteins were analyzed by SDS-PAGE as already described.

## 2.8. Statistical analysis

Statistical analyses were performed in GraphPad Prism 8.1.1. Data is presented as mean ± standard deviation. Statistically significant differences were determined by Student's unpaired and two-tailed t-test. Statistical significances with a *p* value <0.0001 are represented by four asterisks (\*\*\*\*); *p* value <0.001 is represented by three asterisks (\*\*\*); *p* value <0.01 is represented by two asterisks (\*\*); *p* value < 0.05 is represented by a single asterisk (\*).

**Table 1. Sequences of siRNAs**

siRNA	Sequence (5' - 3')	Concentration/nM
Non-targeting siRNA	UGGUUUACAUGUCGACUAA	30
CENP-E 3'UTR siRNA	CCACUAGAGUUGAAAGUA	30
DHC siRNA	GGCCAAGGAGGCGCUGGAATT	30
Spindly siRNA	GAAAGGGUCUCAACUGAA	30
NuMA siRNA	AAGGGCGCAAACAGAGCACUA	30



P150 UTR siRNA	GACUUCACCCCUUGAUUAAUU	30
----------------	-----------------------	----

**Table 2.** List of used primary antibodies

<b>PRIMARY ANTIBODIES</b>				
<b>Antibody</b>	<b>WB dilution</b>	<b>IF dilution</b>	<b>Source</b>	<b>Figures</b>
Mouse monoclonal anti- CENPE	1:1000		Abcam(ab5093)	16, 18, 41
Anti-Vinculin antibody, Mouse monoclonal	1:1000		Sigma-Aldrich SAB4200729-100UL	16
Monoclonal Anti- $\alpha$ -Tubulin antibody produced in mouse		1:1000	Sigma-Aldrich (T9026)	17
Anti-alpha Tubulin antibody monoclonal Mouse		1:1000	Abcam (ab7750)	18, 19, 21, 29, 41,
Rabbit polyclonal Anti-CENPE antibody		1:500	Santa Cruz Biotechnology (ab133583)	17, 18, 34
Anti -GFP Goat IgG		1:500	Rockland (600-101-215)	19, 21, 22, 23, 24, 25, 26
Anti-alpha Tubulin antibody Rabbit	1:2000	1:1000	Abcam (ab15246)	22, 23, 24, 25
Purified Mouse Anti-p150 [Glued] Clone 1/p150Glued (RUO)	1:1000	1:1000	BD Trans.Lab (610474)	22, 23, 24, 25, 34

Mouse Anti-Cytoplasmic Dynein Intermediate chain antibody	1:1000		Abcam (ab23905)	34
---	--------	--	-----------------	----

**Table 3.** List of used secondary antibodies

<b>SECONDARY ANTIBODIES</b>				
<b>Antibody</b>	<b>WB dilution</b>	<b>IF dilution</b>	<b>Source</b>	<b>Figures</b>
Peroxidase AffiniPure Rabbit anti-mouse IgG (H+L)	1:10000		Jackson ImmunoResearch (115-035-003)	16
Alexa Fluor 647 Goat anti-mouse IgG		1:1000	Thermo Fisher Scientific (A21236)	17, 18, 41
Alexa Fluor 488 Goat anti-rabbit IgG		1:1000	Thermo Fisher Scientific (A11034)	17, 18, 41
Alexa Fluor 488 Donkey anti-goat IgG		1:1000	Thermo Fisher Scientific (A11055)	19, 21, 22, 23, 24, 25, 26
Donkey anti Mouse IgG (H+L) Secondary Antibody, Alexa Fluor 647		1:1000	Thermo Fisher Scientific (A31571)	119, 21
Peroxidase AffiniPure Goat anti-mouse IgG (H+L)	1:10000		Jackson ImmunoResearch (115-035-003)	34
Peroxidase AffiniPure Goat anti-rabbit IgG (H+L)	1:10000		Jackson ImmunoResearch (111-035-003)	16, 34
Donkey anti-Mouse IgG (H+L) Highly Cross-Adsorbed Secondary Antibody, Alexa Fluor 568		1:1000	Thermo Fisher Scientific (A10037)	22, 23, 24, 25, 26

Donkey anti-Rabbit IgG (H+L) Highly Cross-Adsorbed Secondary Antibody, Alexa Fluor 647		1:1000	Thermo Fisher Scientific (A31573)	22, 23, 24, 25
--	--	--------	-----------------------------------	----------------

### 3. Results

In order to investigate the effect of different CENP-E mutants on the functionality of CENP-E and its impact on chromosome transport, doxycycline-inducible stable cell lines were generated. GFP-CENP-E-WT cell line, with a full length CENP-E with an N-terminal GFP tag insert, and puromycin resistance. The second cell line, GFP-CENP-E-T422A, with a CENP-E insert with a threonine residue on position 422 mutated to alanine- a phosphonull mutant which Aurora kinases can not phosphorylate, as well as an N-terminal GFP tag and puromycin resistance. A GFP-CENP-E-CC1 mutant line, with a CENP-E insert with 2 alanine residues on positions 242 and 243 mutated to valines, an N-terminal GFP tag and puromycin resistance (kind gifts from Eibes S., postdoc).

#### 3.1. Establishing a stable cell line with CC1-box and T422A mutations

To look into the role of T422 phosphorylation in CENP-E and dynein interaction, a cell line with stable insert of CENP-E cDNA with T422A mutation and A242V, A243V mutations was established. A pBLUESCRIPT plasmid (figure 7) containing CENP-E cDNA with both necessary mutations (figure 8) (9 clones, kind gift from Susana Eibes, postdoc) was first cut by EcoRI to check the sequence. The plasmid contains Kpn and BamHI restriction sites surrounding the cDNA which are needed to produce sticky ends for restriction-ligation cloning with another plasmid, pENTR4-GFP, which contains a GFP tag and Kpn and BamHI restriction sites (figure 9). Both plasmids were cut with the restriction enzymes, and the segments isolated by gel electrophoresis and purified from the gel (figure 10). For CENP-E, the upper band contains cDNA and was isolated. The T4 DNA ligase ligation was then performed to obtain a pENTR4-GFP-CENP-E plasmid with CENP-E cDNA, an N-terminal GFP tag, Kanamycin resistance and attL1 and attL2 sites for Gateway cloning (figure 11). The plasmid was then transfected to *E.coli* TOP10 strain to multiply the plasmid, and the bacteria that accepted the proper plasmid were selected by kanamycin. After miniprep, the plasmid was cut with EcoRI to check the sequence. A clone (clone 4, figure 12) with proper restriction pattern was chosen for further experiments.

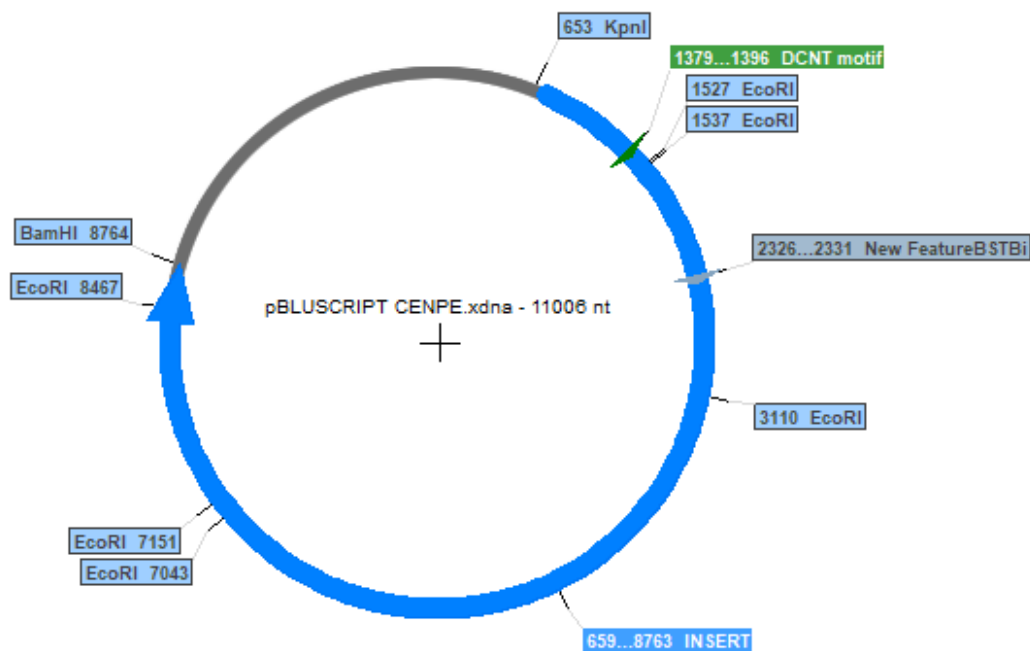


**Figure 7.** Map of pBLUESCRIPT plasmid. Plasmid carrying a cDNA of CENP-E (659-8763) with new mutation (1379-1396). Plasmid map drawn in Serial Cloner V2.5.

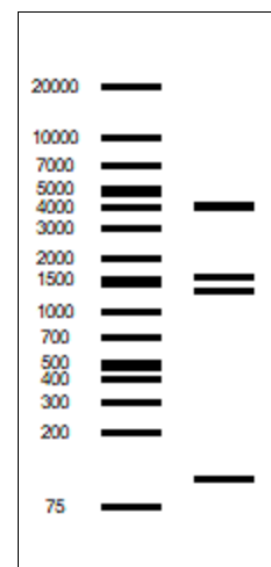
**A)**

<Serial Cloner V2.5> -- <12. aug 2019 15:48>

Restriction analysis of pBLUESCRIPT CENPE.xdna [Circular]  
Incubated with EcoRI

6 fragments generated.

1:	4.066 bp	-	From EcoRI[8467]	To	EcoRI[1527]
2:	3.933 bp	-	From EcoRI[3110]	To	EcoRI[7043]
3:	1.573 bp	-	From EcoRI[1537]	To	EcoRI[3110]
4:	1.316 bp	-	From EcoRI[7151]	To	EcoRI[8467]
5:	108 bp	-	From EcoRI[7043]	To	EcoRI[7151]
6:	10 bp	-	From EcoRI[1527]	To	EcoRI[1537]



**B)**

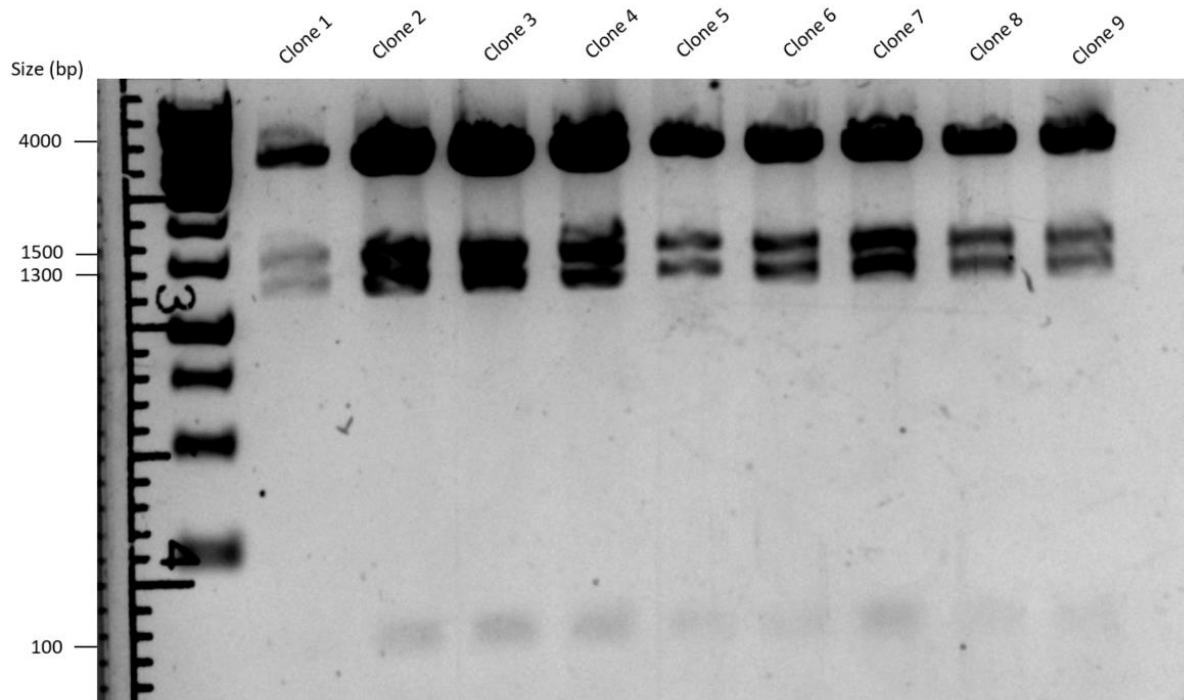


**Figure 8.** Restriction analysis of pBLUESCRIPT with EcoRI. A) Pattern of virtual digestion of plasmid DNA with EcoRI in Serial Cloner V2.5. B) Restriction digestion of plasmid DNA from 9 clones with EcoRI, 1% agarose gel electrophoresis. Clone 2 was picked to continue experiments. Bp denotes the molecular standard Gene Ruler 1kb DNA Ladder (Thermo Fisher Scientific).

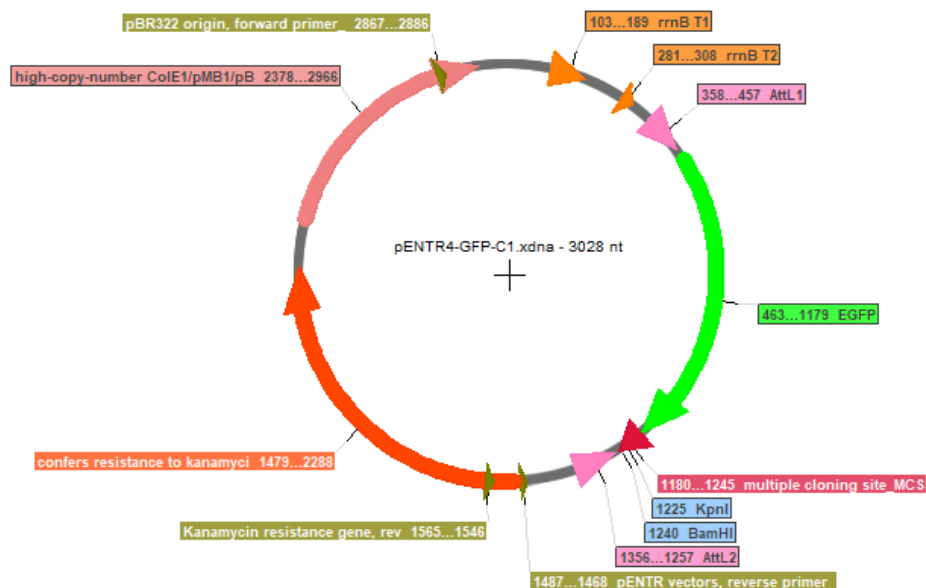


**Figure 9.** Map of pENTR4-GFP plasmid. Plasmid carrying GFP cDNA (463-1179), Kanamycin resistance genes (1479-2288). Map drawn in Serial Cloner V2.5.

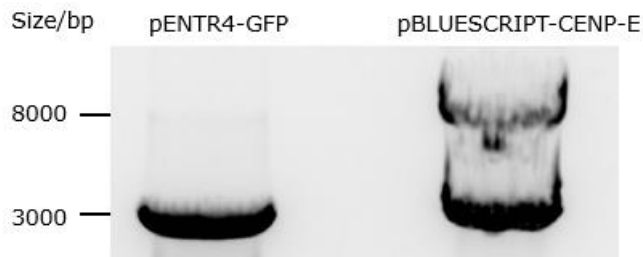


**Figure 10.** pENTR4-GFP and pBLUESCRIPT-CENP-E plasmid DNA cut with Kpn and BamHI. pBLUESCRIPT-CENP-E upper band (8000 bp) contains CENP-E cDNA. 0,8% agarose gel electrophoresis. Bp denotes the molecular standard Gene Ruler 1kb DNA Ladder (Thermo Fisher Scientific).

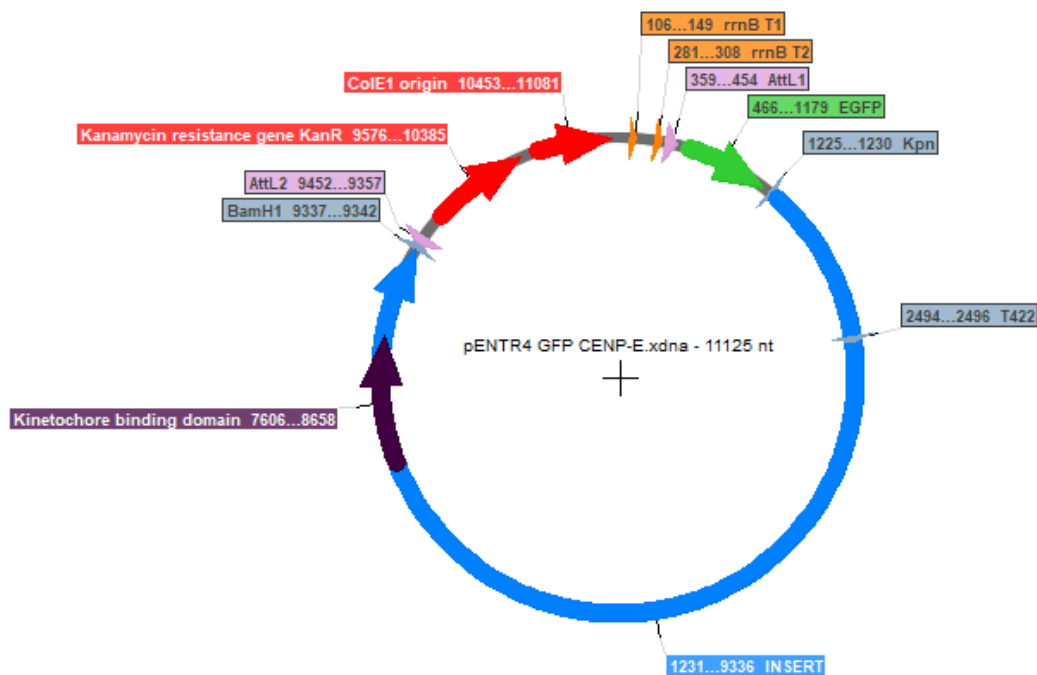


**Figure 11.** Map of pENTR4-GFP CENP-E plasmid. Plasmid carrying CENP-E cDNA (1231-9336), GFP (466-1179), AttL1 (358-454) and AttL2 (9452-9357) sites. Map drawn in Serial Cloner V2.5.

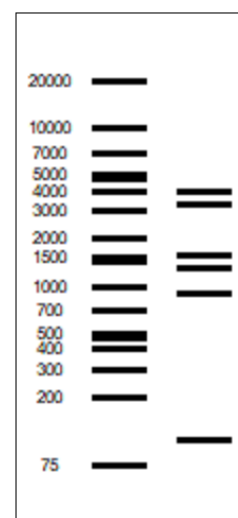
**A)**

<Serial Cloner V2.5> -- <12. aug 2019 15:51>

Restriction analysis of pENTR4 GFP CENP-E.xdna [Circular]  
Incubated with EcoRI

7 fragments generated.

1:	3.933 bp	-	From EcoRI[3682]	To	EcoRI[7615]
2:	3.295 bp	-	From EcoRI[9039]	To	EcoRI[1209]
3:	1.573 bp	-	From EcoRI[2109]	To	EcoRI[3682]
4:	1.316 bp	-	From EcoRI[7723]	To	EcoRI[9039]
5:	890 bp	-	From EcoRI[1209]	To	EcoRI[2099]
6:	108 bp	-	From EcoRI[7615]	To	EcoRI[7723]
7:	10 bp	-	From EcoRI[2099]	To	EcoRI[2109]



**B)**

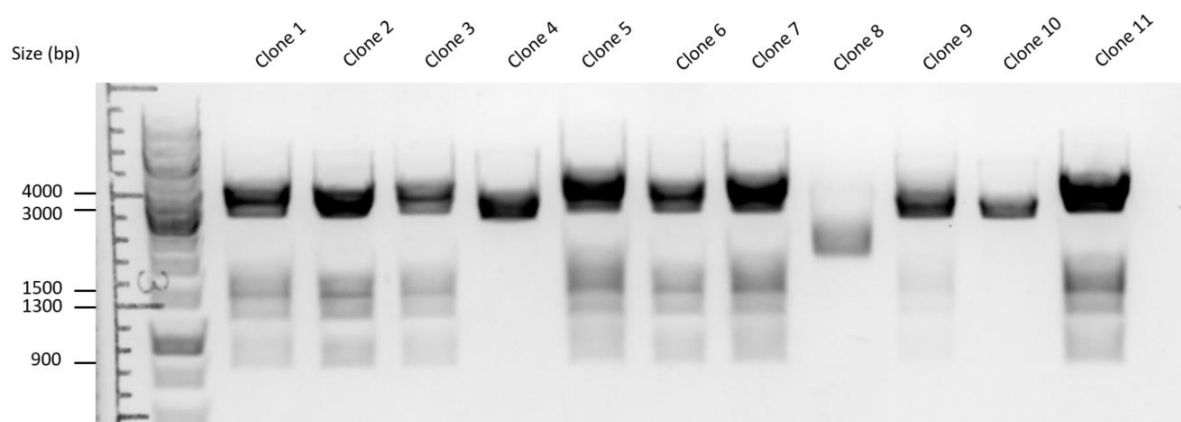


**Figure 12.** Restriction analysis of pENTR4-GFP CENP-E plasmid with EcoRI. A) Pattern of virtual digestion of plasmid DNA with EcoRI in Serial Cloner V2.5. B) Restriction digestion of plasmid DNA from 11 clones with EcoRI, 1% agarose gel electrophoresis. Clone 1 was picked to continue experiments. Bp denotes the molecular standard Gene Ruler 1kb DNA Ladder (Thermo Fisher Scientific).

In Gateway cloning, pLenti CMV-TO Puro destination vector was used, which contains AttR1 and AttR2 sites, puromycin resistance, ampicillin resistance, CMV promotor and enhancer and tet operator (figure 13). The plasmid was cut with EcoRI to check the sequence. After an LR reaction with pENTR4 GFP CENP-E, the mix was transfected to E. coli STABL3 strain, and the



bacteria were selected with ampicillin (1:1000). A miniprep was done for 4 colonies. pLenti CENP-E plasmid was obtained (figure 14, 15), with GFP-CENP-E cDNA, puromycin resistance, ampicillin resistance, CMV promotor and enhancer and tet-operator. Clone 4 was selected for infection.

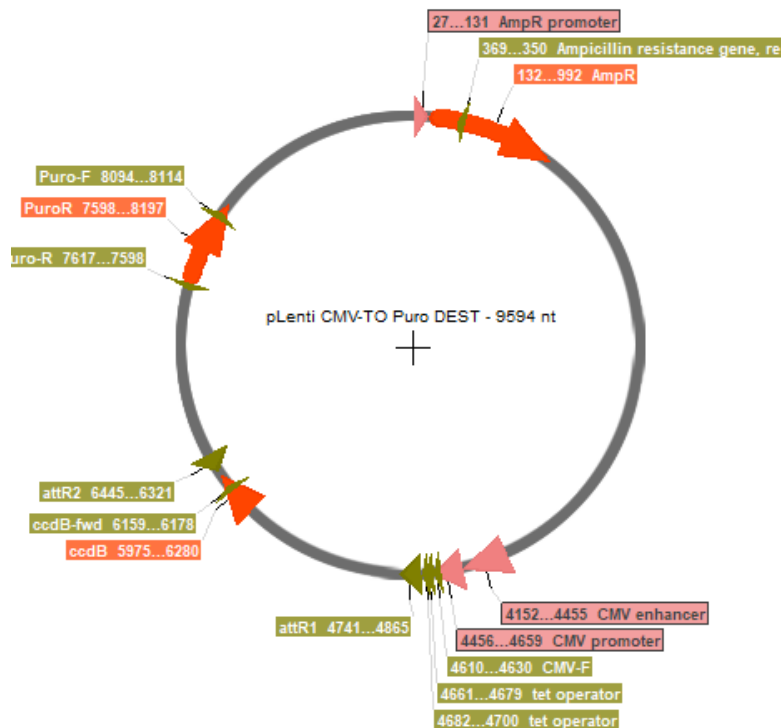


**Figure 13.** Map of pLenti CMV-TO Puro plasmid. Plasmid carrying CMV enhancer (4152-4455), CMV promoter (4456-4659), AttR1 (4741-4865), AttR2 (6445-6321), ampicillin resistance genes (132-992), puromycin resistance genes (7598-8197). Map drawn in Serial Cloner V2.5.

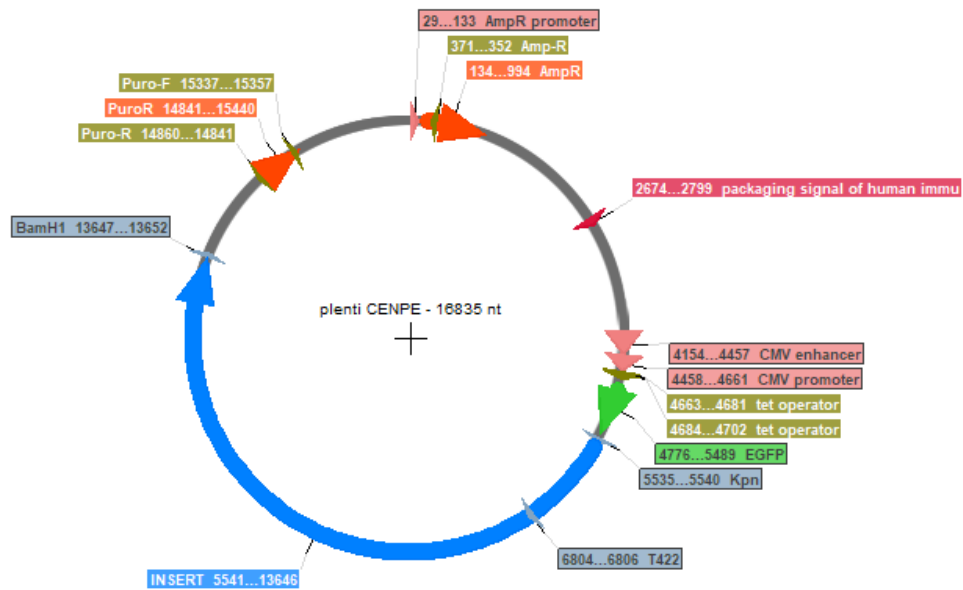


**Figure 14.** Map of pLenti CENPE plasmid. Plasmid carrying CMV enhancer (4154-4457), CMV promoter (4456-4661), tet operator (4663-4702), GFP (4776-5489), CENP-E cDNA (5541-13646), puromycin resistance genes (14860-15357). Map drawn in Serial Cloner V2.5.

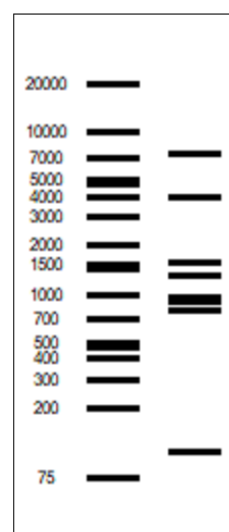
**A)**

<Serial Cloner V2.5> -- <12. aug 2019 15:53>

Restriction analysis of plenti CENPE.xdna [Circular]  
Incubated with EcoRI

9 fragments generated.

1:	7.250 bp	-	From EcoRI[14311]	To	EcoRI[4726]
2:	3.933 bp	-	From EcoRI[7992]	To	EcoRI[11925]
3:	1.573 bp	-	From EcoRI[6419]	To	EcoRI[7992]
4:	1.316 bp	-	From EcoRI[12033]	To	EcoRI[13349]
5:	962 bp	-	From EcoRI[13349]	To	EcoRI[14311]
6:	890 bp	-	From EcoRI[5519]	To	EcoRI[6409]
7:	793 bp	-	From EcoRI[4726]	To	EcoRI[5519]
8:	108 bp	-	From EcoRI[11925]	To	EcoRI[12033]
9:	10 bp	-	From EcoRI[6409]	To	EcoRI[6419]



**B)**

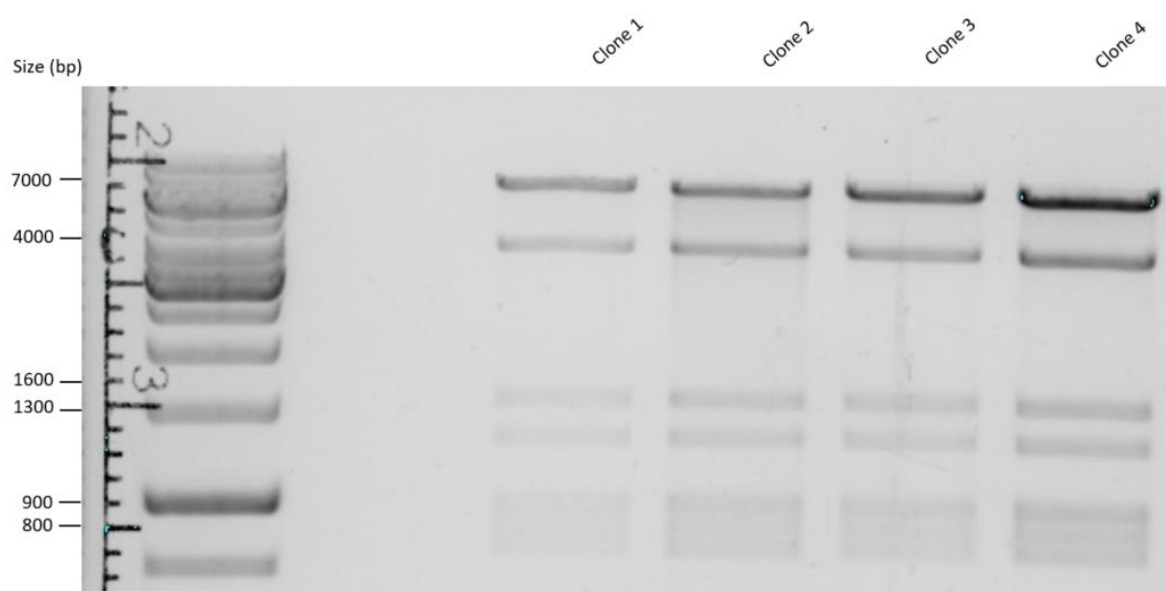


**Figure 15.** Restriction analysis of pLenti CENP-E plasmid with EcoRI. A) Pattern of virtual digestion of plasmid DNA with EcoRI in Serial Cloner V2.5. B) Restriction digestion of plasmid DNA from 4 clones with EcoRI, 1% agarose gel electrophoresis. Clone 4 was selected to continue experiments. Bp denotes the molecular standard Gene Ruler 1kb DNA Ladder (Thermo Fisher Scientific).

## **Lentiviral infection**

HEK293T cells were infected with a mix of pLenti CENP-E, psPax2 (containing HIV1-gag and HIV1-pol, for viral translation) and pVSV-G (encoding a viral envelope protein) to produce lentiviruses. After 2 and 3 days, target cells, U2OS Tet-R Blast, were infected with the lentivirus. Cells were selected with puromycin 5 $\mu$ M, diluted, seeded and left to grow in a 96-well plate.

### **3.2. GFP-CENP-E expression is highest after 16 hours of adding doxycycline**

To establish a most favorable time to add doxycycline before an experiment, when maximum levels of GFP-CENP-E expression are achieved, cells were harvested at the different timepoints after adding doxycycline (1 $\mu$ M, figure 16, A). The cells were harvested after 16h, 24h, 48h and 72h after adding doxycycline. For cells with WT CENP-E, the experiment was repeated two times. Upper band represents induced GFP-CENP-E (figure 16, B, 16kb bigger than endogenous CENP-E). The detected levels of induced protein weren't high, possibly due to transfer to nitrocellulose membrane (GFP-CENP-E is an extremely large protein of 332 kDA, which can cause problems with the transfer). The levels of expression seem highest after 16 hours of adding doxycycline. For GFP-CENP-E-T422A cell line, the levels of expression seem highest 16 and 24 hours after adding doxycycline. Also, there is a band that corresponds to the size of GFP-CENP-E in the control sample, which indicates that the promoter is leaky. For GFP-CENP-E-CC1, in the upper gel, the protein seems degraded, possibly due to inadequate transfer conditions or problems with SDS-PAGE. In the lower band, the last two wells do not contain any protein, because the gel broke at that place before transfer. The approach of adding doxycycline 16h before performing experiments was concluded to be the best.

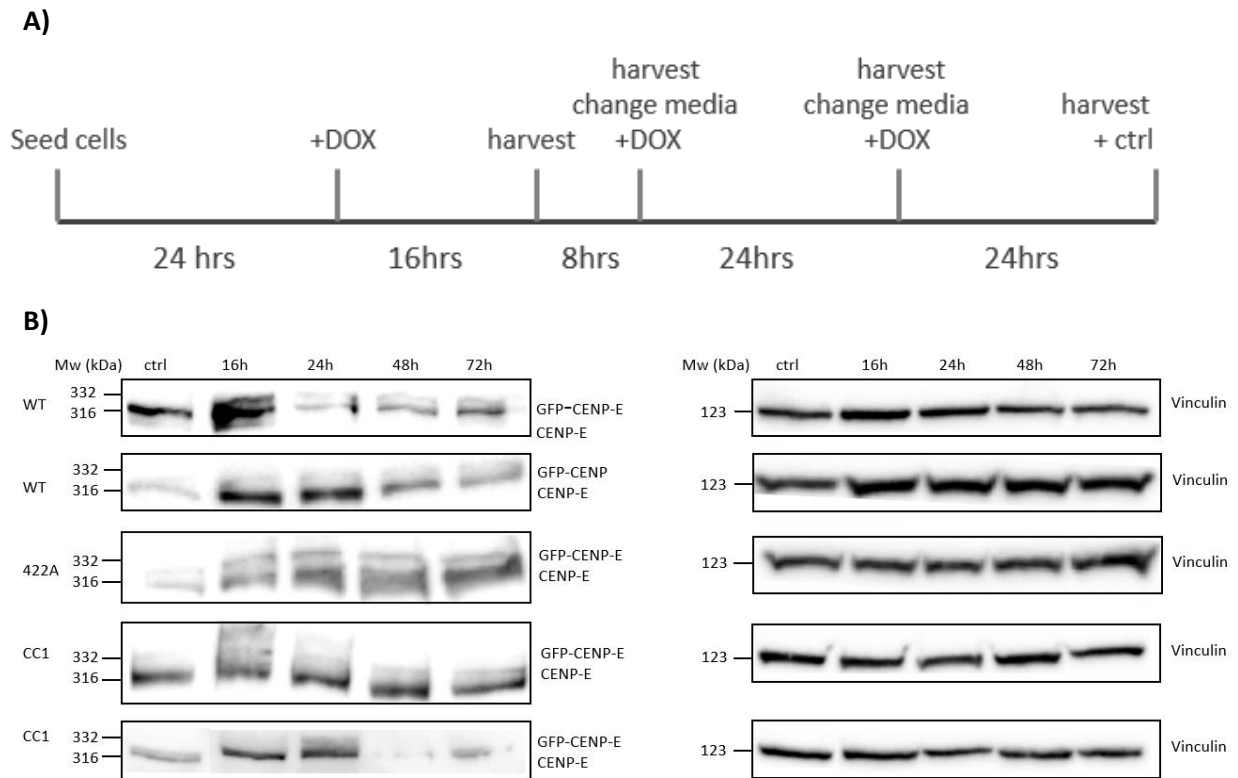


**Figure 16.** GFP-CENP-E expression levels. A) a schematic of the experiment. B) Western blot. Samples from cells expressing GFP-CENP-E WT, 422A and CC1 mutants were collected. For WT and CC1 the Western was repeated, due to low levels of protein. Vinculin (123kDa) was used as loading control. List of used antibodies in tables 2 and 3. kDa represents the molecular standard Precision Plus Protein Standards, Bio Rad.

### 3.3. Phosphorylation by Aurora A prevents stripping of CENP-E towards the spindle poles

To check the effect of T422 phosphorylation in CENP-E, U20S parental cells were treated with Aurora inhibitors (figure 17, A). In control cells (added 1:2000 DMSO as control), CENP-E is located at the kinetochores. In cells where Aurora A is inhibited, there is a significant increase in the amount of CENP-E signal at the poles ( $p$  value  $< 0.05$ , (\*), figure 17, B). When Aurora B is inhibited, CENP-E localizes to the kinetochores, and cells show significant congression problems. This suggests that phosphorylation of CENP-E by Aurora A has a role in preventing premature stripping of CENP-E from kinetochores towards the poles of the mitotic spindle.

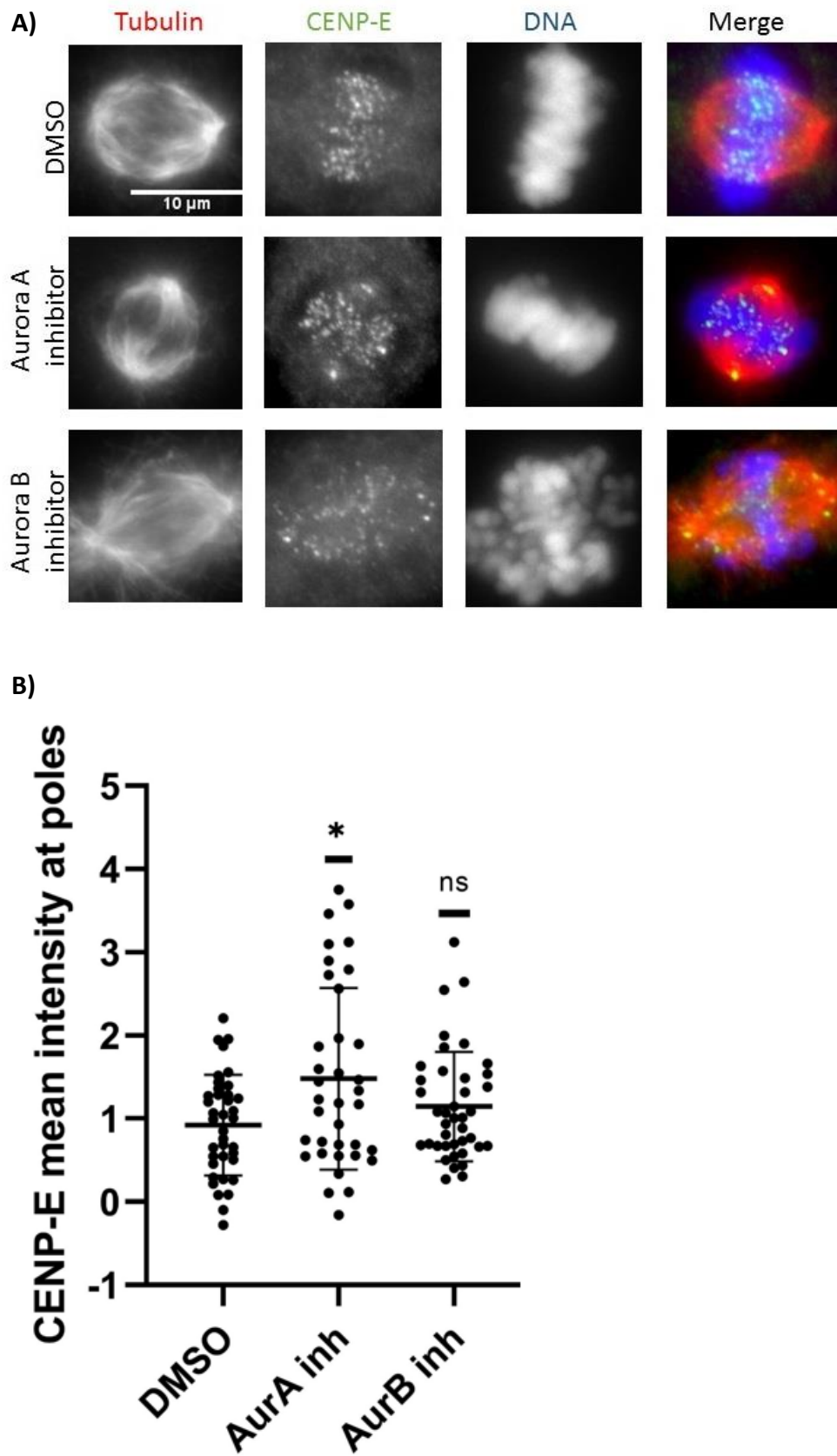


**Figure 17.** Inhibition of Aurora kinases A and B. A) Localization of CENP-E when Aurora kinases are inhibited. Red: tubulin, green: GFP-CENP-E, blue: DNA. List of used antibodies in tables 2 and 3. B).

CENP-E mean intensity at the poles. The intensity was measured in ImageJ, with a region of interest covering the pole of the mitotic spindle and normalized to the background. Statistical analysis was performed in GraphPad Prism 8.1.1, statistically significant differences were determined by the Student's unpaired and two-tailed t-test. Statistical significances with a  $p$  value  $<0.0001$  are represented by four asterisks (\*\*\*\*);  $p$  value  $<0.001$  is represented by three asterisks (\*\*\*);  $p$  value  $<0.01$  is represented by two asterisks (\*\*);  $p$  value  $<0.05$  is represented by a single asterisk (\*). N (cells)=15.

### 3.4. Microtubules have a role in CENP-E stripping

To check whether CENP-E stripping depends on microtubule binding, a nocodazole treatment (3,3  $\mu$ M) was used to eliminate tracks (depolymerizes microtubules). In cells with inhibited Aurora A, CENP-E no longer localizes at the poles, but on kinetochores. In the case with Aurora B inhibition, CENP-E remains located at the kinetochores. In a sample of 15 cells, CENP-E was located at the kinetochores in 100% of the cells (figure 18).

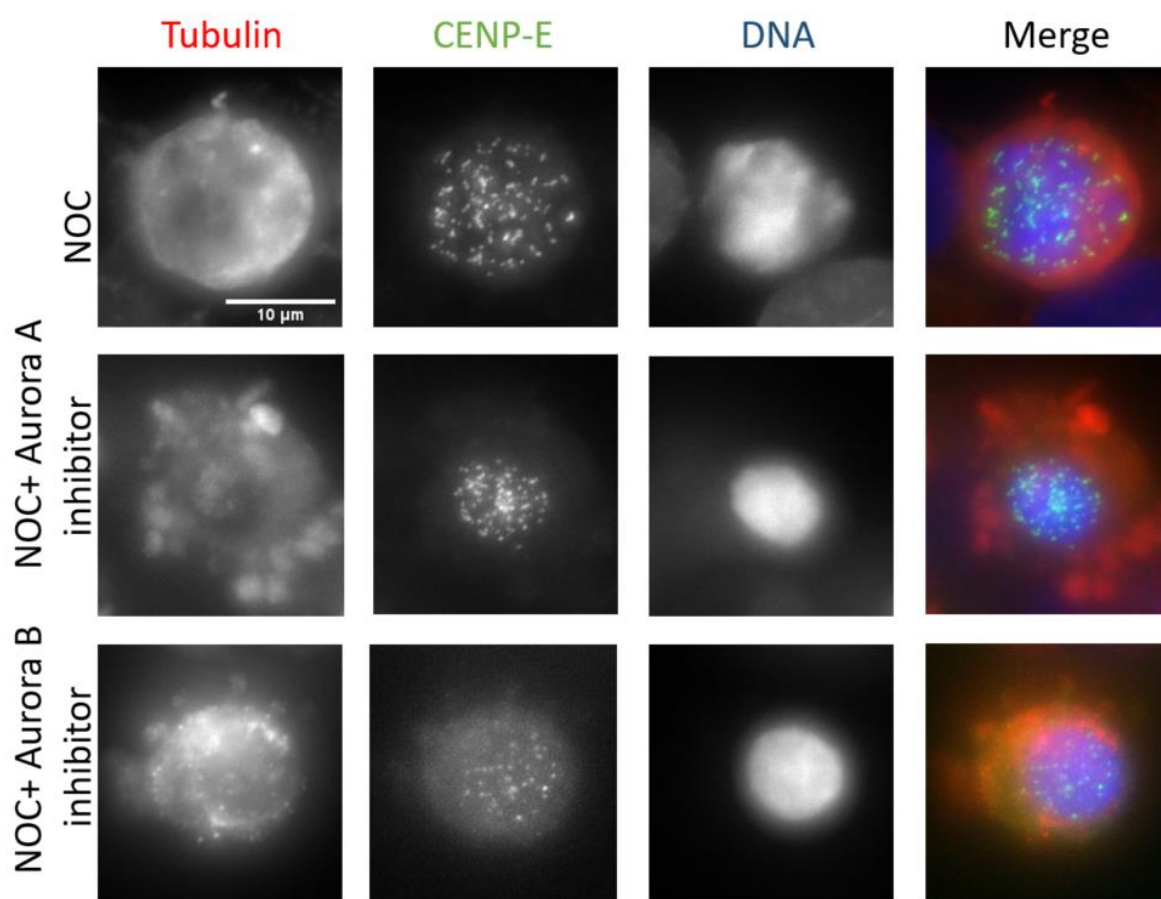


**Figure 18.** Microtubules are needed for CENP-E stripping. CENP-E (endogenous) localizes at the kinetochores in 100% of cells in each sample (cell line: U2OS parental). Red: tubulin, green: CENP-E, blue: DNA. List of used antibodies in table 2 and 3. N (cells)= 15 per sample.

Nocodazole treatment was repeated with cell lines stably expressing GFP-CENP-E WT and GFP-CENP-E 422A. In the WT cell line, CENP-E localizes at the kinetochores, in both cases – with and without nocodazole. The phosphonull mutant when not treated with NOC, shows a similar phenotype to cells with Aurora A inhibited – CENP-E accumulation at the poles. However, when treated with NOC in the same cell line, phosphonull CENP-E localizes at the kinetochores. Thus, microtubules are needed for stripping of CENP-E towards the poles, because upon their depolymerization, CENP-E cannot be transported to the spindle poles, but rather stays at the kinetochores (figure 19).

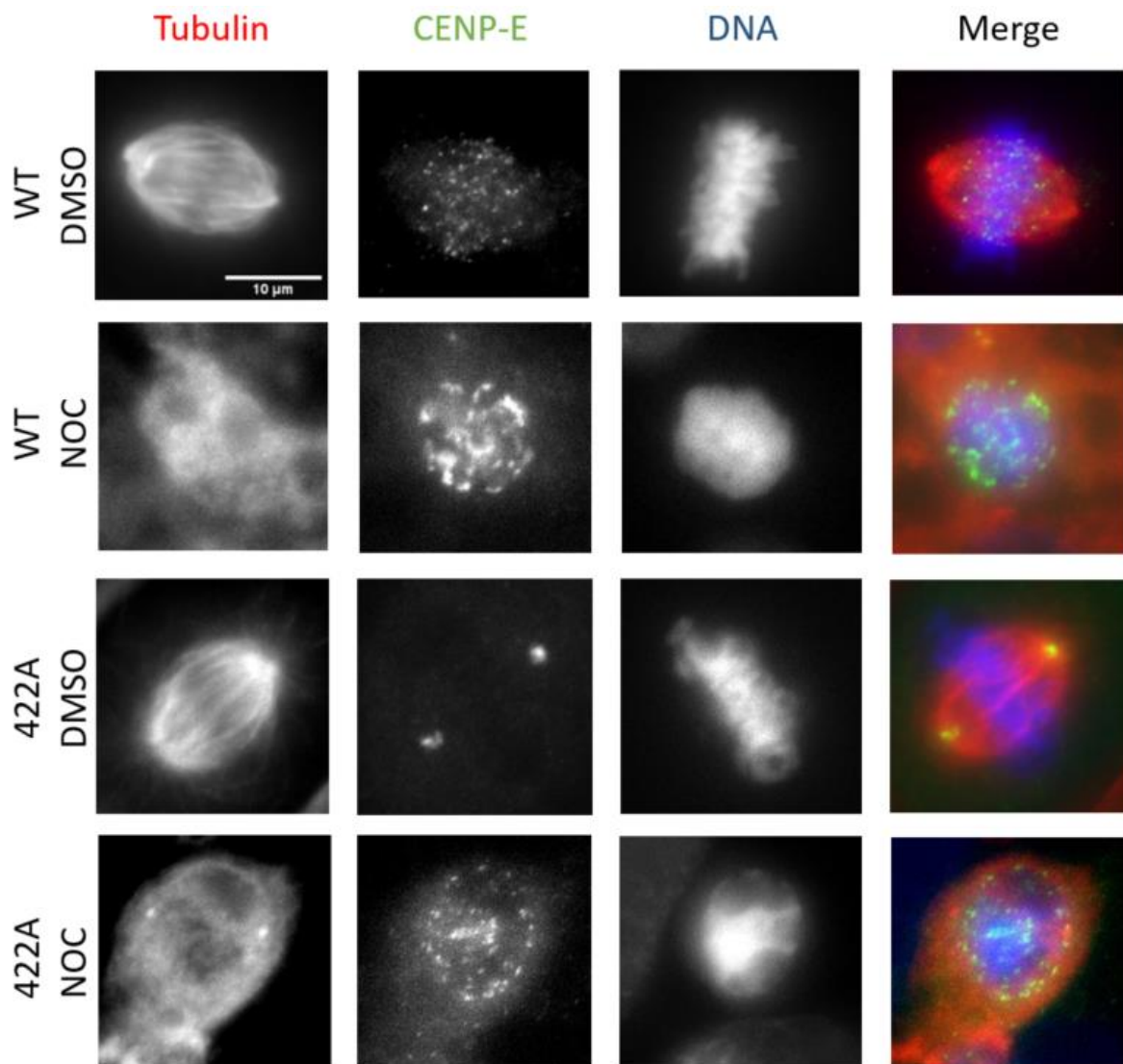


**Figure 19.** Microtubules are needed for CENP-E stripping. Red: tubulin, green: GFP- CENP-E, blue: DNA. List of used antibodies in tables 2 and 3. DMSO 1:2000 used as control. N (cells)= 15 cells per cell line.



### 3.5. Accumulation of CENP-E at the poles is not due to uncongressed chromosomes

To test whether accumulation of CENP-E at the poles is purely due to the uncongressed chromosomes that cannot be transported towards the metaphase plate when the activity of CENP-E is abrogated (Kim, 2010), cells were treated with STLC (an inhibitor of Eg5, a kinesin that promotes the assembly of bipolar spindle). This treatment causes formation of monopolar spindles – a conformation in which spindle poles stay together, surrounded by chromosomes. Two series of live-imaging filming were done for both WT and 422A cell line, first using 0,5  $\mu$ M STLC (N (cells)= 30) and one using 5  $\mu$ M STLC (N (cells)= 39, figure 20). In both conditions, 100% of the 422A cells had GFP-CENP-E located at the poles. The same conditions of Eg5 inhibition were used in immunofluorescence experiments, where CENP-E was located on the poles in 100% of the cells under treatment with both STLC concentrations (N (cells)= 154 for 0,5  $\mu$ M STLC inhibition condition, and N(cells)= 152 for 5  $\mu$ M STLC, figure 21). As for WT cell line, GFP-CENP-E was located at the kinetochores in all conditions (live imaging: N(cells, 0,5  $\mu$ M STLC)= 50, N(cells, 5  $\mu$ M STLC)= 10; immunofluorescence: N(cells, 0,5  $\mu$ M STLC)= 172, N(cells, 5  $\mu$ M STLC)= 150).

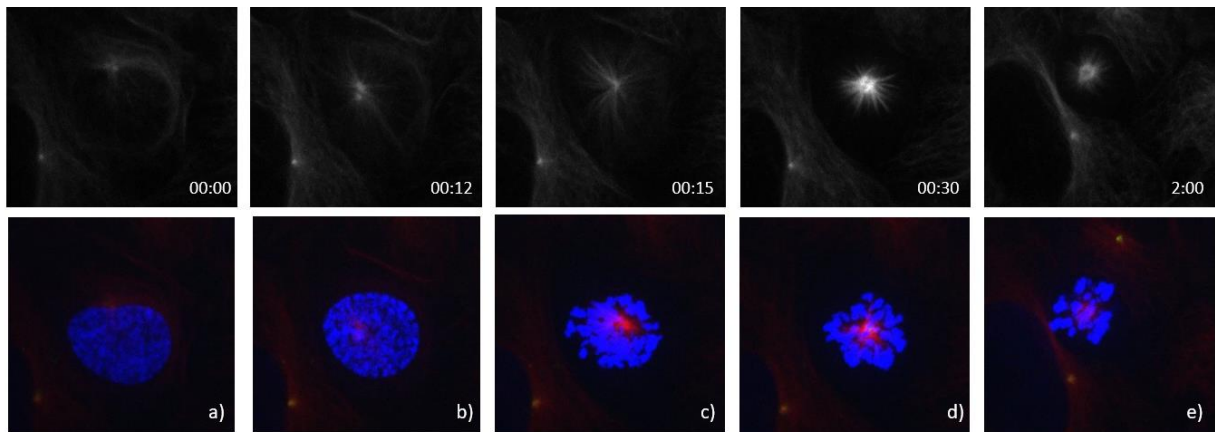


**Figure 20.** Time series of live-cell spinning disk confocal imaging of U2OS cells stably expressing GFP-CENP-E-422A, under 5  $\mu$ M STLC treatment, forming a monopolar spindle. Time is shown in hours:minutes. GFP-CENP-E-422A in green, tubulin (SiRTubulin dye) in red, DNA (Ad-H2B-RFP) in blue. Upper row: tubulin. N (cells)=10.

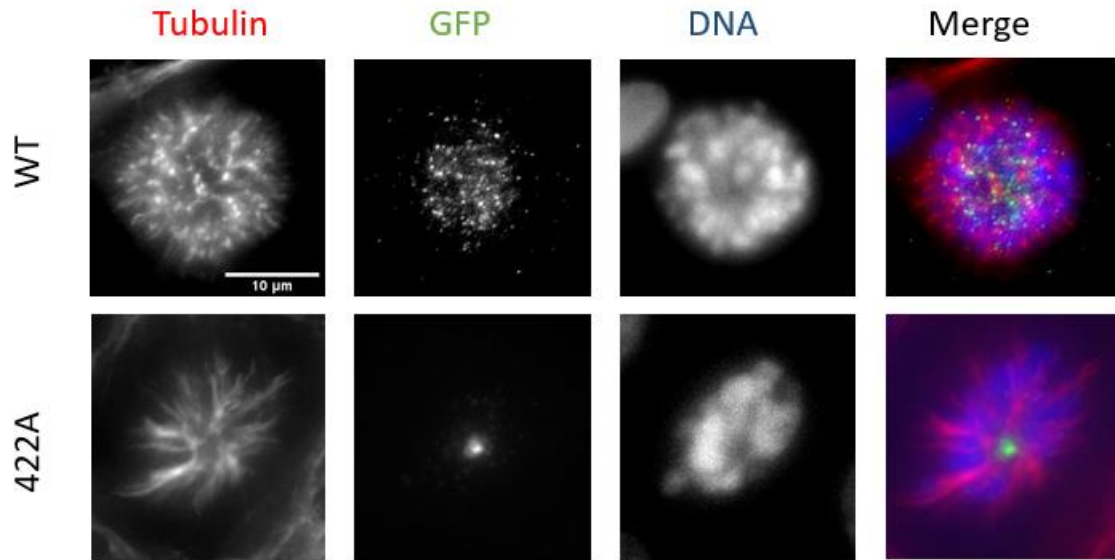


**Figure 21.** Localization of CENP-E under 5  $\mu$ M STLC treatment. Red: tubulin, green: GFP- CENP-E, blue: DNA. List of used antibodies in tables 2 and 3. N (cells) =150 per each cell line.

### 3.6. CENP-E stripping is dependent upon Spindly

To test whether accumulation of phosphonull CENP-E at the poles is caused by premature dynein-dependent stripping of CENP-E from kinetochores, a series of protein knock-downs was performed for proteins with known role in dynein function and immunofluorescence analysis was performed. The cells were immunostained using the antibodies against CENP-E and p150 (a component of dynactin, a known dynein adaptor) to assess their localization. In the control treatment with a non-targeting siRNA, GFP-CENP-E-WT is localized at the kinetochores, while GFP-CENP-E-422A mutant is localized at the poles. In NT and WT cases p150 is more localized at the poles, and in the case with 422A cell line, CENP-E and p150 seem to colocalize, suggesting potential role of dynein in CENP-E-422A accumulation at the poles (figure 22).

## siRNA NT

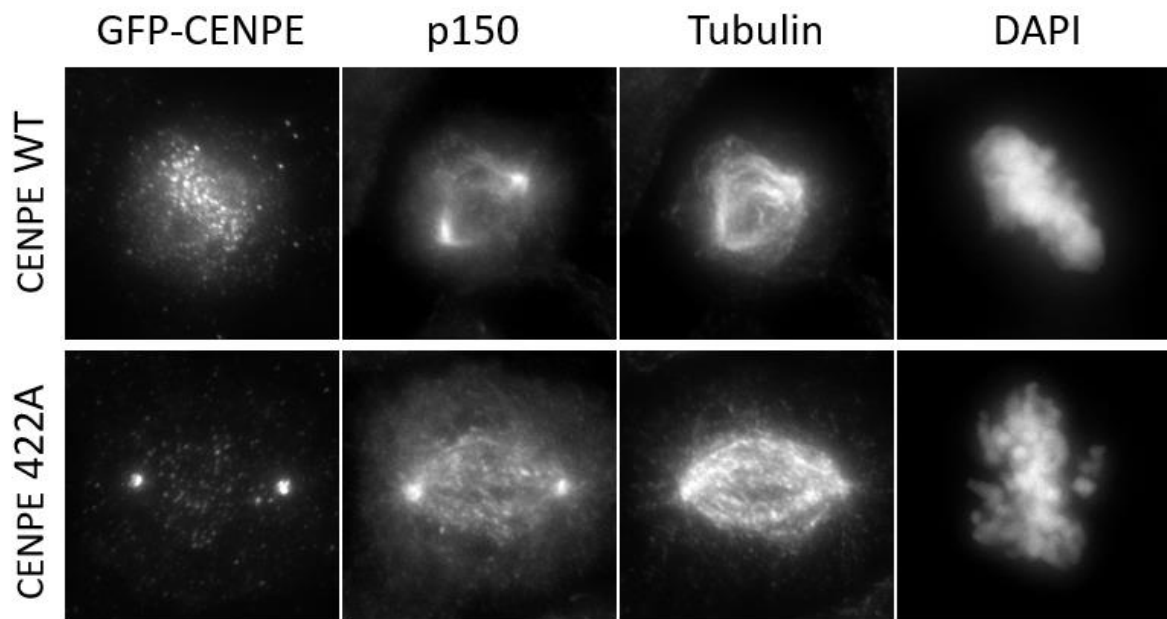
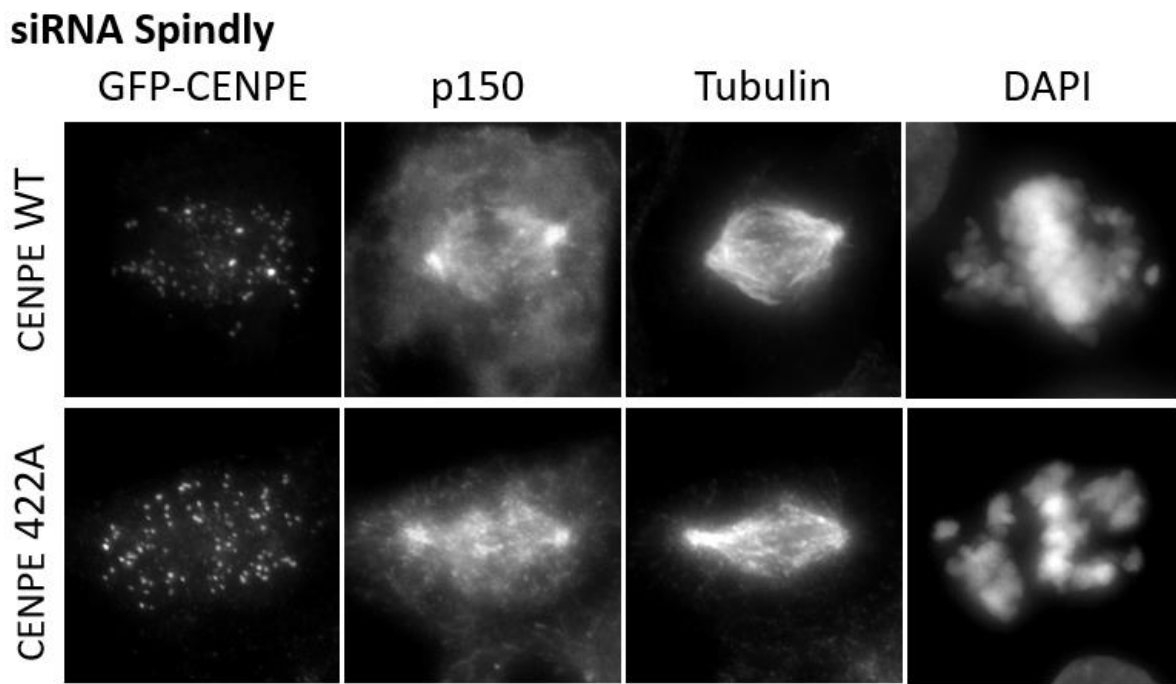


**Figure 22.** Non-targeting siRNA treatment. N(cells)= 15 per sample. List of used antibodies in tables 2 and 3.

Because Spindly is required for dynein localization at the kinetochores, I first tested whether depletion of Spindly could affect the transport of CENP-E-T422A to the poles. Strikingly, in the absence of Spindly, and consequently of kinetochore dynein too, CENP-E-422A could not accumulate at the poles anymore and was localized exclusively at kinetochores. This indicates that in situation when dynein cannot be loaded on kinetochores (Spindly RNAi), CENP-E cannot be transported to the poles, independently of its phosphorylation status. In other words, the accumulation of phosphonull CENP-E at the poles is indeed driven by dynein. (figure 23).



3.

**Figure 23.** Spindly knock down siRNA treatment. N (cells)= 15 per sample. List of used antibodies in tables 2 and 3.

Dynein heavy chain (DHC) is a component of dynein. To test if depletion of DHC will show the same effect on CENP-E-T422A transport as SPINDLY knockdown, I depleted DHC in cell lines expressing GFP-CENP-E-WT and GFP-CENP-E-T422A, respectively. In WT cell line, CENP-E still localizes at the kinetochores. In 422A, CENP-E still localizes at the poles, and the amount of CENP-E at the poles seems to be even higher than in control. Although this treatment did not confirm the Spindly RNAi-derived results, we cannot exclude the possibility that this was due to incomplete depletion of DHC or due to the fact that by depleting DHC we cause much more problems to the cells than by depleting only kinetochore-bound dynein. (figure 24).

# siRNA DHC

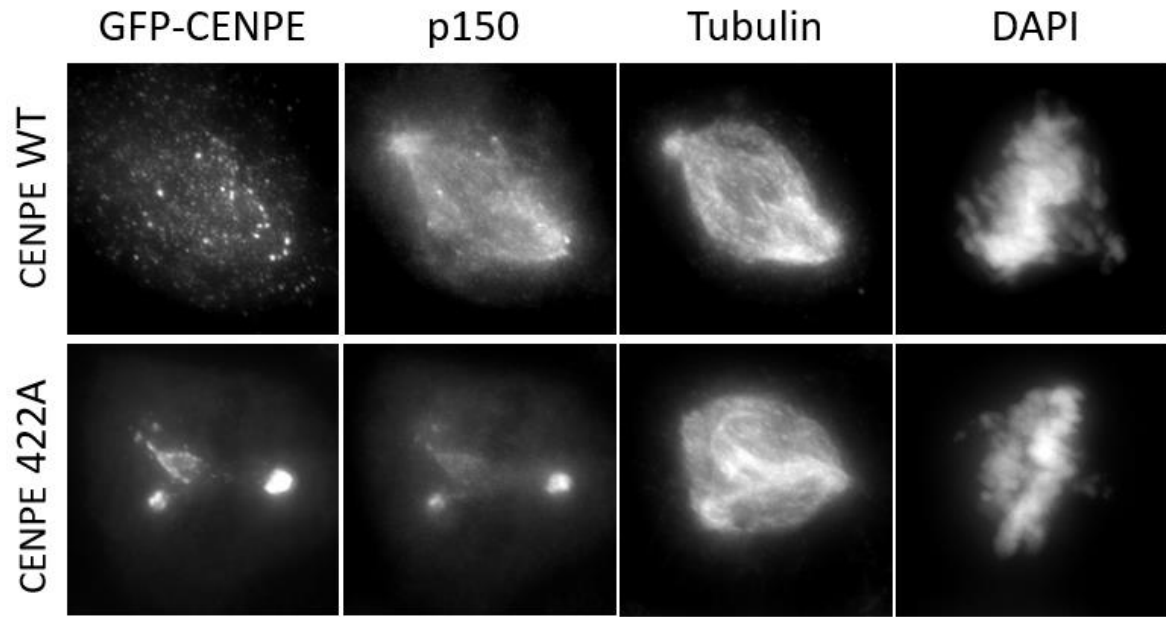


**Figure 24.** Dynein heavy chain knock down siRNA treatment. N (cells) =15 per sample. List of used antibodies in tables 2 and 3.

NuMa has a role in localization of Dynein-Dynactin at the poles. To test whether spindle pole-localized dynein is required for transportation of CENP-E-422A to the poles, I depleted NuMA using RNAi. Upon NuMA depletion WT CENP-E is still normally localized at the kinetochores. As for 422A, CENP-E is still localized at the poles, suggesting that NuMA-bound pool of dynein does not contribute to CENP-E transportation to the spindle poles. (figure 25).

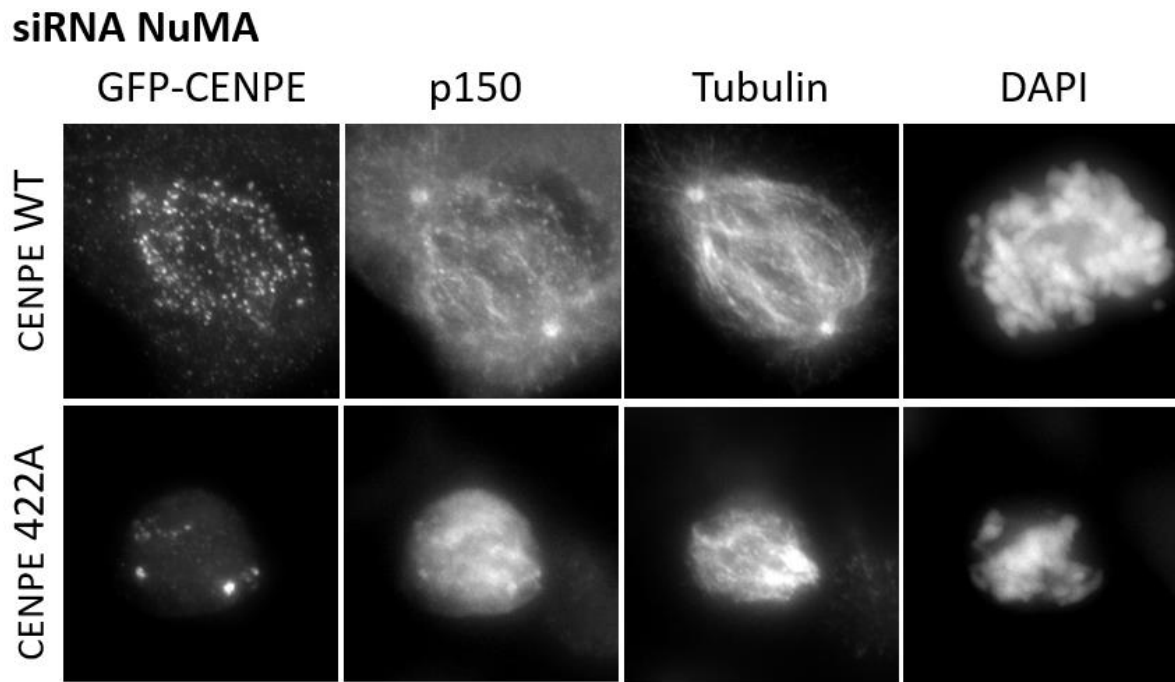


**Figure 25.** NuMa knock down siRNA treatment. N (cells) = 15 per sample. List of used antibodies in tables 2 and 3.

A p150 knock-down experiment was also performed. The siRNA was newly ordered, and further confirmations of the siRNA effectiveness are needed. In the GFP-CENP-E-WT expressing cell line, after p150 KD, CENP-E localizes at the kinetochores. In GFP-CENP-E-T422A cell line, CENP-E is at the poles (figure 26).

Although further analysis is needed, the results collected upon Spindly depletion strongly suggest that the accumulation of CENP-E-T422A at the poles is dynein-driven and that Aurora-dependent phosphorylation of CENP-E might serve to protect CENP-E from being prematurely stripped from kinetochores by dynein.

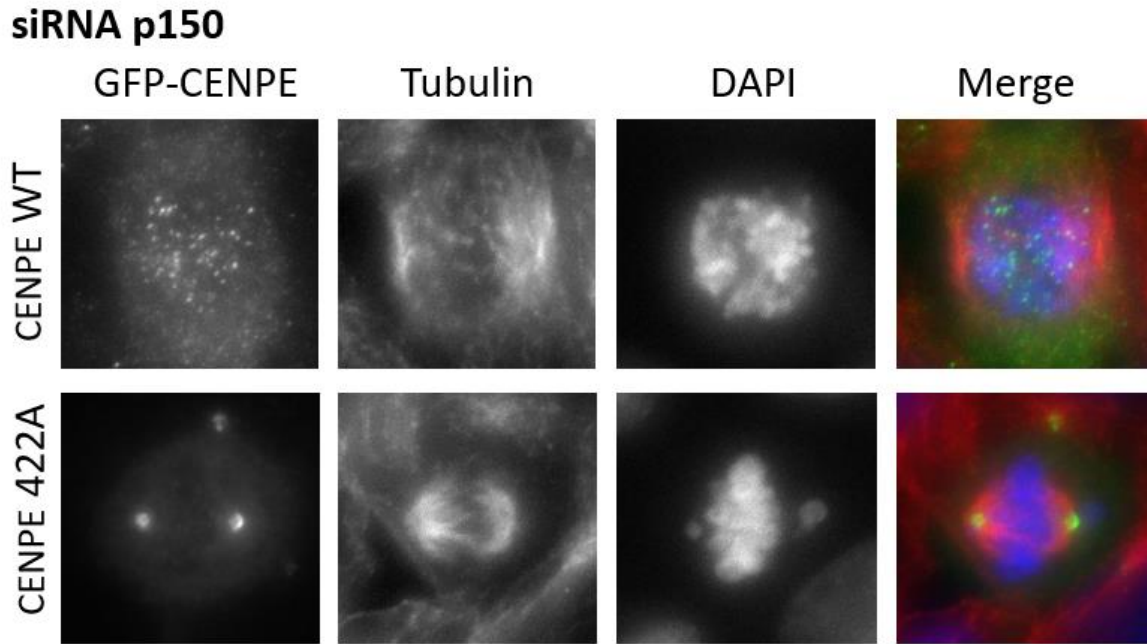


**Figure 26.** p150 knock down siRNA treatment. N (cells)=15 per sample. List of used antibodies in tables 2 and 3.

### 3.7. Characterization of CENP-E CC1-box mutant

To identify whether the newly found CC1-box motif in CENP-E sequence is a motif for Dynein binding, U20S cells expressing GFP-CENP-E with mutations A242V, A243V (generated by Susana Eibes, postdoc in Cell Division and Cytoskeleton Group, Danish Cancer Society Research Center) were stained with Ad-H2B-RFP to visualize DNA, SiR-tubulin dye to visualize tubulin. In order to monitor the effect of the mutant alone, a 48hour siRNA knock-down of endogenous CENP-E (sequence in table 1) was performed prior. Cells entering mitosis were found (10) and filmed for 2 hours (to cover the whole process of mitosis). In the beginning of mitosis (figure 27, a)), CENP-E expression is high, and it is localized to kinetochores. As division is progressing, CENP-E localizes to kinetochores of uncongressed chromosomes (b-e), in all filmed cells. After congression is done, CENP-E levels are diminishing (f -j). This indicates that even with mutated CC1 motif, CENP-E can still be stripped off the kinetochores. The expression levels between the 10 filmed cells variate, and it can not be certainly distinguished whether CENP-E stays at the kinetochores longer e.g. that dynein-mediated stripping is present in a lower extent because the proposed binding motif is disrupted.



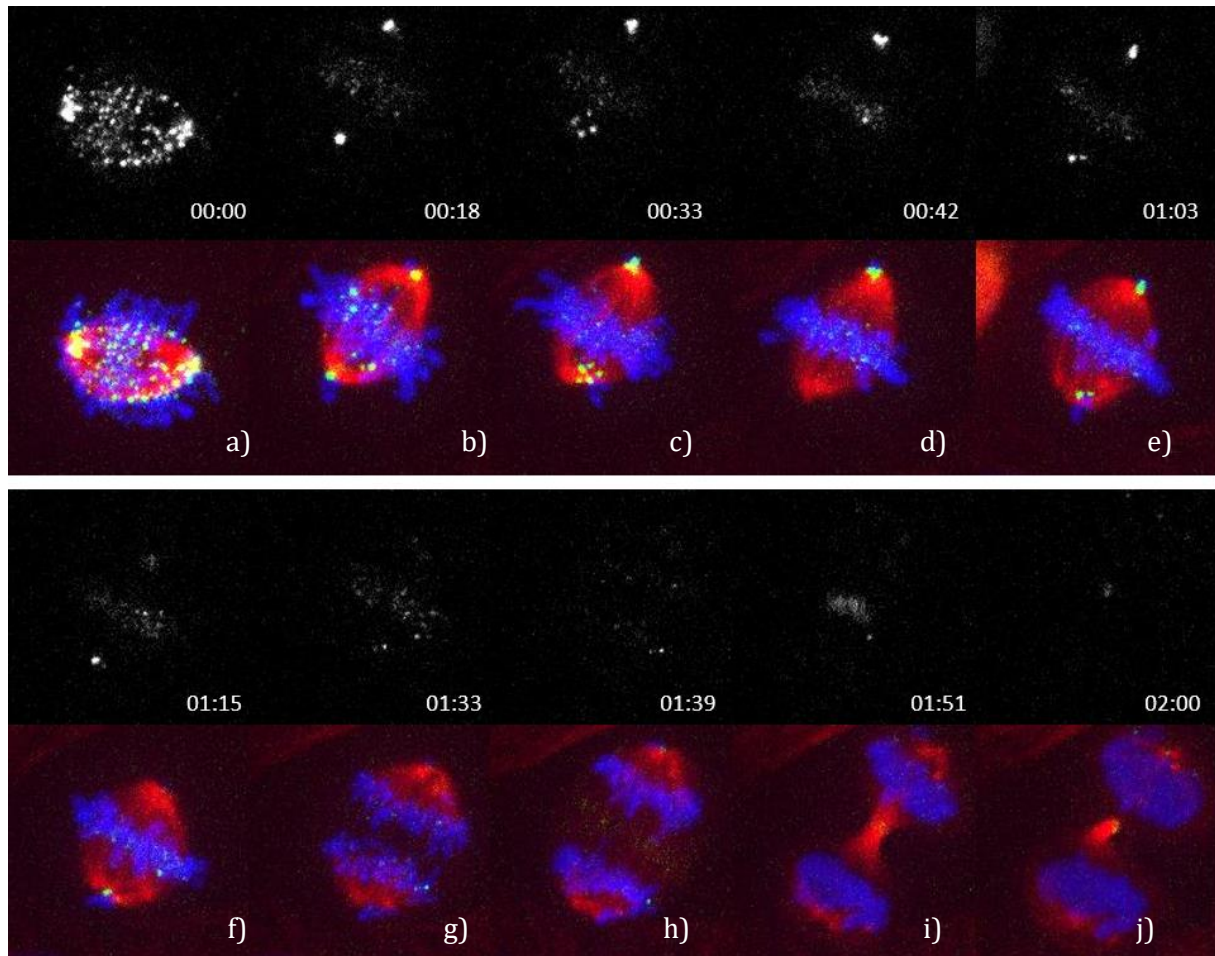


**Figure 27.** Time series of live-cell spinning disk confocal imaging of U2OS cells stably expressing GFP-CENP-E-CC1 to show localization throughout mitosis. Time is shown in hours:minutes. GFP-CENP-E-CC1 in green, tubulin (SiRTubulin dye) in red, DNA (Ad-H2B-RFP) in blue, N (cells)=10.

In order to further confirm whether the proposed motif has a role in Dynein binding, a series of siRNAs was performed on the novel cell line, as was before done for GFP-CENP-E-WT and GFP-CENP-E-T422A cell lines (chapter 3.5). When the cells were treated with a non-targeting siRNA (sequence in table 1.), CENP-E is located at the kinetochores. When it comes to DHC, Spindly and NuMa knock-downs, CENP-E-CC1 is located at the kinetochores in all cases (figure 28.) In the case where p150 is knocked-down, CENP-E-CC1 is located at the kinetochores (figure 29).



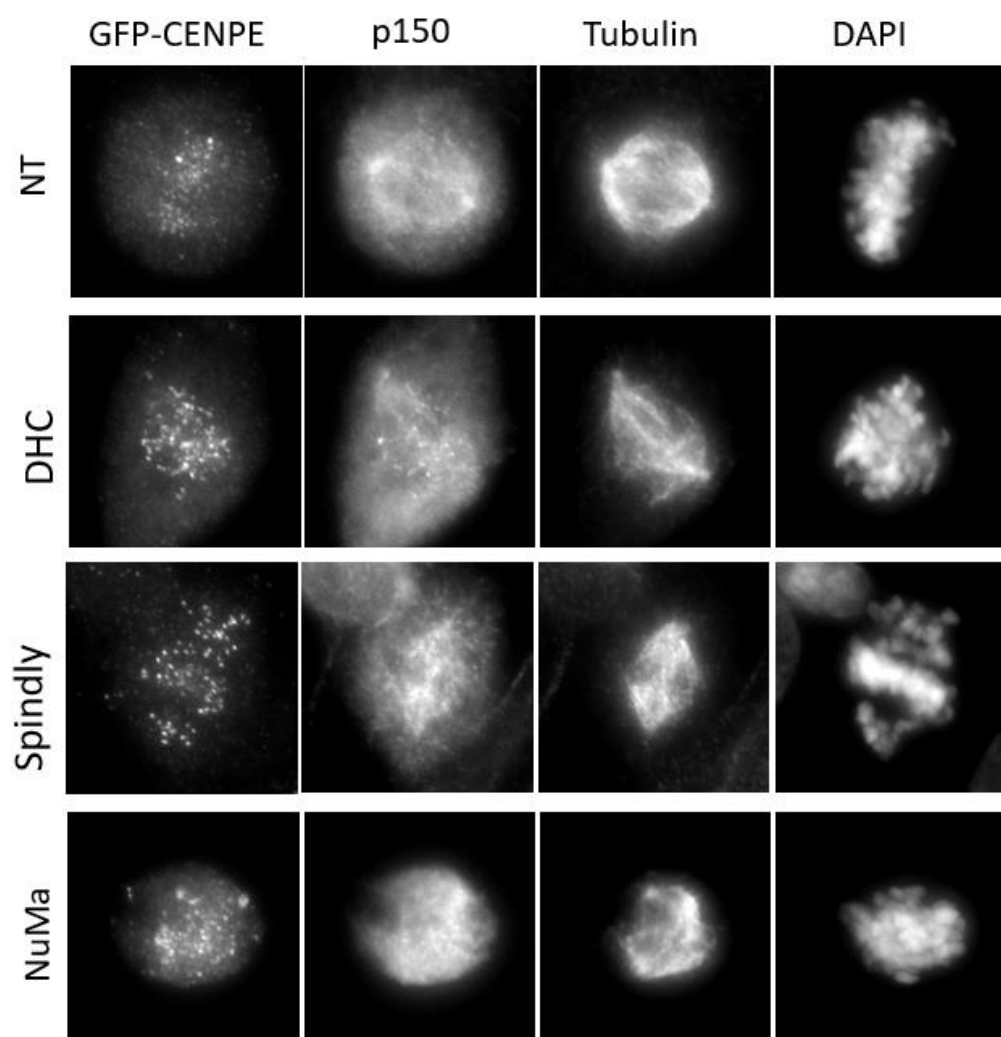


**Figure 28.** siRNA treatment for CC1 cell line. N(cells)= 15 per sample. List of used siRNAs and antibodies in tables 1, 2 and 3.

### siRNA p150

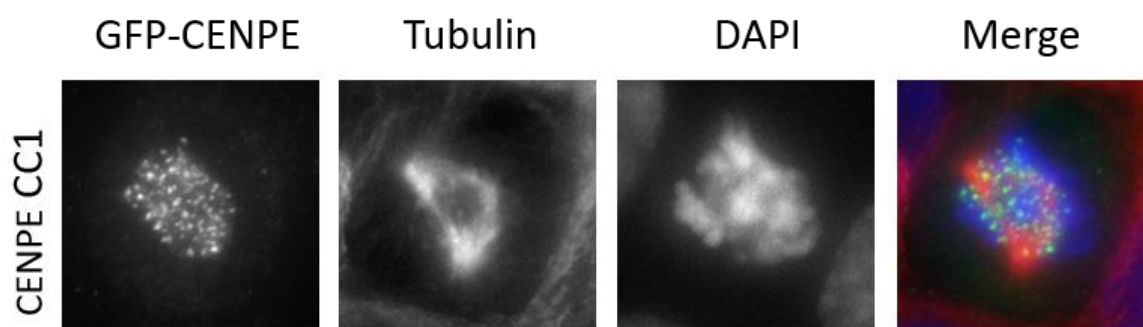


**Figure 29.** p150 knock down siRNA treatment. N (cells)=15 per sample. List of used siRNAs and antibodies in tables 1, 2 and 3.

### 3.8. Quantification of CENP-E amount at the poles after siRNA treatments

In order to further investigate the effect of Aurora-mediated phosphorylation and potential direct interaction between CENP-E and dynein on dynein-mediated stripping of CENP-E from kinetochores, I measured the intensity of GFP-CENP-E at the poles under different conditions. It is evident that GFP-CENP-E intensity at the poles is significantly higher (figure 30,  $p$  value  $<0.0001$ , (\*\*\*\*)) in T422A cells than in WT control in all siRNA knock-down treatments except for Spindly KD (ns, figure 30, 31). Under conditions when Spindly was depleted, the amount of CENP-E at the poles is significantly lower ( $p$  value  $<0.0001$ , (\*\*\*\*), figure 31) than in NT, which means that stripping of CENP-E depends on Spindly, most likely via Spindly-mediated kinetochore dynein function, as previously shown by immunofluorescence (discussed above). In the case where NuMa is knocked-down, when compared to NT in 422A, there is also significantly lower amounts of CENP-E at the poles ( $p$  value  $<0.001$ , (\*\*\*)). NuMa disrupts pole focusing, and the lower amount of CENP-E at the poles was expected. Also, as I showed using immunofluorescence, when DHC is knocked down in 422A treatments compared to 422A NT treatment (figure 31), the amount of CENP-E at the poles is significantly higher ( $p$  value  $<0.0001$ , (\*\*\*\*), figure 31). That doesn't correspond to the expected result that a decrease in amount of dynein should lead to less CENP-E stripping towards the poles. However, as discussed above, we cannot exclude the possibility that this was because of inefficient depletion of DHC or due to the severness of phenotype due to other cellular functions of DHC. As for the CC1 mutant, in NT case, the amount at the poles is higher than in WT, which doesn't go along with the expected results that there should be less stripping of CENP-E towards the poles if the CC1-box was required for dynein binding. This result is in line with the immunofluorescence data showed above and again indicates that even with mutated CC1 motif, CENP-E can still be stripped off the kinetochores. Further experiments will be needed to elucidate if something else in addition to CC1 motif is required for potential CENP-E-dynein interaction. As for NuMA depletion, in both WT and CC1 cell lines there is no significant differences for amount of CENP-E at the poles as compared to the NT sample (figure 30).

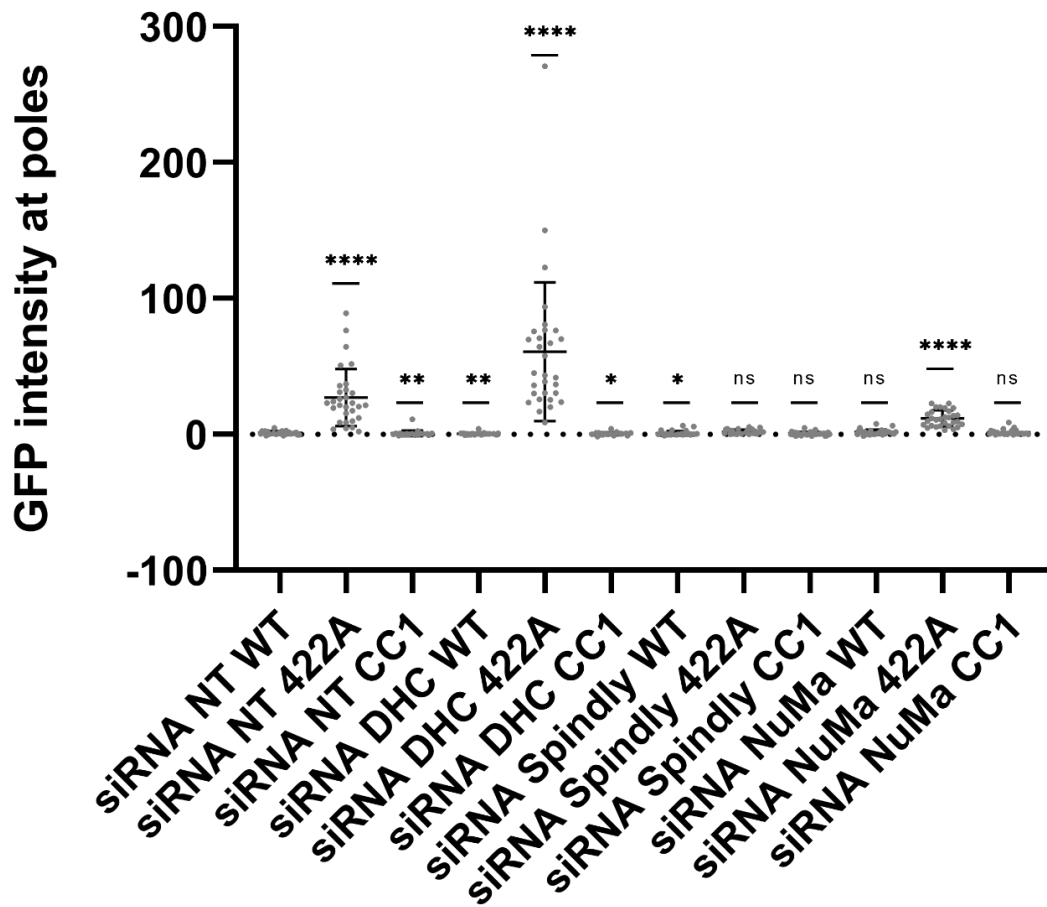


**Figure 30.** GFP intensity at the poles after different siRNA knock-downs. Corresponds to CENP-E amount at the poles. The intensity was measured in ImageJ, with a region of interest covering the pole of the mitotic spindle and normalized to the background. Statistical analysis was performed in GraphPad Prism 8.1.1, statistically significant differences were determined by the Student's unpaired and two-tailed t-test. Statistical significances with a  $p$  value  $<0.0001$  are represented by four asterisks (\*\*\*\*);  $p$  value  $<0.001$  is represented by three asterisks (\*\*);  $p$  value  $<0.01$  is represented by two asterisks (\*\*);  $p$  value  $<0.05$  is represented by a single asterisk (\*). N (cells)=15.

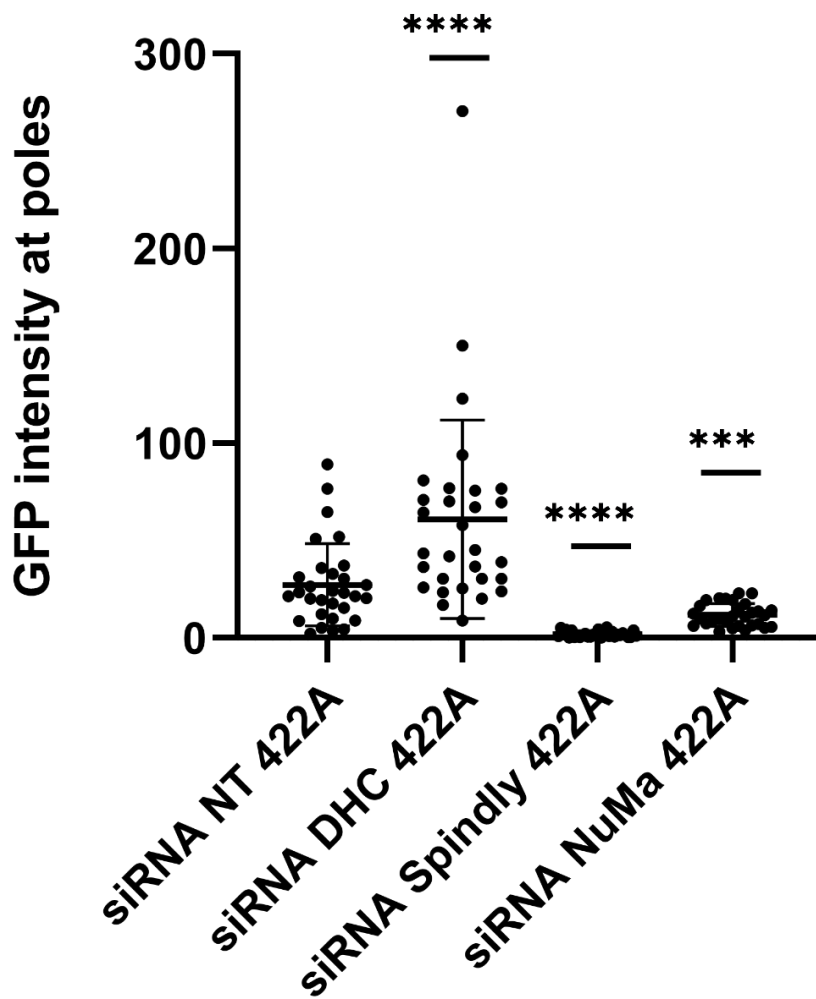


**Figure 31.** GFP intensity at the poles after different siRNA knock-downs in 422A cell line. Corresponds to CENP-E amount at the poles. The intensity was measured in ImageJ, with a region of interest covering the pole of the mitotic spindle and normalized to the background. Statistical analysis was performed in GraphPad Prism 8.1.1, statistically significant differences were determined by the Student's unpaired and two-tailed t-test. Statistical significances with a  $p$  value  $<0.0001$  are represented by four asterisks (\*\*\*\*);  $p$  value  $<0.001$  is represented by three asterisks (\*\*\*);  $p$  value  $<0.01$  is represented by two asterisks (\*\*);  $p$  value  $<0.05$  is represented by a single asterisk (\*). N (cells)=15.

A p150 knock-down experiment was also performed. The siRNA was newly ordered, and further confirmations of the siRNA effectiveness are needed. In the WT CENP-E expressing cell line, after p150 KD, CENP-E localizes at the kinetochores. The amount of GFP-CENP-E in both 422A NT and p150 KD is higher than in WT NT control ( $p$  value  $<0.0001$  (\*\*\*\*), figure 32). 422A NT and p150 RNAi, when compared, show lower amounts of CENP-E in the p150 KD case ( $p$  value  $<0.0001$  (\*\*\*\*), figure 33). That was expected, since p150 is a component of dynactin, which is a known dynein interactor. This shows that less dynactin means less dynein-dynactin mediated

stripping of CENP-E towards the poles. When it comes to CC1 cell line, no significant differences were found (figure 32).

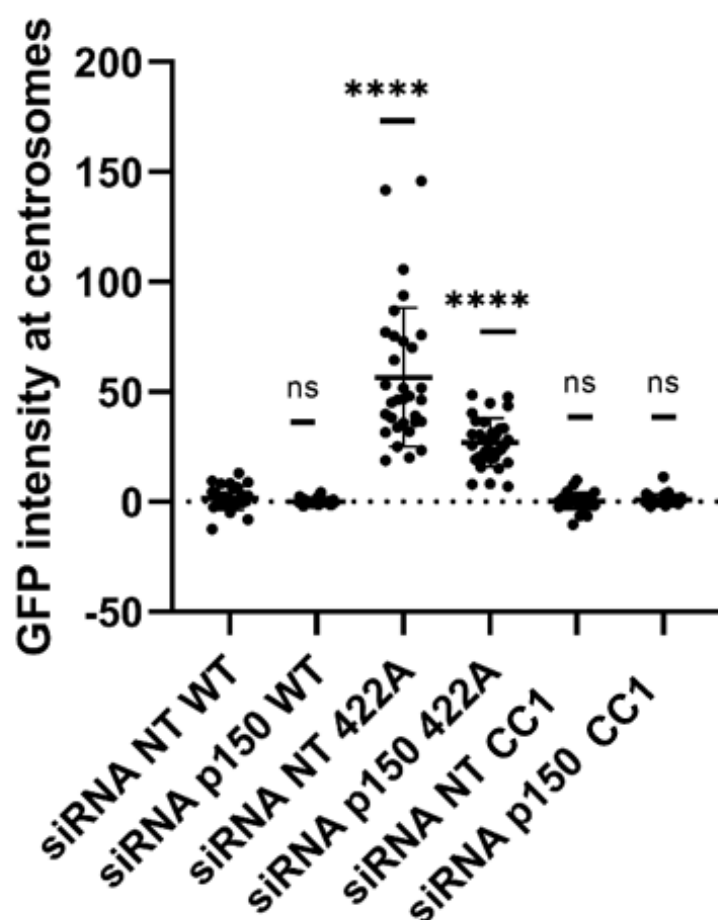


**Figure 32.** The intensity was measured in ImageJ, with a region of interest covering the pole of the mitotic spindle and normalized to the background. Statistical analysis was performed in GraphPad Prism 8.1.1, statistically significant differences were determined by the Student's unpaired and two-tailed t-test. Statistical significances with a  $p$  value  $<0.0001$  are represented by four asterisks (\*\*\*\*);  $p$  value  $<0.001$  is represented by three asterisks (\*\*\*);  $p$  value  $<0.01$  is represented by two asterisks (\*\*);  $p$  value  $<0.05$  is represented by a single asterisk (\*). N (cells)=15.

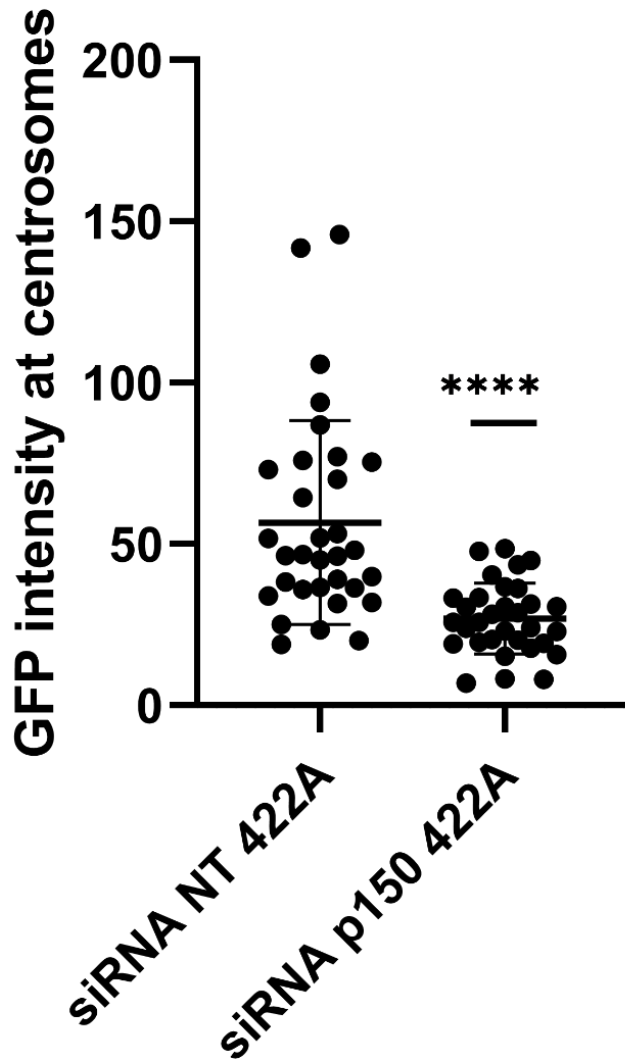


**Figure 33.** The intensity was measured in ImageJ, with a region of interest covering the pole of the mitotic spindle and normalized to the background. Statistical analysis was performed in GraphPad Prism 8.1.1, statistically significant differences were determined by the Student's unpaired and two-tailed t-test. Statistical significances with a  $p$  value  $<0.0001$  are represented by four asterisks (\*\*\*\*);  $p$  value  $<0.001$  is represented by three asterisks (\*\*\*);  $p$  value  $<0.01$  is represented by two asterisks (\*\*);  $p$  value  $<0.05$  is represented by a single asterisk (\*). N (cells)=15.

### 3.9. Immunoprecipitation

To further test whether CENP-E interacts with dynein-dynactin, an immunoprecipitation was performed. In addition to a sample containing asynchronous cell population, another sample with cell enriched in mitosis (using nocodazole block followed by mitotic shake-off) was collected. Immunoprecipitation was performed with a GFP antibody (since CENP-E has an N-terminus GFP tag, figure 34). On the blot in figure 34 we can see that CENP-E

was successfully immunoprecipitated. The proteins tested were p150 (a dynactin component) and DIC (Dynein Intermediate Chain). In the asynchronous cells sample, p150 was detected, but it was also present in the control. We can not conclude about the interaction, because it seems the antibody is sticky. As for DIC, there are also bands present in the control, so we can not conclude about the interaction. In the mitotic fraction of cells, except for CENP-E, other proteins weren't clearly detected. There is a low amount of proteins in CENP-E and p150 control present, so the conditions of IP have to be optimized.

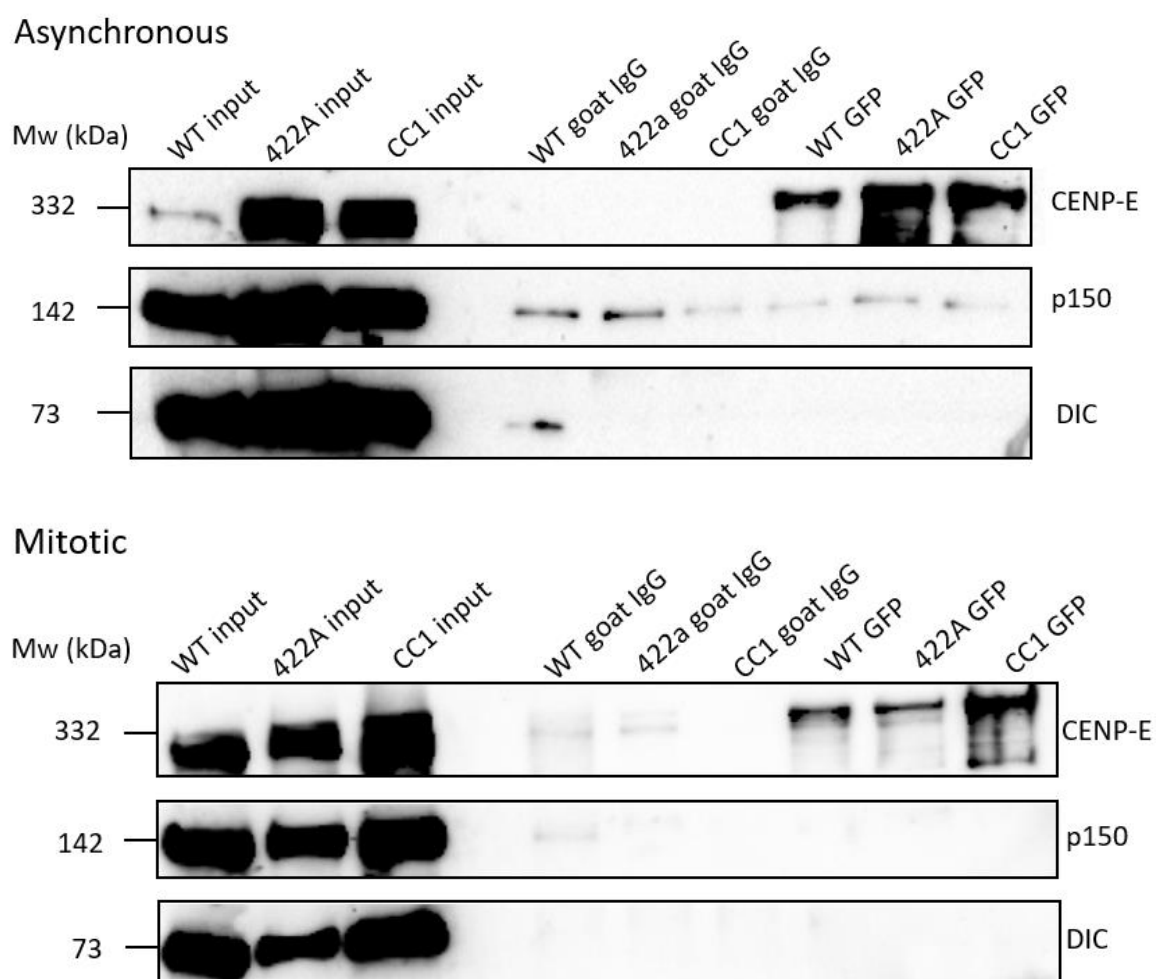


**Figure 34.** CENP-E interaction with Dynein/Dynactin. A Western blot of asynchronous fraction and mitotic fraction of the cells. List of used antibodies in tables 2 and 3. kDa represents the molecular standard Precision Plus Protein Standards, Bio Rad.

### 3.10. T422A mutant establishes bipolar spindles under treatment with STLC

Interestingly, when performing a live-cell imaging of U2OS cells expressing GFP-CENP-E-422A (chapter 3.4., figure 35), I observed that 46,67% (30 cells) establish bipolarity as opposed to 18% of WT cells (50 cells) treated with 0.5  $\mu$ M STLC (table 4, figure 36). STLC is an inhibitor of Eg5, a kinesin required for the assembly of bipolar spindle. Since bipolar cells were present during STLC treatment in both cell lines, we concluded that the Eg5 inhibition was not complete, and the experiment was repeated with higher STLC concentration (5  $\mu$ M) to fully inhibit Eg5. 0% of WT cells (N=10) established bipolarity as opposed to 28,21% of 422a cells (N=39, table 5, figures 37).

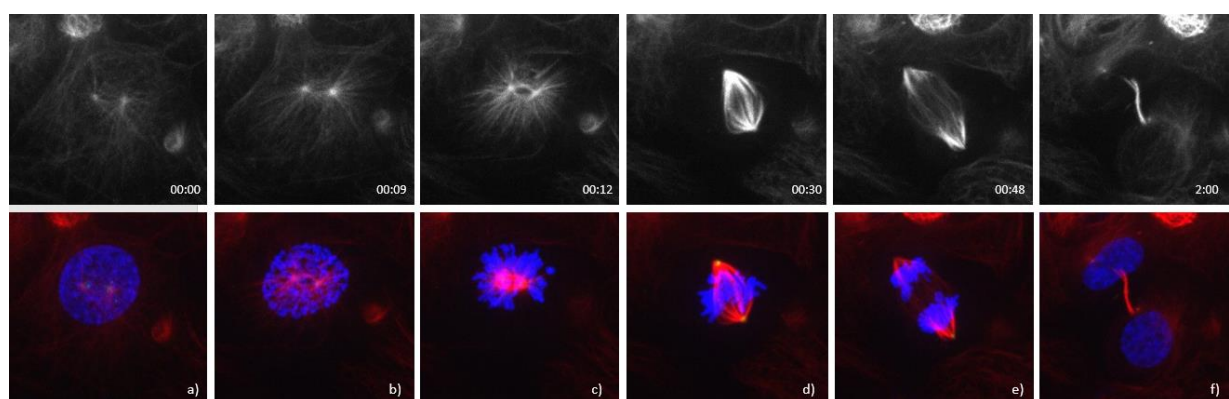


**Figure 35.** Time series of live-cell spinning disk confocal imaging of U2OS cells stably expressing GFP-CENP-E-422A, under 5  $\mu$ M STLC treatment, forming a bipolar spindle. Time is shown in hours:minutes. GFP-CENP-E-422A in green, tubulin (SiR-Tubulin dye) in red, DNA (Ad-H2B-RFP) in blue, N (cells)=10.

**Table 4.** Monopolar and bipolar cells in each cell line after 0,5  $\mu$ M STLC treatment. Live imaging.

	WT	422A
monopolar	41	16
bipolar	9	14
%/bipolar	18	46,67



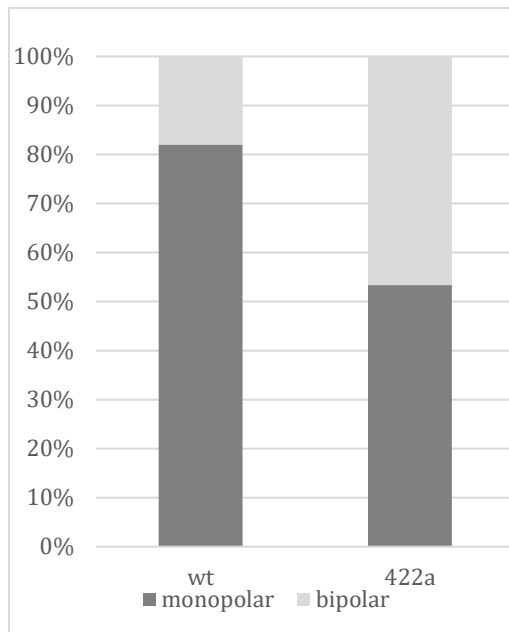


**Figure 36.** Amount of monopolar and bipolar spindles in cell lines. STL treatment 0.5  $\mu$ M. Live imaging.

**Table 5.** Monopolar and bipolar cells in each cell line after 5  $\mu$ M STL treatment. Live imaging.

	WT	422A
monopolar	10	28
bipolar	0	11
%/bipolar	0	28,21

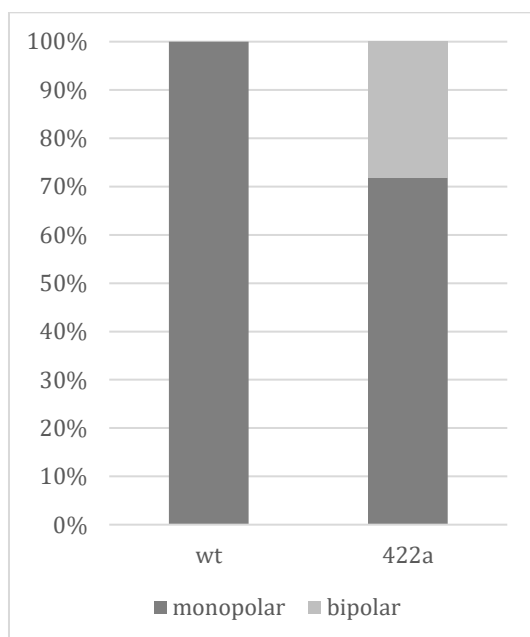


**Figure 37.** Amount of monopolar and bipolar spindles in cell lines. STL treatment 5  $\mu$ M. Live imaging.

To further confirm the presence of higher number of bipoles in 422A cell line, a series of immunofluorescence experiments (figure 38) was performed on all three cell line samples. (GFP-CENP-E-WT, GFP-CENP-E-T422A, GFP-CENP-E-CC1) Both 0,5 and 5  $\mu$ M concentrations of STLC were used, on a sample of 150 cells per each cell line. Under 0,5  $\mu$ M STLC treatment 8% WT cells established bipolarity, 27,92% 422A, and 2% CC1 (table 6, figure 39). Under higher concentration of STLC, 0,67% of WT, 18,4% of 422A and 0% of CC1 cells established bipolarity (table 7, figure 40). Once again, the amount of bipoles in 422A is significantly higher in any other cell lines, suggesting that unphosphorylated CENP-E counteracts Eg-5 inhibition, supporting the establishment of bipolar spindles when Eg-5 is inhibited.

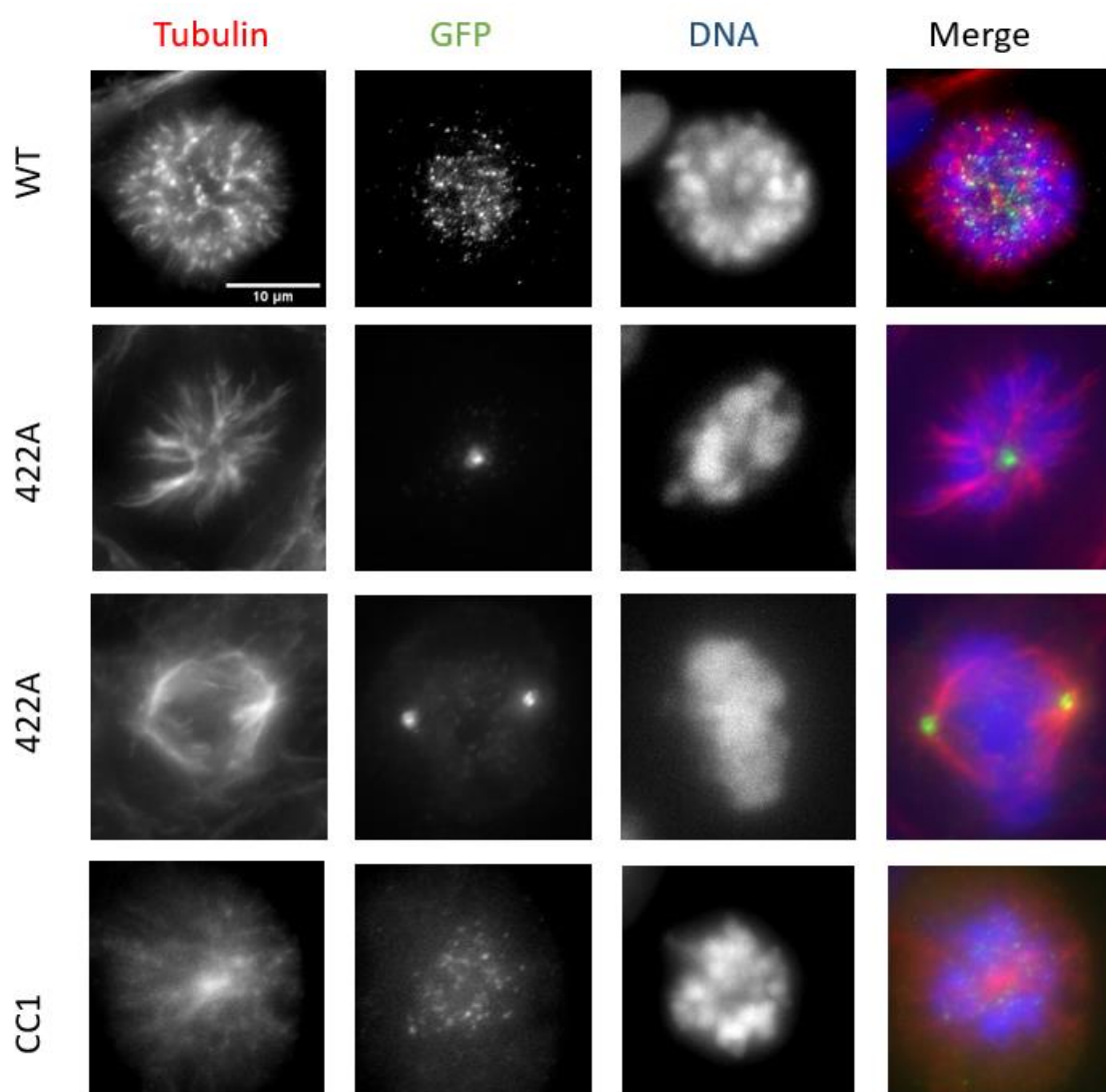


**Figure 38.** Monopolar and bipolar spindles after treatment with 5  $\mu$ M STLC. Immunofluorescence. Red: tubulin, green: CENP-E, blue: DNA. List of used antibodies in table 2 and 3. N (cells)= 150 per sample.

**Table 6.** Monopolar and bipolar cells in each cell line after 0,5  $\mu$ M STLC treatment. Immunofluorescence.

	WT	422A	CC1
monopolar	158	111	147
bipolar	14	43	3
%/bipolar	8	27,92	2

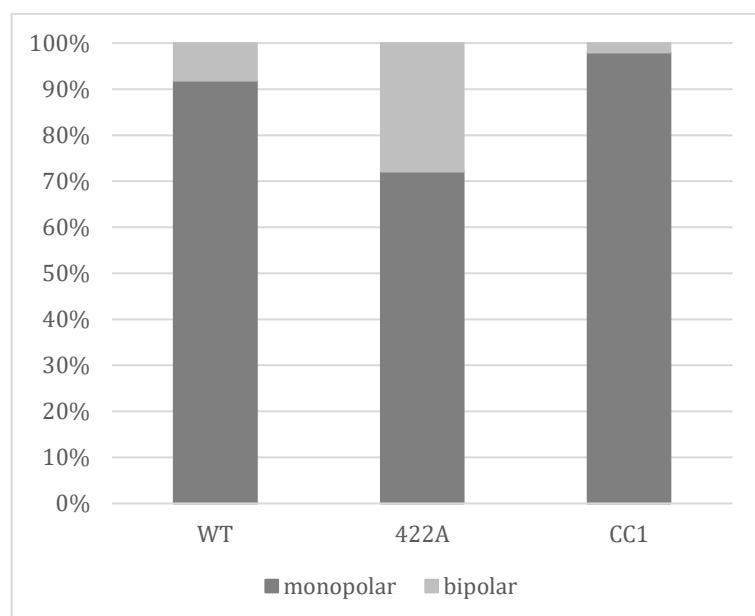


**Figure 39.** Amount of monopolar and bipolar spindles in cell lines. STLC treatment 0,5  $\mu$ M.

**Table 7.** Monopolar and bipolar cells in each cell line after 5  $\mu$ M STLC treatment. Immunofluorescence.

	WT	422A	WT/DCTN
monopolar	149	124	150
bipolar	1	28	0
%/bipolar	0,67	18,4	0

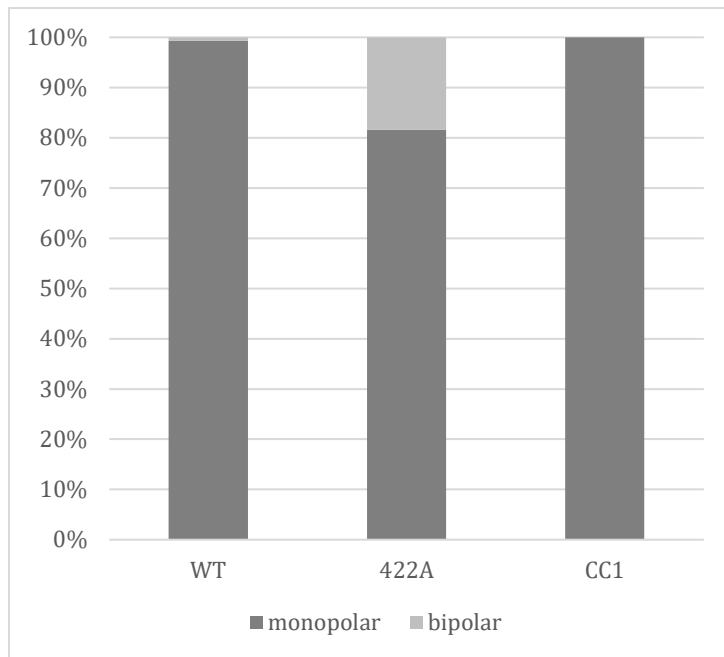


**Figure 40.** Amount of monopolar and bipolar spindles in cell lines. STLC treatment 5  $\mu$ M.

### 3.10. Establishment of bipolarity is due to CENP-E's phosphorylation state, not activity

To test whether the establishment of bipolarity upon STLC treatment in U2OS-GFP-CENP-E-422A cells is due to CENP-E activity or its phosphorylation state, in addition to STLC, CENP-E inhibitor was also added (3 hours prior fixing, figure 41). The amount of bipoles was 46% in the cells treated with 0,5  $\mu$ M STLC, and 45% in the cells treated with 0,5  $\mu$ M STLC+ 20nM CENP-E inhibitor (table 8, figure 42). When 5 $\mu$ M STLC was used, 21,4% in STLC treated, and 20,75% in 5  $\mu$ M STLC+ 20nM CENP-E inhibitor, which shows no significant differences (table 9, figure 43). Thus, the phenotype is a result of CENP-E phosphorylation state, rather than its activity.

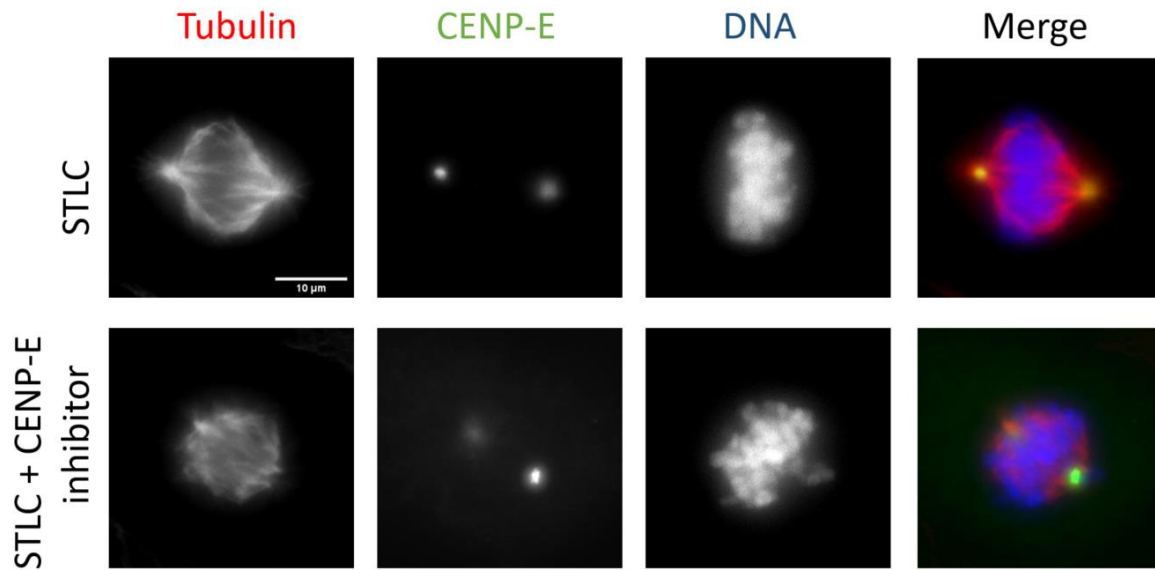


**Figure 41.** Establishment of bipolarity is due to CENP-E's phosphorylation state, not activity Red: tubulin, green: GFP- CENP-E, blue: DNA. List of used antibodies in tables 2 and 3. N (cells)=52 for 5 $\mu$ M STLC treatment, N (cells)=51 for 5 $\mu$ M STLC + 20 nM CENP-E inhibitor.

**Table 8.** Monopolar and bipolar cells in each cell line after 0,5  $\mu$ M STLC and 0,5  $\mu$ M STLC and 20nM CENP-E inhibitor treatment. Immunofluorescence.

	422a+STLC 0,5 $\mu$ M	422a+STLC 0,5 $\mu$ M + 20 nM CENP-E inhibitor
monopolar	28	28
bipolar	24	23
%/bipolar	46	45

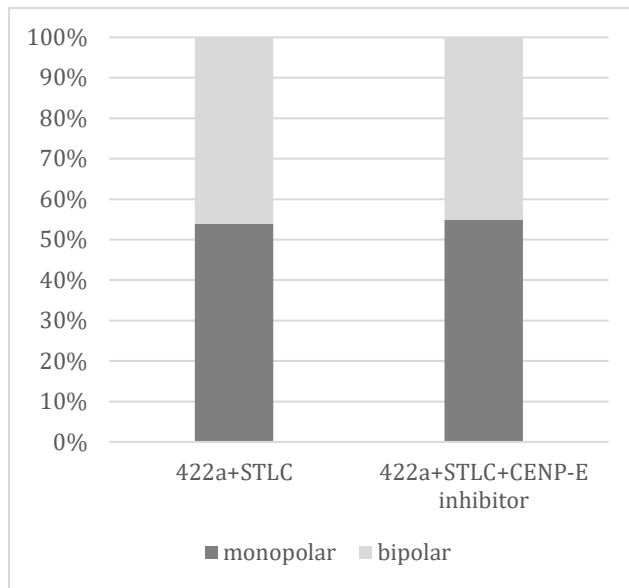


**Figure 42.** Amount of monopolar and bipolar spindles in cell lines. STLC treatment 0,5  $\mu$ M, CENP-E inhibitor 20 nM.

**Table 9.** Monopolar and bipolar cells in each cell line after 5  $\mu$ M STLC and 5  $\mu$ M STLC and 20nM CENP-E inhibitor treatment. Immunofluorescence.

	422a+STLC 5 $\mu$ M	422a+STLC 5 $\mu$ M + 20 nM CENP-E inhibitor
monopolar	44	42
bipolar	12	11
%/bipolar	21,43%	20,75%

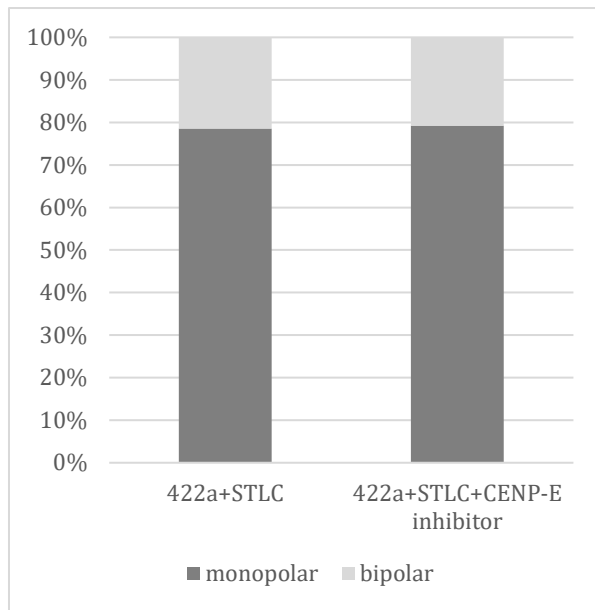


**Figure 43.** Amount of monopolar and bipolar spindles in cell lines. STLC treatment 5  $\mu$ M, CENP-E inhibitor 20 nM.

## 4. Discussion

In this work, I propose that phosphorylation of a conserved residue (T422) of CENP-E by Aurora kinases A and B has a role in Dynein-mediated stripping of CENP-E from the kinetochores. Kim et al. (2010) proposed that T422 phosphorylation has a role in controlling CENP-E directionality and activating the motor protein when transferring pole-proximal chromosomes to the metaphase plate during mitosis. They showed, that this consensus site in CENP-E gets phosphorylated by both Aurora kinases A and B, and identified a docking motif for PP1 that overlaps T422. They proposed an Aurora/PP1 phosphorylation switch that modulates motor properties of CENP-E, thus regulating congression of polar chromosomes. When at the poles, CENP-E is phosphorylated by Aurora A, and as it glides along k-fibers of already bioriented chromosomes, it moves away from the Aurora A gradient. Once away from the Aurora A concentration, it binds PP1 and is dephosphorylated. The group proposed that at the metaphase plate, the absence of tension on improperly attached chromosomes (monooriented or sintelically attached) brings CENP-E in close proximity of an Aurora B pool, allowing its phosphorylation. This phosphorylation would then have a role in modulating processivity of CENP-E attached to kinetochores with reduced tension. Furthermore, Aurora B- dependent phosphorylation in and around the inner centromeres of sister kinetochores would destabilize incorrect attachments of CENP-E to microtubules that reach across the inter-kinetochore space.

The Dynein/Dynactin complex has a long-proposed role in stripping of kinetochore substrates once bi-orientation of chromosomes is achieved (Howell, 2001), and it is already established that CENP-E motors are displaced from kinetochores as end-on attachments and bi-orientation is established (Bancroft, 2015; Hoffman, 2001). In 2019, Auckland and McAinsh confirmed CENP-E as one of the substrates being stripped from the kinetochore in a Dynein-dependent manner. They proposed, that CENP-F acts as a dynein-brake, which limits the rate of CENP-E stripping through physical interaction with dynein regulators Nde1/Ndel1/Lis1 (Stehman, 2007; Vergnolle and Taylor, 2007). They suggest that unloading of CENP-E is happening in two phases. First, as kinetochores transition from being unattached to being laterally attached to the microtubules, the corona is contracted, and this unloads a third of the motor pool. As the lateral attachments are converted to end-on and subsequently bi-oriented attachments, dynein strips away a further ~50% of the remaining CENP-E. Loss of the CENP-F dynein-brake enables the rest to be stripped.



Under treatment with Aurora A inhibitor, a significant increase in the amount of CENP-E signal at the poles (p value < 0.05, (\*), figure 17, B) can be noticed. Kim et al. (2010) obtained similar results but interpreted that the higher levels of CENP-E at the poles originate from uncongressed chromosomes, which are trapped at the poles upon CENP-E inactivation. As it can be seen in figure 17, A), a sample of cells without congression problems was selected, and CENP-E can be detected at the poles. Moreover, to confirm CENP-E localization at the poles, an STLC treatment was performed (causes monopolar spindles) and in all phosphonull cells CENP-E is located at the poles (figures 20, 35, 37), which brings a further confirmation that localization at the poles is not due to uncongressed chromosomes. When Aurora B is inhibited (figure 17), CENP-E is at the kinetochores, and cells show significant congression problems, which is in line with an already established role of Aurora B in correction of erroneous kinetochore-microtubule attachments. When microtubule tracks were eliminated (nocodazole treatment, figures 18 and 19), both in U2OS parental (under treatment with Aurora inhibitors) and in U2OS cells stably expressing CENP-E (WT and 422A phosphonull mutant), CENP-E could not be removed from kinetochores, indicating that the accumulation of CENP-E-422A at the poles depended on its transport along the microtubules. U2OS cells with inhibited Aurora A and phosphonull cell line show same phenotype, confirming the role of Aurora A in keeping CENP-E at the kinetochores.

When testing a potential role of different proteins in CENP-E stripping from the kinetochores, the results were versatile. In the scenario where p150 and NuMa were knocked-down, the results were in line with the predictions – a smaller amount of CENP-E was present on the poles. In DHC KD, the expected result was less CENP-E at the poles in the 422A cell line – if dynein is the one stripping CENP-E towards the poles, KD of a dynein subunit should reduce the amount of CENP-E being stripped towards the poles. Instead, the results indicate more CENP-E at the spindle poles. As for Spindly, once it is depleted, CENP-E phosphonull no longer localizes at the poles – it stays at the kinetochores. Moreover, when looking at p150 localization in comparison to CENP-E, in control, DHC and NuMa knock-downs they seem to colocalize. In other cell lines they do not seem to colocalize. When Spindly is knocked down, they no longer colocalize in the 422A cell line. That insinuates that Spindly is the mediator between CENP-E and Dynein/Dynactin complex – when Spindly is depleted, there is no CENP-E stripping (figures 22-25). An immunoprecipitation was performed to find direct CENP-E interactors, but it wasn't successful.

The recurrence of bipolar cells after STLC treatment in the phosphonull cell line (figures 20, 35, 37) raised some new questions. A potential answer comes from Raaajmakers et al. in 2013. STLC is an inhibitor of Eg-5, which is a key player in bipolar spindle assembly. It does so by

sliding anti- parallel microtubules apart (Kashina, 1996; Kapitein, 2005). Without Eg5 activity, human cells fail to separate their centrosomes and form a monopolar spindle (Sawin, 1992; Blangy, 1995; Kashina, 1996). The authors have shown that dynein can antagonize the outward force in the spindle generated by Eg5, as inhibition of Dynein function was shown to rescue spindle bipolarity in Eg5-inhibited cells (Mitchison, 2005; Tanenbaum, 2008; Ferenz, 2009). When DHC is depleted in cells under STLC treatment, a large fraction of cells form bipolar spindles (Raaajimakers, 2013; Tanenbaum, 2008). Depletion of the dynein subunits DIC2, Roadblock-1, and DLIC1/DLIC2 also leads to a prominent rescue of spindle bipolarity in STLC-treated cells. As we proposed the potential interaction between CENP-E and the LIC domain of dynein, it might be that, when dephosphorylated and accumulated at the poles, CENP-E could sequester dynein, consequently triggering an inhibitory effect. Moreover, there was no difference in amount of established bipoles when CENP-E was inhibited in STLC-treated cells, indicating that the bipolarity recurrence is due to the phosphorylation state of CENP-E, rather than its motor activity. Altogether, this goes in line with the hypothesis that dephosphorylated CENP-E interacts with dynein, whereas T422 phosphorylation disrupts CENP-E/Dynein interaction.

## 5. Conclusions

Bringing the obtained results in consideration, a conclusion can be drawn that phosphorylation of CENP-E by Aurora kinases has a role in preventing premature stripping of CENP-E from kinetochores during mitosis. T422 phosphorylation disrupts binding of components of the dynein/dynactin complex and CENP-E can not be stripped. As chromosomes bi-orient, and proper kinetochore-microtubule attachment and tension is achieved, CENP-E is being displaced from the region of Aurora B activity. PP1 then dephosphorylates CENP-E and it is able to interact with the dynein/dynactin complex, thus getting stripped polewards in a dynein-dependent manner. Although further analysis is needed, the results strongly suggest that the accumulation of CENP-E-T422A at the poles is dynein-driven and that Aurora-dependent phosphorylation of CENP-E might serve to protect CENP-E from being prematurely stripped from kinetochores by dynein.

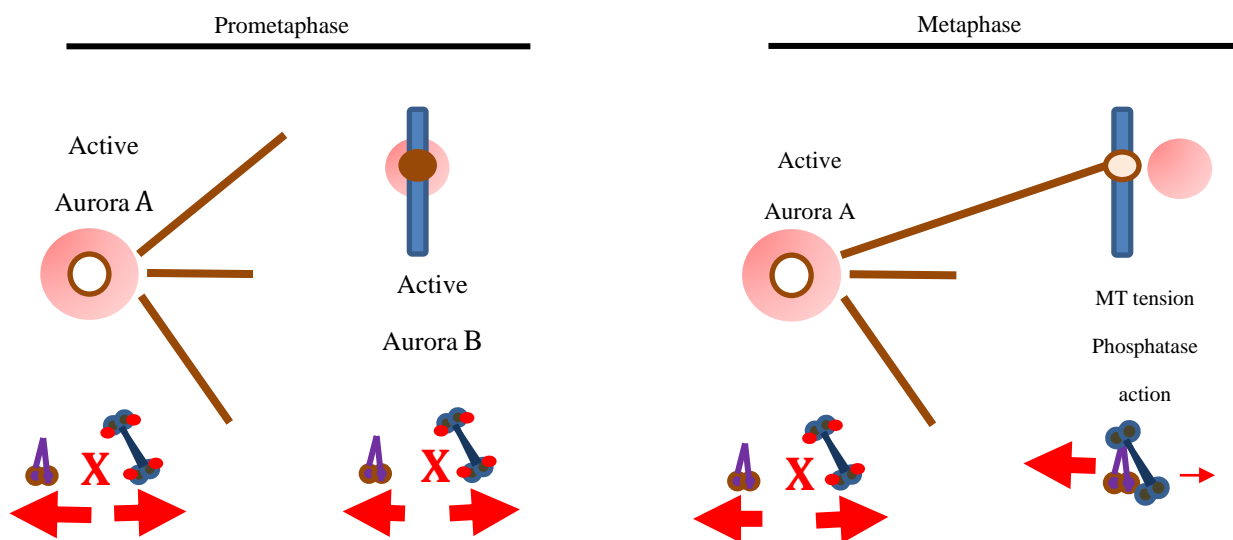


**Figure 44.** A proposed model of regulation of Dynein-mediated stripping of CENP-E by phosphorylation by Aurora kinases A and B. At the poles, CENP-E is in the vicinity of an Aurora A gradient, and is phosphorylated in T422. Once it moves away from the poles, PP1 binds to CENP-E and dephosphorylates it. At unattached kinetochores, CENP-E reaches into the Aurora B pool, and gets phosphorylated. The phosphorylation disrupts its interaction with Dynein/Dynactin complex. Once chromosomes bi-orient, and proper kinetochore tension is achieved, CENP-E is being displaced from the Aurora B pool. PP1 dephosphorylates CENP-E and it can now interact with the Dynein/Dynactin complex and be stripped polewards (modified from Eibes S., unpublished).

## 6. References

- Adams R. R., Maiato H., Earnshaw W. C., Carmena M. (2001): Essential roles of *Drosophila* inner centromere protein (INCENP) and Aurora-B in histone H3 phosphorylation, metaphase chromosome alignment, kinetochore disjunction, and chromosome segregation. *J. Cell Biol.* 153:865–880.
- Alberts B., Johnson A., Lewis J., Morgan D., Raff M., Roberts K., Walter P. (2004): *Molecular biology of the Cell*. Garland Science.
- Alushin G.M., Ramey V.H., Pasqualato S., Ball D.A., Grigorieff N., Musacchio A., Nogales E. (2010): The Ndc80 kinetochore complex forms oligomeric arrays along microtubules. *Nature* 467:805–810.
- Andrews P.D., Ovechkina Y., Morrice N., Wagenbach M., Duncan K., Wordeman L., Swedlow J. R. (2004): Aurora B regulates MCAK at the mitotic centromere. *Dev. Cell* 6:253-268.
- Auckland P, McAinsh A. P.. (2019): CENP-F controls force generation and dynein dependant stripping of CENP-E at the kinetochores. 10.1101/627380.
- Bakhoun S.F., Silkworth W.T., Nardi I.K., Nicholson J.M., Compton D.A., Cimini D. (2014): The mitotic origin of chromosomal instability. *Curr. Biol.* 24:148–149.
- Bakhoun S.F., Compton D.A. (2012): Chromosomal instability and cancer: a complex relationship with therapeutic potential. *J. Clin. Invest.* 122:1138–1143.
- Barisic M., Aguiar P., Geley S., Maiato H. (2014): Kinetochore motors drive congression of peripheral polar chromosomes by overcoming random armejection forces. *Nat. Cell Biol.* 16:1249-1256.
- Barisic M., Geley S. (2011): Spindly switch controls anaphase: Spindly and RZZ functions in chromosome attachment and mitotic checkpoint control. *Cell Cycle* 10:449–456.
- Barisic M., Silva e Sousa R., Tripathy S.K., Magiera M.M., Zaytsev A.V., Pereira A.L., Janke C., Grishchuk E.L., Maiato H. (2015): Mitosis. Microtubule detyrosination guides chromosomes during mitosis. *Science* 348:799-803.
- Barr A.R., Gergely F. (2007): Aurora-A: the maker and breaker of spindle poles. *J Cell Sci.* 120: 2987–96.

- Barros T.P., Kinoshita K., Hyman A.A., Raff J.W. (2005): Aurora A activates D-TACC-Msps complexes exclusively at centrosomes to stabilize centrosomal microtubules. *J Cell Biol.* 170:1039–46.
- Basto R., Scaerou F., Mische S., Wojcik E., Lefebvre C., Gomes R., Hays T., Karess, R. (2004): In vivo dynamics of the rough deal checkpoint protein during *Drosophila* mitosis. *Curr. Biol.* 14:56-61.
- Belmont L.D., Hyman A.A., Sawin K.E., Mitchison T.J. (1990): Real-time visualization of cell cycle-dependent changes in microtubule dynamics in cytoplasmic extracts. *Cell* 63:579-589.
- Biology of the Cell, 6th edition. New York, Garland Science.
- Booth D.G., Hood F.E., Prior I.A., Royle S.J. (2011): A TACC3/ch-TOG/clathrin complex stabilises kinetochore fibres by inter-microtubule bridging. *EMBO J.* 30:906-919.
- Brouhard G.J., Hunt A.J. (2005): Microtubule movements on the arms of mitotic chromosomes: Polar ejection forces quantified in vitro. *Proc. Natl. Acad. Sci.* 102:13903–13908.
- Brown K.D., Coulson R.M., Yen T.J., Cleveland D.W. (1994): Cyclin-like accumulation and loss of the putative kinetochore motor CENP-E results from coupling continuous synthesis with specific degradation at the end of mitosis. *J. Cell Biol.* 125:1303-1312.
- Brust-Mascher I., Scholey J.M. (2011): Mitotic motors and chromosome segregation: The mechanism of anaphase B. *Biochem Soc Trans* 39:1149-1153.
- Brust-Mascher I., Sommi P., Cheerambathur D.K., Scholey J.M. (2009): Kinesin-5-dependent poleward flux and spindle length control in *Drosophila* embryo mitosis. *Mol. Biol. Cell.* 20:1749–1762.
- Buffin E., Lefebvre, C., Huang, J., Gagou, M.E., Karess, R.E. (2005): Recruitment of Mad2 to the kinetochore requires the Rod/Zw10 complex. *Curr. Biol.* 15:856–861.
- Caballe, A. (2015): ULK3 regulates cytokinetic abscission by phosphorylating ESCRT-III proteins. *Elife* 4, e06547.
- Cai S., O'Connell C.B., Khodjakov A., Walczak C.E. (2009): Chromosome congression in the absence of kinetochore fibres. *Nat. Cell Biol.* 11:832-838
- Caldas G.V., Lynch T.R., Anderson R., Afreen S., Varma D., DeLuca J.G. (2015): The RZZ complex requires the N-terminus of KNL1 to mediate optimal Mad1 kinetochore localization in human cells. *Open Biol.* 5:110-119.

- Carlton J. G., Caballe A., Agromayor M., Kloc M., Martin-Serrano, J. (2012): ESCRT-III governs the Aurora B-mediated abscission checkpoint through CHMP4C. *Science* 336:220–225.
- Carmena M., Earnshaw W.C. (2003): The cellular geography of Aurora kinases. *Nat. Rev. Mol. Cell Biol.* 1:842.
- Carmena M., Ruchaud S., Earnshaw W.C. (2009): Making the Auroras glow: regulation of Aurora A and B kinase function by interacting proteins. *Curr. Opin. Cell Biol.* 21:796–805.
- Carmena M., Wheelock M., Funabiki H., Earnshaw W.C. (2012): The chromosomal passenger complex (CPC): from easy rider to the godfather of mitosis. *Nat. Rev. Mol. Cell Biol.* 13:789–803
- Carvalho, A., Carmena, M., Sambade, C., Earnshaw, W. C., Wheatley, S. P. (2003): Survivin is required for stable checkpoint activation in taxol-treated HeLa cells. *J. Cell Sci.* 116:2987–2998.
- Chan E.H.Y., Santamaria A., Silljé H.H.W., Nigg E.A. (2008): Plk1 regulates mitotic Aurora A function through  $\beta$ TrCP-dependent degradation of hBora. *Chromosoma* 117:457–69.
- Chan G.K., Schaar B.T., Yen T.J. (1998): Characterization of the kinetochore binding domain of CENP-E reveals interactions with the kinetochore proteins CENP-F and hBUBR1. *J. Cell Biol.* 143:49–63
- Chao W.C.H. (2012): Structure of the mitotic checkpoint complex. *Nature* 484:208–213.
- Cheeseman I. (2014): The kinetochore. *Cold Spring Harb. Perspect Biol.* 6: a015826.
- Cheeseman I.M., Anderson S., Jwa M., Green E.M., Kang J., Yates J.R., Chan C.S., Drubin D.G., Barnes G. (2002): Phospho-regulation of kinetochore-microtubule attachments by the Aurora kinase Ipl1p. *Cell* 111:163–172.
- Cheeseman I.M., Chappie J.S., Wilson-Kubalek E.M., Desai A. (2006): The conserved KMN network constitutes the core microtubule-binding site of the kinetochore. *Cell* 127:983–997.
- Cheeseman I.M., Desai A. (2008): Molecular architecture of the kinetochore-microtubule interface. *Nature Reviews Molecular Cell Biology* 9:33–46.
- Cheeseman, I.M., Niessen, S., Anderson, S., Hyndman, F., Yates, J.R., Oegema, K., Desai, A. (2004): A conserved protein network controls assembly of the outer kinetochore and its ability to sustain tension. *Genes Dev.* 18:2255–2268.

Chen H.Z., Tsai S.Y., Leone G. (2009): Emerging roles of E2Fs in cancer: an exit from cell cycle. *Nat. Rev. Cancer* 9:785-797.

Chou, Y.H., Bischoff, J.R., Beach, D., Goldman, R.D. (1990): Intermediate filament reorganization during mitosis is mediated by p34cdc2 phosphorylation of vimentin. *Cell* 62:1063–1071.

Cimini, D. (2014): The mitotic origin of chromosomal instability. *Curr. Biol.* 24:148–149.

Cohen-Fix, O., Peters J.M., Kirschner, D. (1996): Anaphase initiation in *saccharomyces cerevisiae* is controlled by the APC-dependent degradation of the anaphase inhibitor Pds1p. *Genes Dev.* 10:3081–3093.

Cooke C.A., Schaar B., Yen T.J., Earnshaw W.C. (1997): Localization of CENP-E in the fibrous corona and outer plate of mammalian kinetochores from prometaphase through anaphase. *Chromosoma* 106:446-455.

Coue M., Lombillo V.A., McIntosh J.R. (1991): Microtubule depolymerization promotes particle and chromosome movement in vitro. *J. Cell Biol.* 112: 1165–1175.

Cowley D.O., Rivera-Pérez J.A., Schliekelman M., He Y.J., Oliver T.G., Lu L. (2009): Aurora-A kinase is essential for bipolar spindle formation and early development. *Mol. Cell Biol.* 29(4):1059–71.

Cuylen, S. (2013) Entrapment of chromosomes by condensin rings prevents their breakage during cytokinesis. *Dev. Cell* 27:469–478.

Dai J., Sullivan B.A., Higgins J.M.G. (2006): Regulation of mitotic chromosome cohesion by haspin and Aurora B. *Dev Cell.* 11:741–50.

Damodaran A.P., Vaufrey L., Gavard O., Prigent C. (2017): Aurora A kinase is a priority pharmaceutical target for the treatment of cancers. *Trends Pharmacol. Sci.* 38:687–700.

De Luca M., Brunetto L., Asteriti I.A., Giubettini M., Lavia P., Guarguaglini G. (2008): Aurora-A and ch-TOG act in a common pathway in control of spindle pole integrity. *Oncogene* 27:6539–49.

De Wulf, P., McAinsh, A.D., Sorger, P.K. (2003): Hierarchical assembly of the budding yeast kinetochore from multiple subcomplexes. *Genes Dev.* 17:2902–2921.

DeLuca, J.G., Gall, W.E., Ciferri, C., Cimini D., Musacchio A., Salmon E.D. (2006): Kinetochore microtubule dynamics and attachment stability are regulated by Hec1. *Cell* 127:969-982.

DeLuca, K.F., Lens, S.M., DeLuca, J.G. (2011): Temporal changes in Hec1 phosphorylation control kinetochore-microtubule attachment stability during mitosis. *J. Cell Sci.* 124:622-634.

DeLuca K.F., Meppelink A., Broad A.J., Mick J.E., Peersen O.B., Pektas S., Lens S.M.A., DeLuca J.G. (2017): Aurora A kinase phosphorylates Hec1 to regulate metaphase kinetochore-microtubule dynamics. *J. Cell Biol.* 217:163-177.

Dephoure N., Zhou C., Villén J., Beausoleil S.A., Bakalarski C.E., Elledge S.J. (2008): A quantitative atlas of mitotic phosphorylation. *Proc. Natl. Acad. Sci.* 105:10762–7.

der Horst A., Vromans M.J.M., Bouwman K., van der Waal M.S., Hadders M.A., Lens S.M.A. (2015): Inter-domain cooperation in INCENP promotes Aurora B relocation from centromeres to microtubules. *Cell Rep.* 12(3):380–7.

Dimitrova, Y.N.; Jenni, S.; Valverde, R.; Khin, Y.; Harrison, S.C. St Wei, R.R.; Al-Bassam, J.; Harrison, S.C. The Ndc80/HEC1 complex is a contact point for kinetochoremicrotubule attachment. *Nat. Struct. Mol. Biol.* 2007, 14, 54–59.

Dong Y., Vanden Beldt K.J., Meng X., Khodjakov A., McEwen B.F. (2007): The outer plate in vertebrate kinetochores is a flexible network with multiple microtubule interactions. *Nat. Cell Biol.* 9:516-522.

Dou Z., von Schubert C., Korner R., Santamaria A., Elowe S., Nigg, E.A. (2011): Quantitative mass spectrometry analysis reveals similar substrate consensus motif for human Mps1 kinase and Plk1. *PLoS ONE* 6: e18793.

Dynlacht B.D., Moberg K., Lees J.A., Harlow E., Zhu L. (1997): Specific regulation of E2F family members by cyclin-dependent kinases. *Mol. Cell Biol.* 17:3867-75.

Echeverri C.J., Paschal B.M., Vaughan K.T., Vallee R.B. (1996): Molecular characterization of the 50-kD subunit of dynactin reveals function for the complex in chromosome alignment and spindle organization during mitosis. *J. Cell Biol.* 132:617-633.

Foley E.A., Kapoor T.M. (2012): Microtubule attachment and spindle assembly checkpoint signalling at the kinetochore. *Nat. Rev. Mol. Cell Biol.* 14:25–37.



Fung T.K., Poon R.Y. (2005): A roller coaster ride with the mitotic cyclins. *Semin. Cell. Dev. Biol.* 16:335-342.

Gachet Y., Reyes C., Tournier S. (2016): Aurora B kinase controls the separation of centromeric and telomeric heterochromatin. *Mol. Cell. Oncol.* 3:1043039.

Gama J.B., Pereira C., Simões P.A. (2017): Molecular mechanism of dynein recruitment to kinetochores by the Rod-Zw10-Zwilch complex and Spindly. *J. Cell Biol.* 216:943–960

Ganem, N.J., Pellman, D. (2012): Linking abnormal mitosis to the acquisition of DNA damage. *J. Cell Biol.* 199:871–881.

Garcia-Saez I., Yen T., Wade R.H., Kozielski F. (2004): Crystal structure of the motor domain of the human kinetochore protein CENP-E. *J. Mol. Biol.* 340:1107-1116

Gascoigne K.E., Takeuchi K., Suzuki A., Hori T., Fukagawa T., Cheeseman I.M. (2011). Induced ectopic kinetochore assembly bypasses the requirement for CENP-A nucleosomes. *Cell* 145:410-422.

Gassmann, R. (2004): Borealin: a novel chromosomal passenger required for stability of the bipolar mitotic spindle. *J. Cell Biol.* 166, 179–191.

Giet R., McLean D., Descamps S., Lee M.J., Raff J.W., Prigent C. (2002): *Drosophila* Aurora A kinase is required to localize D-TACC to centrosomes and to regulate astral microtubules. *J. Cell Biol.* 156:437–51.

Giet R., Prigent C. (2001): The non-catalytic domain of the *Xenopus laevis* aurora A kinase localises the protein to the centrosome. *J Cell Sci.* 114(11):2095-2104.

Glötzer M. (2016): Cytokinesis in fungi and metazoa. *Cold Spring Harb Perspect Biol* 9(10). pii: a022343

Glover D.M., Leibowitz M.H., Mclean D.A., Parry H. (1995): Mutations in aurora prevent centrosome separation leading to the formation of monopolar spindles. *Cell* 81:95–105.

Gruneberg U., Neef R., Honda R., Nigg E.A., Barr F.A. (2004): Relocation of Aurora B from centromeres to the central spindle at the metaphase to anaphase transition requires MKlp2. *J Cell Biol.* 166:167–72.

Gudimchuk N., Tarasovets E.V., Mustyatsa V., Drobyshev A.L., Vitre B., Cleveland D.W., Ataullakhanov F.I., Grishchuk E.L. (2018): Probing Mitotic CENP-E Kinesin with the Tethered Cargo Motion Assay and Laser Tweezers. *Biophys. J.* 114:2640-2652.

Gulluni F., Martini M., De Santis M.C., Campa C.C., Ghigo A., Margaria J.P., Ciruolo E., Franco I., Ala U., Annaratone L. (2017): Mitotic spindle assembly and genomic stability in breast cancer require PI3K-C2alpha scaffolding function. *Cancer Cell* 32:444-459.

Gupta S., Mana-Capelli S., McLean J.R., Chen C.T., Ray S., Gould K.L., McCollum D. (2013): Identification of SIN pathway targets reveals mechanisms of crosstalk between NDR kinase pathways. *Curr. Biol.* 23:333–338.

Hammond JW, Huang CF, Kaech S, Jacobson C, Banker G, Verhey KJ. (2010): Posttranslational modifications of tubulin and the polarized transport of kinesin-1 in neurons. *Mol Biol Cell.* 21:572–583.

Hannak E., Kirkham M., Hyman A.A., Oegema K. (2001): Aurora-A kinase is required for centrosome maturation in *Caenorhabditis elegans*. *J. Cell Biol.* 155(7):1109–15.

Hardwick K.G., Murray A.W. (1995): Mad1p, a phosphoprotein component of the spindle assembly checkpoint in budding yeast. *J. Cell Biol.* 131:709–720.

Hartwell L.H., Weinert T.A. (1989): Checkpoints: controls that ensure the order of cell cycle events. *Science* 246:629-634.

Henley S.A., Dick F.A. (2012) The retinoblastoma family of proteins and their regulatory functions in the mammalian cell division cycle. *Cell Div.* 14:7-10.

Herzog F. (2009): Structure of the anaphase-promoting complex/cyclosome interacting with a mitotic checkpoint complex. *Science* 323:1477–1481.

Hinchcliffe E.H., Sluder G. (2001) “It takes two to tango”: understanding how centrosome duplication is regulated throughout the cell cycle. *Genes Dev.* 15:1167-1181.

Hirota T., Kunitoku N., Sasayama T., Marumoto T., Zhang D., Nitta M. (2003): Aurora-A and an interacting activator, the LIM protein Ajuba, are required for mitotic commitment in human cells. *Cell* 114(5):585–98.

Hoffman D.B., Pearson C.G., Yen T.J., Howell B.J., Salmon E.D. (2001): Microtubule-dependent changes in assembly of microtubule motor proteins and mitotic spindle checkpoint proteins at PtK1 kinetochores. *Mol. Biol. Cell* 12:1995-2009.

Holland, A.J. and Cleveland D.W. (2012): Losing balance: the origin and impact of aneuploidy in cancer. *EMBO Rep.* 13:501–514.

Honda, R., Korner, R., Nigg, E. A. (2003): Exploring the functional interactions between Aurora B, INCENP, and survivin in mitosis. *Mol. Biol. Cell* 14, 3325–3341.

Hoyt M.A. (2001): A new view of the spindle checkpoint. *J. Cell Biol.* 154:909–911.

Hsu L.C., White R.L. (1998): BRCA1 is associated with the centrosome during mitosis. *Proc. Natl. Acad. Sci.* 95:12983–12988.

Huis In 't Veld P.J., Jeganathan S., Petrovic A., Singh P., John J., Krenn V., Weissmann F., Bange T., Musacchio A. (2016): Molecular basis of outer kinetochore assembly on CENP-T. *eLife* 5 e21007.

Hutterer A., Berdnik D., Wirtz-Peitz F., Žigman M., Schleiffer A., Knoblich J.A. (2006): Mitotic activation of the kinase Aurora-A requires its binding partner bora. *Dev. Cell.* 11:147–57.

Iemura K., Tanaka, K. (2015): Chromokinesin Kid and kinetochore kinesin CENP-E differentially support chromosome congression without end-on attachment to microtubules. *Nat. Commun.* 6:6447

Jang C.Y., Coppinger J.A., Seki A., Yates J.R, Fang G. (2009): Plk1 and Aurora A regulate the depolymerase activity and the cellular localization of Kif2a. *J. Cell Sci.* 122(9):1334–1341.

Janssen, A. (2011) Chromosome segregation errors as a cause of DNA damage and structural chromosome aberrations. *Science* 333:895–898.

Jelluma, N. (2010) Release of Mps1 from kinetochores is crucial for timely anaphase onset. *J. Cell Biol.* 191:281–290.

Jokelainen P.T. (1967): The ultrastructure and spatial organization of the metaphase kinetochore in mitotic rat cells. *J. Ultrastruct. Res.* 19:19-44.

Kalinina I., Nandi A., Delivani P., Chacon M.R., Klemm A.H, Ramunno- Johnson D., Krull A., Lindner B., Pavin N., Tolic-Nørrelykke I.M. (2013): Pivoting of microtubules around the spindle pole accelerates kinetochore capture. *Nat. Cell Biol.* 15:82–87.

Kamasaki T., O'Toole E., Kita S., Osumi M., Usukura J., McIntosh J.R., Goshima G. (2013): Augmin-dependent microtubule nucleation at microtubule walls in the spindle. *J. Cell Biol.* 202:25–33.

- Kapitein L.C., Peterman E.J.G., Kwok B.H., Kim J.H., Kapoor T.M., Schmidt C.F. (2005): The bipolar mitotic kinesin Eg5 moves on both microtubules that it crosslinks. *Nature* 435(7038):114–8.
- Kapoor T.M., Lampson M.A., Hergert P., Cameron L., Cimini D., Salmon D., McEwen B.F., Khodjakov A. (2006): Chromosomes can congress to the metaphase plate before biorientation. *Science* 311:388–391.
- Khodjakov A., Cole R.W., Oakley B.R., Rieder C.L. (2000): Centrosome-independent mitotic spindle formation in vertebrates. *Curr. Biol.* 10:59–67.
- Khodjakov A., Rieder C.L. (2009): Mitosis: Too much of a good thing (can be bad). *Curr. Biol.* 19:1032–1034.
- Kim S., Yu H. (2015): Multiple assembly mechanisms anchor the KMN spindle checkpoint platform at human mitotic kinetochores. *J. Cell Biol.* 208:181-196.
- Kim Y., Heuser J.E., Waterman C.M., Cleveland D.W. (2008): CENP-E combines a slow, processive motor and a flexible coiled coil to produce an essential motile kinetochore tether. *J. Cell Biol.* 181:411-419
- Kim Y., Holland A.J., Lan W., Cleveland D.W. (2010): Aurora kinases and protein phosphatase 1 mediate chromosome congression through regulation of CENP-E. *Cell* 142:444-455
- Kinoshita K, Noetzel TL, Pelletier L, Mechtler K, Drechsel DN, Schwager A. (2005): Aurora A phosphorylation of TACC3/maskin is required for centrosome-dependent microtubule assembly in mitosis. *J Cell Biol.* 170:1047–55.
- Kinoshita K., Noetzel T.L., Pelletier L., Mechtler K., Drechsel D.N., Schwager A. (2005): Aurora A phosphorylation of TACC3/maskin is required for centrosome-dependent microtubule assembly in mitosis. *J Cell Biol.* 170:1047–55.
- Kirschner M., Mitchison T. (1986): Beyond self-assembly: From microtubules to morphogenesis. *Cell* 45:329–342.
- Kitamura E., Tanaka K., Komoto S., Kitamura Y., Antony C., Tanaka T.U. (2010): Kinetochores generate microtubules with distal plus ends: Their roles and limited lifetime in mitosis. *Dev. Cell* 18:248–259.
- Kline-Smith S.L., Khodjakov A., Hergert P., Walczak C.E. (2004): Depletion of centromeric MCAK leads to chromosome congression and segregation defects due to improper kinetochore attachments. *Mol. Biol. Cell* 15(3):1146-1159.

- Kops, G.J.; Kim, Y.; Weaver, B.A.; Mao, Y.; McLeod, I.; Yates, J.R., 3rd; Tagaya, M.; Cleveland, D.W. (2005): ZW10 links mitotic checkpoint signaling to the structural kinetochore. *J. Cell Biol.* 169:49–60.
- Kuhn J., Dumont S. (2017): Spindle assembly checkpoint satisfaction occurs via end-on but not lateral attachments under tension. *J. Cell Biol.* 216:1533-1542.
- Kumar A., Purohit R. (2012): Computational screening and molecular dynamics simulation of disease associated nsSNPs in CENP-E. *Mutat. Res.* 738:28-37.
- Lafaurie-Janvore, J. (2013): ESCRT-III assembly and cytokinetic abscission are induced by tension release in the intercellular bridge. *Science* 339:1625–1629.
- LaFountain J.R., Cohan C.S., LaFountain D.J. (2004): Direct visualization of microtubule flux during metaphase and anaphase in crane-fly spermatocytes. *Mol. Biol. Cell* 15:5724–5732.
- Lan W., Zhang X., Kline-Smith S.L., Rosasco S.E., Barrett-Wilt G.A., Shabanowitz J. (2004): Aurora B phosphorylates centromeric MCAK and regulates its localization and microtubule depolymerization activity. *Curr. Biol.* 14:273–86.
- Lawrence C.J., Dawe R.K., Christie K.R., Cleveland D.W., Dawson S.C., Endow S.A., Goldstein L.S., Goodson H.V., Hirokawa N., Howard J., Malmberg R.L., McIntosh J.R., Miki H., Mitchison T.J., Okada Y., Reddy A.S., Saxton W.M., Schliwa M., Scholey J.M., Vale R.D., Walczak C.E., Wordeman L. (2004) A standardized kinesin nomenclature. *J. Cell Biol.* 167:19-22.
- Lesage B., Qian J., Bollen M. (2011): Spindle checkpoint silencing: PP1 tips the balance. *Curr. Biol.* 21(21):898-903.
- Li S., Deng Z., Fu J., Xu C., Xin G., Wu Z. (2015): Spatial compartmentalization specializes function of Aurora-A and Aurora-B. *J. Biol. Chem.* 290(28):17546-58.
- Li Y., Yu W., Liang Y., Zhu X. (2007): Kinetochore dynein generates a poleward pulling force to facilitate congression and full chromosome alignment. *Cell Research* 17:701–712
- Lindqvist A., Rodriguez-Bravo V., Medema R.H. (2009): The decision to enter mitosis: feedback and redundancy in the mitotic entry network. *J. Cell Biol.* 185(2):193-202.
- Liu D., Vleugel M., Backer C.B., Hori T., Fukagawa T., Cheeseman I.M., Lampson M.A. (2010): Regulated targeting of protein phosphatase 1 to the outer kinetochore by KNL1 opposes Aurora B kinase. *J. Cell Biol.* 188:809-820.

- Liu Q., Ruderman J.V. (2006): Aurora A, mitotic entry, and spindle bipolarity. *Proc. Natl. Acad. Sci. USA.* 103:5811–6.
- Luo, X.; Yu, H. (2004): Protein metamorphosis: The two-state behavior of Mad2. *Structure* 16:1616–1625.
- Ma H.T., Poon R.Y.C. (2011): How protein kinases co-ordinate mitosis in animal cells. *Biochem J.* 435(1):17–31.
- Mackay, D.R. (2010): Defects in nuclear pore assembly lead to activation of an Aurora B-mediated abscission checkpoint. *J. Cell Biol.* 191: 923–931 12.
- Mackay, D.R. and Ullman K.S. (2015): ATR and a Chk1–Aurora B pathway coordinate postmitotic genome surveillance with cytokinetic abscission. *Mol. Biol. Cell* 26:2217–2226.
- Magidson V., O’Connell C.B., Loncarek J., Paul R., Mogilner A., Khodjakov A. (2011): The spatial arrangement of chromosomes during prometaphase facilitates spindle assembly. *Cell* 146:555-567.
- Magidson V., Paul R., Yang N., Ault J.G., O’Connell C.B., Tikhonenko I., McEwen B.F., Mogilner A., Khodjakov A. (2015): Adaptive changes in the kinetochore architecture facilitate proper spindle assembly. *Nat. Cell Biol.* 17:1134-1144.
- Maiato, H., Afonso O., Matos I. (2015): A chromosome separation checkpoint: a midzone Aurora B gradient mediates a chromosome separation checkpoint that regulates the anaphase–telophase transition. *Bio Essays* 37:257–266
- Maldonado M., Kapoor T.M. (2011): Constitutive Mad1 targeting to kinetochores uncouples checkpoint signalling from chromosome biorientation. *Nat. Cell Biol.* 13:475–482
- Malumbres M., Harlow E., Hunt T., Lafti J.M., Manning G., Morgan D.O., Tsai L.H., Olgemuth D.J. (2009): Cyclin – dependant kinases: a family portrait, *Nat. Cell Biol.* 11:1275-1276.
- Malumbres M., Barbacid M. (2001): To cycle or not to cycle: a critical decision in cancer. *Nat. Rev. Cancer*, 1:222-231.
- Malvezzi F., Litos G., Schleiffer A., Heuck A., Mechtler K., Clausen T., Westermann S. (2013): A structural basis for kinetochore recruitment of the Ndc80 complex via two distinct centromere receptors. *EMBO J.* 32:409-423.

Manning G. (2002): The protein kinase complement of the human genome. *Science* 298:1912–1934.

Mao Y., Desai A., Cleveland D.W. (2005): Microtubule capture by CENP-E silences BubR1-dependent mitotic checkpoint signaling. *J. Cell Biol.* 170:873–880

Mapelli M., Massimiliano L., Santaguida S., Musacchio A. (2007): The Mad2 conformational dimer: structure and implications for the spindle assembly checkpoint. *Cell* 131(4):730–743.

Mapelli, M.; Musacchio, A. (2007): MAD contortions: Conformational dimerization boosts spindle checkpoint signaling. *Curr. Opin. Struct. Biol.* 17:716–725.

Martinez-Balbas M.A., Dey A., Rabindran S.K., Ozato K., Wu C. (1995): Displacement of sequence-specific transcription factors from mitotic chromatin. *Cell* 83:29–38.

Masai H., Matsumoto S., You Z., Yoshizawa- Sugata N., Oda M. (2010): Eukaryotic chromosome DNA replication: where, when, and how?. *Annu. Rev. Biochem.* 79:89–130.

McEwen B.F., Arena J.T., Frank J., Rieder C.L. (1993): Structure of the colcemid-treated PtK1 kinetochore outer plate as determined by high voltage electron microscopic tomography. *J. Cell Biol.* 120:301–312.

McEwen, B. F., Chan, G. K. T., Zubrowski, B., Savoian, M. S., Sauer, M. T. and Yen, T. J. (2001). CENP-E is essential for reliable bioriented spindle attachment, but chromosome alignment can be achieved via redundant mechanisms in mammalian cells. *Mol. Biol. Cell* 12, 2776–2789.

McIntosh J.R. (1991): Structural and mechanical control of mitotic progression. *Symp. Quant. Biol.* 56:613–619.

McIntosh J.R., McDonald K.L., Edwards M.K., Ross B.M. (1979): Three-dimensional structure of the central mitotic spindle of *Diatoma vulgare*. *J. Cell Biol.* 83: 428–442.

McIntosh J.R., Molodtsov M., Ataullakhanov F.I. (2012): Biophysics of mitosis. *Quart Rev Biophys* 45: 147–207.

McIntosh J.R., Volkov V., Ataullakhanov F.I., Grishchuk E.L. (2010): Tubulin depolymerization may be an ancient biological motor. *J Cell Sci* 123: 3425–3434.

McKenney R.J., Huynh W., Tanenbaum M.E., Bhabha G., Vale R.D. (2014): Activation of cytoplasmic dynein motility by dynactin-cargo adapter complexes. *Science* 345:337–341.

- Meraldi P., Honda R., Nigg E.A. (2002): Aurora-A overexpression reveals tetraploidization as a major route to centrosome amplification in p53<sup>-/-</sup> cells. *EMBO J.* 21(4):483-492.
- Nelson D.A., Krucher N.A., Ludlow J.W. (1997): High molecular weight protein phosphatase type 1 dephosphorylates the retinoblastoma protein. *J. Biol. Chem.* 272(7):4528-35.
- Nicklas R.B. (1997): How cells get the right chromosomes. *Science* 275:632–637.
- Nishino T., Rago F., Hori T., Tomii K., Cheeseman I.M., Fukagawa T. (2013): CENP-T provides a structural platform for outer kinetochore assembly. *EMBO J.* 32:424-436.
- Nixon F.M., Honnor T.R., Clarke N.I., Starling G.P., Beckett A.J., Johansen A.M., Brettschneider J.A., Prior I.A., Royle S.J. (2017): Microtubule organization within mitotic spindles revealed by serial block face scanning electron microscopy and image analysis. *J. Cell Sci.* 130:1845-1855.
- Nousiainen M., Silljé H.H., Sauer G., Nigg E.A., Körner R. (2006): Phosphoproteome analysis of the human mitotic spindle. *Proc. Natl. Acad. Sci. USA.* 103:5391-5396
- Nurse, P. (1990): Universal control mechanism regulating onset of M-phase. *Nature.* 344:503–508.
- O'Toole E.T., Giddings T.H., McIntosh J.R., Dutcher S.K. (2003): Three-dimensional organization of basal bodies from wild-type and d-tubulin deletion strains of *Chlamydomonas reinhardtii*. *Mol. Biol. Cell* 14:2999–3012.
- Olenick M.A., Tokito M., Boczkowska M., Dominguez R., Holzbaur E.L. (2019): Hook Adaptors Induce Unidirectional Processive Motility by Enhancing the Dynein-Dynactin Interaction. *J. Biol. Chem.* 291(35):18239–18251.
- Ouchi M., Fujiuchi N., Sasai K., Katayama H., Minamishima Y.A., Ongusaha P.P. (2004): BRCA1 phosphorylation by Aurora-A in the regulation of G2 to M transition. *J. Biol. Chem.* 279(19):19643–8.
- Petretti C., Savoian M., Montembault E., Glover D.M., Prigent C., Giet R. (2006): The PITSLRE/CDK11(p58) protein kinase promotes centrosome maturation and bipolar spindle formation. *EMBO Rep.* 7(4):418–24.
- Petry S., Groen A.C., Ishihara K., Mitchison T.J., Vale R.D. (2013): Branching microtubule nucleation in *Xenopus* egg extracts mediated by augmin and TPX2. *Cell* 152:768–777.
- Przewloka M.R., Venkei Z., Bolanos-Garcia V.M., Debski J., Dadlez M., Glover D.M. (2011): CENP-C is a structural platform for kinetochore assembly. *Curr. Biol.* 21:399-405.



- Rago F., Gascoigne K.E., Cheeseman I.M. (2015): Distinct organization and regulation of the outer kinetochore KMN network downstream of CENP-C and CENP-T. *Curr. Biol.* 25:671-677.
- Rattner J.B., Rao A., Fritzler M.J., Valencia D.W., Yen T.J. (1993): CENPF is a 400 kDa kinetochore protein that exhibits a cell-cycle dependent localization. *Cell Motil. Cytoskelet* 26:214-226.
- Redwine W.B., DeSantis M.E., Hollyer I. (2017): The human cytoplasmic dynein interactome reveals novel activators of motility. *Elife*. 2017;6:e28257.
- Renshaw M.J., Ward J.J., Kanemaki M., Natsume K., Nedelec F.J., Tanaka T.U. (2010): Condensins promote chromosome recoiling during early anaphase to complete sister chromatid separation. *Dev. Cell* 19:232–244.
- Rieder C.L. (1982): The formation, structure, and composition of the mammalian kinetochore and kinetochore fiber. *Int. Rev. Cytol.* 79:1-58.
- Rieder C.L., Alexander S.P. (1990): Kinetochores are transported poleward along a single astral microtubule during chromosome attachment to the spindle in newt lung cells. *J. of Cell Biol.* 110:81–95.
- Rieder C.L., Cole R.W., Khodjakov A., Sluder G. (1995): The checkpoint delaying anaphase in response to chromosome monoorientation is mediated by an inhibitory signal produced by unattached kinetochores. *J. Cell Biol.* 130:941–948.
- Rieder C.L., Salmon E.D. (1994): Motile kinetochores and polar ejection forces dictate chromosome position on the vertebrate mitotic spindle. *J Cell Biol* 124: 223–233.
- Rosenfeld S.S., van Duffelen M., Behnke-Parks W.M., Beadle C., Correia J., Xing J. (2009): The ATPase cycle of the mitotic motor CENP-E. *J. Biol. Chem.* 284:32858-32868
- Sadasivam, J., Arsen, P., Singh, P., John, J., Krenn, V., Florian, W., Tanja, B., Musacchio, A. (2016): Molecular basis of outer kinetochore assembly on CENP-T. *Elife* 5
- Santaguida, S., Tighe, A., D'Alise, A.M., Taylor, S.S., Musacchio, A. (2010): Dissecting the role of MPS1 in chromosome biorientation and the spindle checkpoint through the small molecule inhibitor reversine. *J. Cell Biol.* 190:73–87.
- Saurin A.T., van der Waal M.S., Medema R.H., Lens S.M., Kops G.J. (2011): Aurora B potentiates Mps1 activation to ensure rapid checkpoint establishment at the onset of mitosis. *Nat Commun.* 2:316.

- Schaar B.T., Chan G.K., Maddox P., Salmon E.D., Yen T.J. (1997): CENP-E function at kinetochores is essential for chromosome alignment. *J. Cell Biol.* 139:1373-1382
- Schleiffer A., Maier M., Litos G., Lampert F., Hornung P., Mechtler K., Westermann S. (2012): CENP-T proteins are conserved centromere receptors of the Ndc80 complex. *Nat. Cell Biol.* 14:604-613.
- Schroeder C.M., Ostrem J.M., Hertz N.T., Vale R.D. (2014): A Ras-like domain in the light intermediate chain bridges the dynein motor to a cargo-binding region. *Elife.* 3:e03351.
- Schroeder C.M., Vale R.D. (2016): Assembly and activation of dynein-dynactin by the cargo adaptor protein Hook3. *J. Cell Biol.* 214(3):309–318.
- Screpanti E., De Antoni A., Alushin G.M., Petrovic A., Melis T., Nogales E., Musacchio A. (2011): Direct binding of Cenp-C to the Mis12 complex joins the inner and outer kinetochore. *Curr. Biol.* 21:391-398.
- Scrittore L., Skoufias D.A., Hans F., Gerson V., Sassone-Corsi P., Dimitrov S. (2005): A small C-terminal sequence of Aurora B is responsible for localization and function. *Mol. Biol. Cell* 16(1):292–305.
- Sherr C.J., McCormick F. (2002): The RB and p53 pathways in cancer. *Cancer Cell* 2:103-112.
- Shimada M., Goshima T., Matsuo H., Johmura Y., Haruta M., Murata K. (2016): Essential role of autoactivation circuitry on Aurora B-mediated H2AXpS121 in mitosis. *Nat. Commun.* 7:12059.
- Silio, V., McAnish, A.D., Millar, J.B. (2015): KNL1-Bubs and RZZ Provide Two Separable Pathways for Checkpoint Activation at Human Kinetochores. *Dev. Cell* 35:600–613.
- Splinter D., Razafsky D.S., Schlager M.A. (2012): BICD2, dynactin, and LIS1 cooperate in regulating dynein recruitment to cellular structures. *Mol. Biol. Cell.* 23(21):4226–4241.
- Steigemann, P. (2009): Aurora B-mediated abscission checkpoint protect against tetraploidization. *Cell* 136:473–484.
- Steinhardt R.A., Alderton J. (1988): Intracellular free calcium rise triggers nuclear envelope breakdown in the sea urchin embryo. *Nature* 332:364–366.
- Sudakin, V., D. Ganioth, A. Dahan, H. Heller, J. Hershko, F.C. Luca, J. V Ruderman, and A. Hershko. (1995): The cyclosome, a large complex containing cyclin-selective ubiquitin ligase activity, targets cyclins for destruction at the end of mitosis. *Mol. Biol. Cell.* 6:185–197.

- Sumara I., Quadroni M., Frei C., Olma M.H., Sumara G., Ricci R. (2007): A Cul3-based E3 ligase removes Aurora B from mitotic chromosomes, regulating mitotic progression and completion of cytokinesis in human cells. *Dev. Cell* 12:887–900.
- Tanaka K., Mukae N., Dewar H., van Breugel M., James E.K., Prescott A.R., Antony C., Tanaka T.U. (2005): Molecular mechanisms of kinetochore capture by spindle microtubules. *Nature* 434: 987-994.
- Thrower D.A., Jordan M.A., Wilson L. (1996): Modulation of CENP-E organization at kinetochores by spindle microtubule attachment. *Cell Motil. Cytoskelet.* 35:121-133.
- Uhlmann F. (2001): Chromosome cohesion and segregation in mitosis and meiosis. *Curr. Opin. Cell Biol.* 13:754–761.
- Uhlmann F. (2014): A silent revolution in chromosome biology. *Nat. Rev. Mol. Cell Biol.* 15:431.
- Uzunova K., Dye B.T., Schutz H., Ladurner R., Petzold G., Toyoda Y., Jarvis M.A., Brown N.G., Poser I., Novatchkova M., Mechtler K., Hyman A.A., Stark H., Schulman B.A., Peters J.M. (2012): APC15 mediates CDC20 autoubiquitylation by APC/CMCC and disassembly of the mitotic checkpoint complex. *Nat. Struct. Mol. Biol.* 19:1116–1123
- Vader, G., Kauw, J. J., Medema, R. H., Lens, S. M. (2006): Survivin mediates targeting of the chromosomal passenger complex to the centromere and midbody. *EMBO Rep.* 7:85–92.
- van der Waal, M. S., Hengeveld, R. C., van der Horst, A., Lens, S. M. (2012): Cell division control by the chromosomal passenger complex. *Exp. Cell Res.* 318:1407–1420.
- Vandre DD, Davis F.M., Rao P.N., Borisy G.G. (1984): Phosphoproteins are components of mitotic microtubule organizing centers. *Proc. Natl. Acad. Sci. USA* 81(14):4439-43.
- Vigneron, S.; Prieto, S.; Bernis, C.; Labbe, J.C.; Castro, A.; Lorca, T. (2004): Kinetochore localization of spindle checkpoint proteins: Who controls whom? *Mol. Biol. Cell* 15:4584–4596.
- Vorozhko V.V., Emanuele M.J., Kallio M.J., Stukenberg P.T., Gorbsky G.J. (2008): Multiple mechanisms of chromosome movement in vertebrate cells mediated through the Ndc80 complex and dynein/dynactin. *Chromosoma* 117:169–179.
- Walczak C.E., Heald R. (2008): Mechanisms of mitotic spindle assembly and function. *Int. Rev. Cytol.* 265:111–158.

Wang G., Jiang Q., Zhang C. (2014): The role of mitotic kinases in coupling the centrosome cycle with the assembly of the mitotic spindle. *J. Cell Sci.* 127:4111–4122.

Wang, H., Hu, X., Ding, X., Dou, Z., Yang, Z., Shaw, A.W., Teng, M., Cleveland, D.W., Goldberg, M.L., Niu, L. (2004): Human Zwint-1 specifies localization of Zeste White 10 to kinetochores and is essential for mitotic checkpoint signaling. *J. Biol. Chem.* 279:54590–54598.

Weaver B.A., Bonday Z.Q., Putkey F.R., Kops G.J., Silk A.D., Cleveland D.W. (2003): Centromere-associated protein-E is essential for the mammalian mitotic checkpoint to prevent aneuploidy due to single chromosome loss. *J. Cell Biol.* 162:551-563.

Welburn J.P.I., Grishchuk E.L., Backer C.B., Wilson-Kubalek E.M., Yates J.R., Cheeseman I.M. (2009): The human kinetochore Skl complex facilitates microtubule depolymerization-coupled motility. *Dev. Cell* 16:374-385.

Welburn, J.P., Vleugel, M., Liu, D., Yates, J.R., Gascoigne, K.E., Cheeseman, I.M. (2013): CDK-dependent phosphorylation and nuclear exclusion coordinately control kinetochore assembly state. *J. Cell Biol.* 201:23–32.

Wendell K.L., Wilson J., Jordan M.A. (1993): Mitotic block in HeLa cells by vinblastine: ultrastructural changes in kinetochore-microtubule attachment and in centrosomes. *J. Cell Sci.* 104: 261-274.

Wood K.W., Lad L., Luo L., Qian X., Knight S.D., Nevins N., Brejc K., Sutton D., Gilmartin A.G., Chua P.R., Desai R., Schauer S.P., McNulty D.E., Annan R.S., Belmont L.D., Garcia C., Lee Y., Diamond M.A., Faucette L.F., Giardiniere M., Zhang S., Sun C.M., Vidal J.D., Lichtsteiner S., Cornwell W.D., Greshock J.D., Wooster R.F., Finer J.T., Copeland R.A., Huang P.S., Morgans D.J. Jr., Dhanak D., Bergnes G., Sakowicz R., Jackson J.R. (2010): Antitumor activity of an allosteric inhibitor of centromere-associated protein-E. *Proc. Natl. Acad. Sci. USA* 107:5839-5844

Wordeman L., Steuer E.R., Sheetz M.P., Mitchison T. (1991): Chemical subdomains within the kinetochore domain of isolated CHO mitotic chromosomes. *J. Cell Biol.* 114:285-290.

Yang Z., Tulu U.S., Wadsworth P., Rieder C.L. (2007). Kinetochore dynein is required for chromosome motion and congression independent of the spindle checkpoint. *Current Biology* 17:973–980.

Yang-Feng T.L., Lee W.H. (1995): Characterization of a novel 350- kilodalton nuclear phosphoprotein that is specifically involved in mitotic-phase progression. *Mol. Cell. Biol.* 15:5017-5029.

Yen T.J., Compton D.A., Wise D., Zinkowski R.P., Brinkley B.R., Earnshaw W.C., Cleveland D.W. (1991): CENP-E, a novel human centromere-associated protein required for progression from metaphase to anaphase. *EMBO J.* 10:1245-1254.

Zhang X., Ems-McClung C., Walczak C. (2008): Aurora A phosphorylates MCAK to control ran-dependent spindle bipolarity. *Mol. Biol. Cell.* 19(11):2752–2765.

Zheng F., Yue C., Li G., He B., Cheng W., Wang X. (2016): Nuclear AURKA acquires kinase independent transactivating function to enhance breast cancer stem cell phenotype. *Nat Commun.* 7:10180

Zhu X., Mancini M.A., Chang K.H., Liu C.Y., Chen C.F., Shan B., Jones D. (1995): Characterization of a novel 350-kilodalton nuclear phosphoprotein that is specifically involved in mitotic-phase progression. *Mol. Cell Biol.* 15:5017-29.

## 7. Curriculum vitae

### Personal information

Name: Mirela Kubat  
Contact: mirela.kubat@gmail.com

### Education

10/2017 - 02/2020  
MASTER'S DEGREE IN MOLECULAR BIOLOGY  
Faculty of Science | University of Zagreb |  
Master's Thesis: Functional study of CENP-E phosphorylation by Aurora kinases A and B

10/2013 – 09/2017  
BACHELOR'S DEGREE IN MOLECULAR BIOLOGY  
Faculty of Science | University of Zagreb |  
Bachelor's Thesis: Application of CRISPR/Cas9 technology in plants and its implication on legislative regulations

### Experience

03/2019 – 09/2019  
Cell Division and Cytoskeleton Group | Danish Cancer Society Research Center | Copenhagen, Denmark |  
Internship under the mentorship of Associate Prof. Marin Barišić

02/2016 – 07/2016  
Division of Molecular Biology | Department of Biology | Faculty of Science | University of Zagreb |  
Internship under the mentorship of Assistant Prof. Nenad Malenica,

### Languages

Croatian: Native proficiency  
English: C1.1. level according to CEFR  
German: B1.1. level according to CEFR

